

Studies of Tricyclic β -lactams as Novel Antimicrobial Agents

Jun Sato

2023

Contents

Chapter I	General Introduction	1
Chapter II	Discovery of a Tricyclic β-lactam Sulfoxide Core	16
Chapter III	Optimization of Aminothiazole Side Chain	69
Chapter IV	Stereoselective Synthesis of Tricyclic β-lactam Core..	105
Chapter V	Conclusion	128
Appendix	Ni-catalyzed Arylcyanation Reaction of Norbornene and Norbornadiene	136
	List of publications	168
	Other Publications.....	170
	Acknowledgment.....	172

Chapter I General Introduction

I-1. Antimicrobial Agents and Antimicrobial Resistance (AMR)

Since the discovery of penicillin by Alexander Fleming, numerous antibiotics have been developed and have contributed to therapy for infectious diseases. Among them, β -lactam antibiotics, which have various skeletons such as penam, cephem, carbapenem, and monobactam, are clinically used as very effective and safe antibiotics (Figure 1-1).

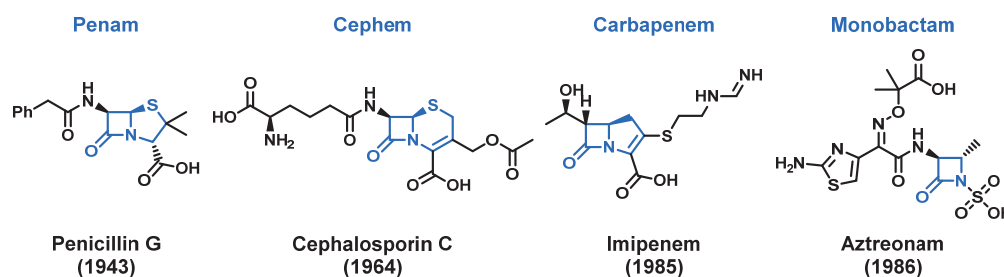


Figure 1-1. Series of β -lactam Antibiotics

Behind the development of many β -lactam antibiotics in this way is the fact that many studies have been conducted aiming at expanding the antibacterial spectrum, changing the administration route, the half-life in blood associating with releasing stress of frequent use for patients and medical workers, and overcoming antimicrobial resistance. However, while new therapeutic options with enhanced antibacterial activities and/or expanded antibacterial spectrum, including β -lactam antibiotics with different skeletons such as carbapenem and monobactam, become available, the battle against antimicrobial resistant bacteria repeats the development of new drugs and the emergence of resistant bacteria such as “cat-and-mouse game” (Figure 1-2).¹ In particular, carbapenem antibiotics are

effective against antimicrobial resistant bacteria to other antibiotics and are currently used as a "Last resort" against resistant bacteria.²

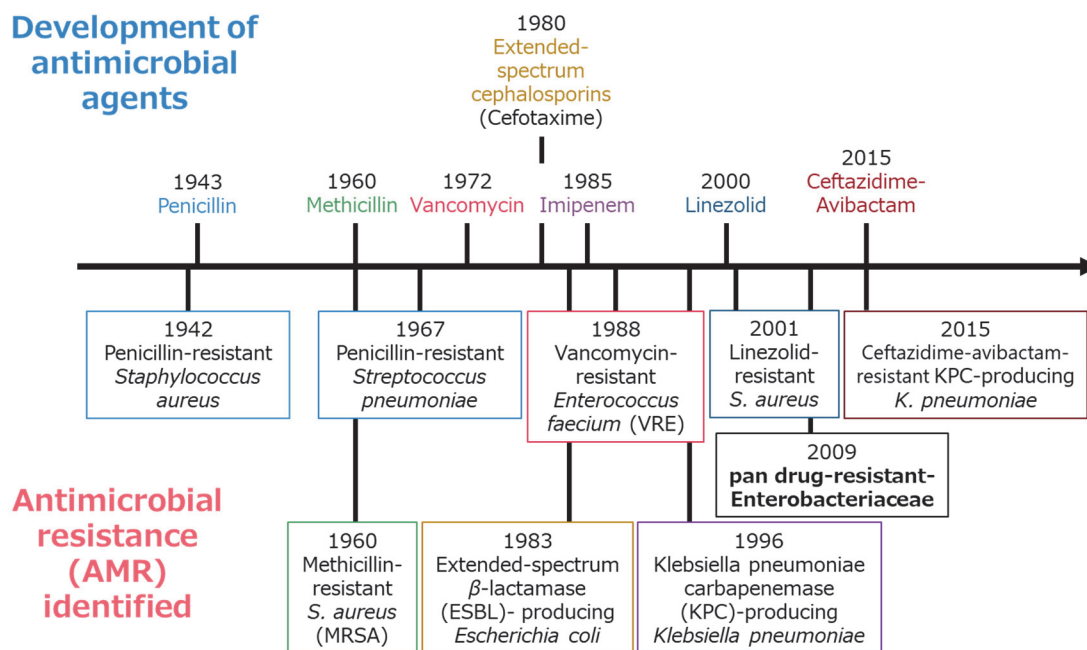


Figure 1-2. Battle against Antimicrobial Resistance¹

On the other hand, the problem of multidrug-resistant bacteria caused by excessive or inappropriate use of those antibiotics is becoming much more serious against our expectation. According to the “Global priority list of antibiotic-resistant bacteria to guide research, discovery, and development of new antibiotics.” published by the World Health Organization (WHO) in 2017,³ carbapenem-resistant *Acinetobacter baumannii* (CRAB), carbapenem-resistant *Pseudomonas aeruginosa* (CRPA), and carbapenem-resistant Enterobacterales (CRE) are positioned as “Priority 1: Critical”. (Table 1-1). Also, in 2019, the United States Centers for Disease Control and Prevention (CDC) had sent out urgent threats about CRAB and CRE, and reported that CRE has a higher estimated number of

infections and deaths than CRAB.¹ CRE organisms are multidrug-resistance, and almost all antibiotics, not just β -lactam antibiotics, are ineffective, therefore new treatment options are urgently needed.⁴ Therefore, the author set the goal of this thesis to identify new treatment options for infections caused by CREs.

Table 1-1. Global Priority List of Antibiotic-Resistant Bacteria to Guide Research, Discovery, and Development of New Antibiotics³

Priority 1 : CRITICAL	<i>Acinetobacter baumannii</i> , carbapenem-resistant	<i>Pseudomonas aeruginosa</i> , carbapenem-resistant	Enterobacterales* , carbapenem-resistant, 3rd generation cephalosporin- resistant
Priority 2: HIGH	<i>Enterococcus faecium</i> , vancomycin-resistant	<i>Staphylococcus aureus</i> , methicillin-resistant, vancomycin intermediate and resistant	<i>Helicobacter pylori</i> , clarithromycin-resistant
	<i>Campylobacter</i> , fluoroquinolone-resistant	<i>Salmonella spp.</i> , fluoroquinolone-resistant	<i>Neisseria gonorrhoeae</i> , 3rd generation cephalosporin-resistant, fluoroquinolone-resistant
Priority 3: MEDIUM	<i>Streptococcus pneumoniae</i> , penicillin-non-susceptible	<i>Haemophilus influenzae</i> , ampicillin-resistant	<i>Shigella spp.</i> , fluoroquinolone-resistant

*Enterobacterales include: *Klebsiella pneumoniae*, *Escherichia coli*, *Enterobacter spp.*, and *Serratia spp.*

I-2. Bacterial Structure

Bacteria are roughly divided into two types, Gram-positive and Gram-negative, according to the Gram stain method devised by Hans Gram. *Acinetobacter baumannii*, *Pseudomonas aeruginosa*, and Enterobacterales mentioned in the previous section as problematic bacteria are Gram-negative. Gram-negative bacteria have a characteristic membrane structure called the outer membrane on the outside of the cell wall (Figure 1-3).

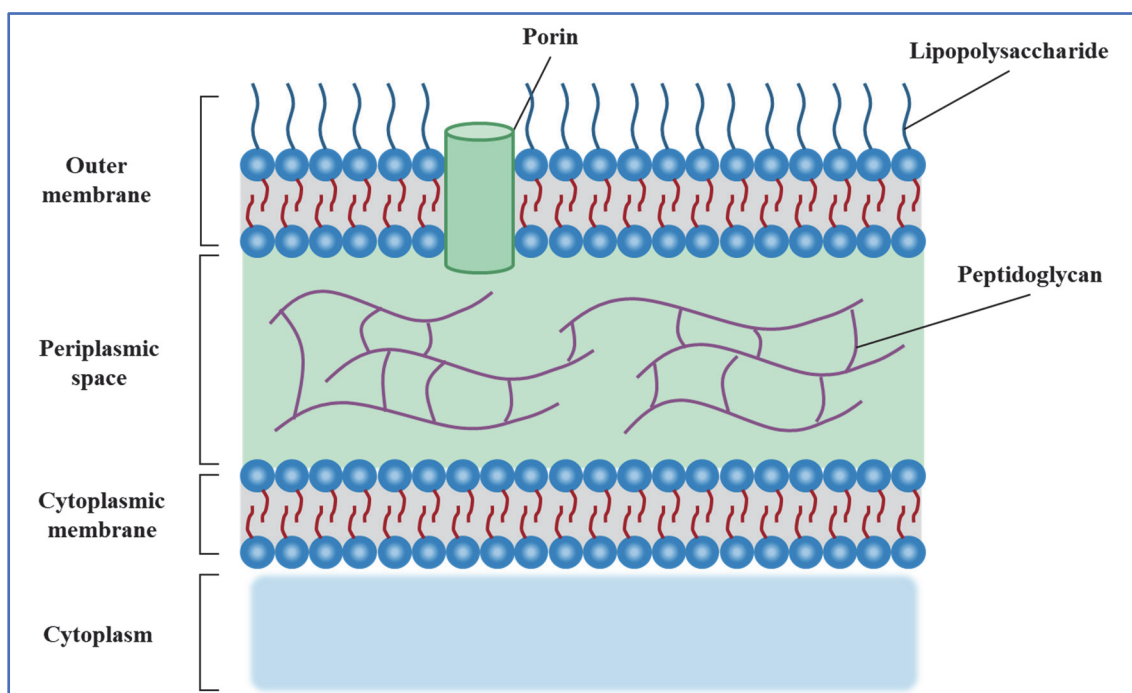


Figure 1-3. Structures of Gram-Negative Bacteria

The outer membrane is formed of a lipid bilayer such as the cell membrane, but the sugar chain of lipopolysaccharide extends outward. Considering drug permeability, adequate lipophilicity is required to permeate the lipid bilayer membrane, whereas it should be a hydrophilic molecule to permeate the outer lipopolysaccharide. In other words, the outer membrane has a structure that neither hydrophobic molecules nor hydrophilic molecules pass through. On the other hand, in order to take up nutrients (hydrophilic substances), the outer membrane has a protein structure called porin, and it is said that hydrophilic antibiotics such as β -lactam antibiotics enter the cells of Gram-negative bacteria via porin.⁵

I-3 Drug Resistance Mechanism

The resistance mechanisms that bacteria acquire at the cellular level can be broadly divided into three categories: 1) production of enzymes that inactivate antibiotics (e.g. β -lactamase which degrades β -lactam antibiotics and aminoglycoside modifying enzymes that inactivate aminoglycoside antibiotics), 2) mutation of target molecules and/or acquisition of alternative routes (e.g. mutations of β -lactam antibiotics target molecule PBP2 (penicillin-binding protein 2) to PBP2'), and 3) changes in membrane permeability of drugs (e.g. development of drug efflux pumps that expel the drug extracellularly and deficiency of porin that antibiotics use to permeate the outer membrane) (Figure 1-4).⁶

Among these resistance mechanisms, the most important determinant of resistance in Gram-negative bacteria, including CRE, is the production of β -lactamase which degrades β -lactam antibiotics.

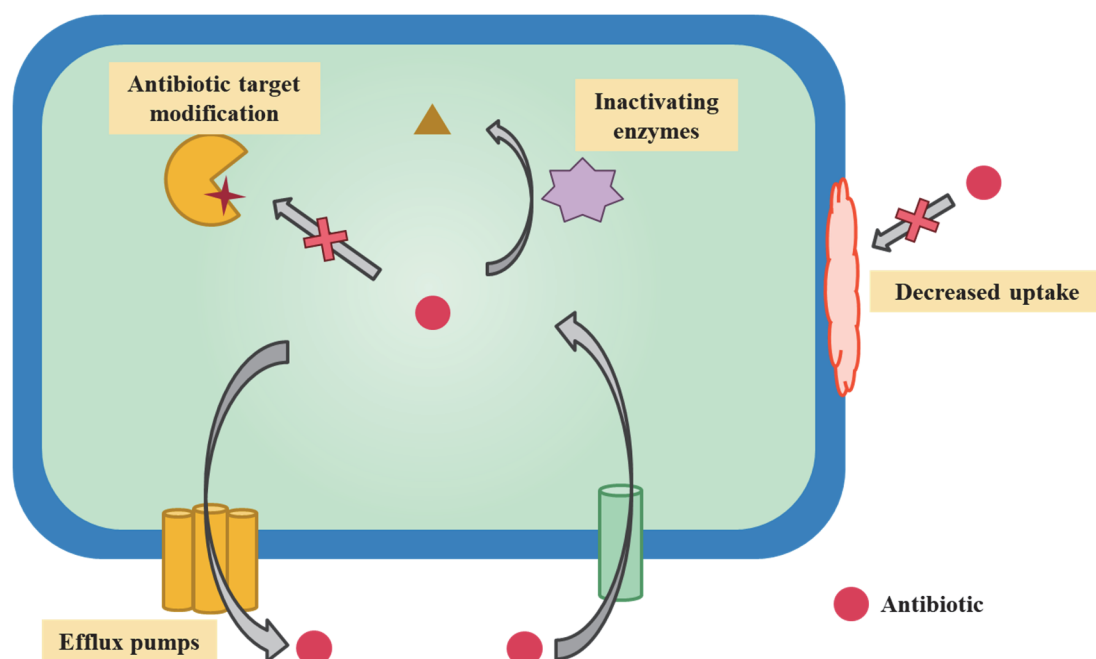


Figure 1-4. Major Mechanisms of Antimicrobial Resistance

β -lactamase is an enzyme that inactivates β -lactam antibiotics by hydrolyzing them. These are a series of enzymes with diverse substrate specificities and are classified from various points of view.⁷ The most commonly used classification is the method by Ambler based on the homology of amino acid sequences.⁸ According to this classification, β -lactamase can be classified into four classes (classes A, B, C, D). β -lactamase belonging to classes A, C and D is a serine- β -lactamase having a serine residue in the active center, and class B is a metallo- β -lactamase having a zinc ion in the active center.⁹

The mechanism of β -lactam antibiotics hydrolysis by serine- β -lactamase (classes A, C and D) is shown below (Figure 1-5A). The hydroxyl group of a serine residue in the active center is activated by a basic residue such as lysine to attack the carbonyl carbon of β -lactam ring and generates the acylenzyme intermediate. The acylenzyme intermediate is then hydrolyzed by a water molecule activated by a basic residue to regenerate β -lactamase and yield the hydrolyzed product.

Next, the reaction mechanism of metallo- β -lactamase (class B) is exhibited (Figure 1-5B). A zinc ion in the active center is coordinated to the carboxylic acid group, then the hydroxyl anion nucleophilically attacks the carbonyl carbon of β -lactam ring and forms an anionic intermediate. This intermediate is then protonated to regenerate β -lactamase and yield the hydrolyzed product.

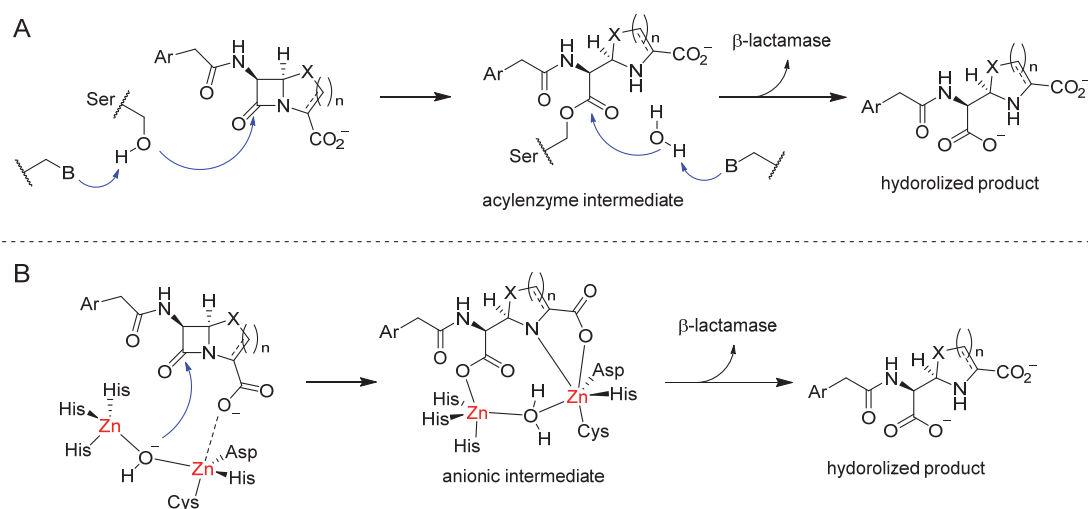


Figure 1-5. Hydrolysis Mechanism of β -lactams by Serine- β -Lactamase (A) and Metallo- β -Lactamase (B)

The substrate scopes in each class of β -lactamase and typical enzymes are shown (Table 1-2).¹⁰ In particular, carbapenem-hydrolyzing β -lactamases ‘carbapenemases’, which degrade almost all approved β -lactam antibiotics including carbapenems, are one of the major resistance mechanisms of carbapenem resistance that have become a significant worldwide public health issue in recent years. Among serine- β -lactamase, class A β -lactamase such as KPC (*K. pneumoniae* carbapenemase)¹¹ and class D β -lactamase such as OXA-23, 24/40, and 48¹² are known as carbapenemases. Class B β -lactamases, which are metallo- β -lactamases (MBLs), also possess carbapenemase activity as they could degrade all classes of β -lactam antibiotics except monobactams.¹³

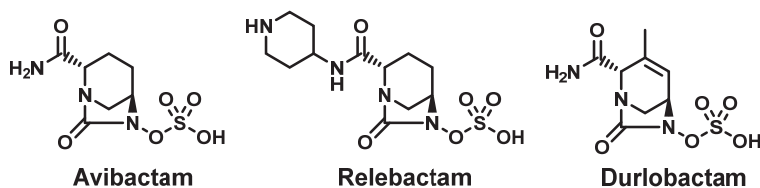
Table 1-2. Substrate Scope and Relevant Examples of β -Lactamases

Class	Type	Substrates				Most relevant examples
		Penicillins	Cephalosporins	Carbapenems	Monobactams	
A	Serine-	○	×	×	×	Penicillinases from Gram-positive bacteria
		○	△	×	×	TEM-1, TEM-2, SHV-1
	(ESBL)	○	○	×	△	SHV-2, TEM-10, CTX-M, GES-1
	(Serin carbapenemase)	○	○	○	△	KPC, SME, NMC-A, GES-2
B	Metallo-	○	○	○	×	IMP, VIM, NDM
C	Serine-	○	○	×	○	AmpC, CMY, ACT-1, DHA
D	Serine-	○	○	△	○	OXA-23, OXA-24/40, OXA-48

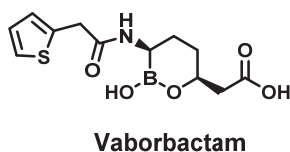
I-4. Combination of β -lactam and β -lactamase Inhibitor

For β -lactamase-producing strains, the combination of β -lactamase inhibitor (BLI) and a β -lactam antibiotic (BL) is one of the treatment options. Since the clinical use of clavulanic acid in combination with amoxicillin in the United States in 1982, some BLIs exert still important role in clinical. On the other hand, these classical BLIs cannot inhibit β -lactamases produced by carbapenem-resistant Enterobacterales (CRE). Developing a new BLI being effective against CRE under these circumstances,, and avibactam (AVI) with a 1,6-diazabicyclo[3.2.1]octane (DBO) skeleton was approved by the FDA in 2015.¹⁴ Since then, new BLIs such as relebactam¹⁵ and durlobactam,¹⁶ having DBO-based BLIs, and vaborbactam,¹⁷ being a boronic acid analogue, have appeared one after another, and research on new BLIs has been actively conducted centering on these two skeletons (Figure 1-6).⁶

DBO type



Cyclic boronate type

**Figure 1-6.** New β -lactamase Inhibitors

In these combinations, the BLI hinders hydrolysis and inactivation by β -lactamases to restore the activity of the β -lactam antibiotic. The BL/BLI strategy should be one of the therapeutic options for infections caused by CREs; however, they do not offer sufficient antibacterial activities against MBL-producing strains and these activities would be lost against clinical isolates with resistance mechanisms other than β -lactamase production. Examples include reduction of the outer membrane permeability caused by porin deficiency with β -lactamase production¹⁸ and degradation of target affinity by mutations in penicillin-binding proteins (PBPs)¹⁹.

I-5. Overview of This Thesis

The author would like to resolve the problem of CRE by using a single molecule of β -lactam, without the β -lactamase inhibitor, as a different from using the BL/BLI strategy. To achieve this goal, it is necessary to discover a new β -lactam agent, which is not easily recognized and hydrolyzed by various classes of β -lactamases and can provide sufficient

antibacterial activities against CREs without a BLI.

Chapter II describes the details the identification of the tricyclic β -lactam sulfoxide **3** with potent antibacterial activities against CREs.

The author was interested in the antibacterial activities of the lactivicin (LTV) analog **1**²⁰, which have a unique ring structure consisting of a cycloserine linked to a γ -lactone ring, and tricyclic β -lactam analog **2**²¹, in which cycloserine had been converted to a β -lactam ring, especially those acting against β -lactamase producers. And as a result of some modifications to **2**, the author have discovered tricyclic β -lactam sulfoxide **3** which exhibited potent antibacterial activities against all tested β -lactamase producers including CRE (Figure 1-7).

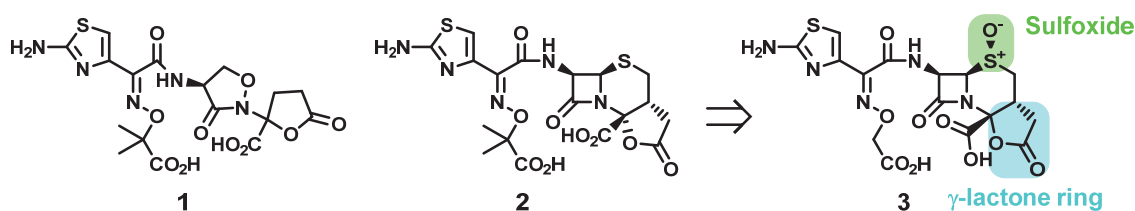


Figure 1-7. Overview of Chapter II

Chapter III details the discovery of compound **4** that overcome resistance mechanisms other than β -lactamase production. These mechanisms are the reduction of outer membrane permeability with the production of β -lactamases¹⁸ and the insertion mutation of four amino acids into penicillin-binding protein 3 (PBP 3).¹⁹ The author identified a potent compound **4** that overcomes these resistance mechanisms by converting the alkoxyimino moiety of the aminothiazole side chain (Figure 1-8).

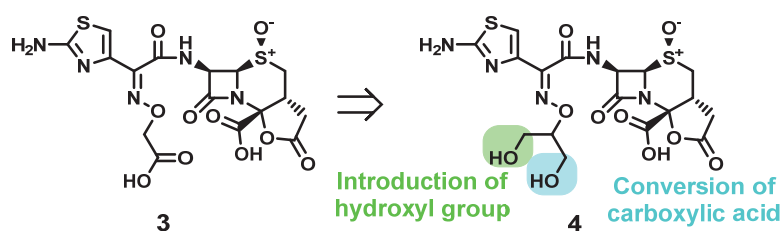
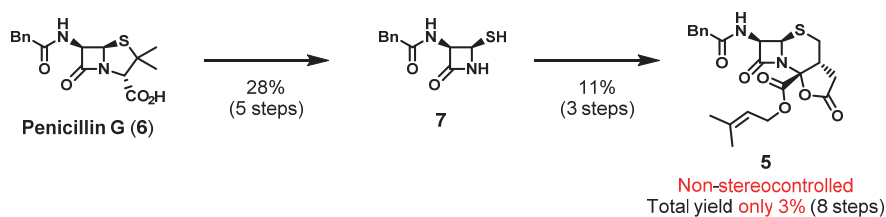


Figure 1-8. Overview of Chapter III

Chapter IV described the development of a new synthetic method for tricyclic β -lactam antibiotic found in Chapters III. In the 1980s, the synthesis of a key intermediate **5** from penicillin leading to tricyclic β -lactam sulfoxide **4** was reported.²¹ But this synthesis route requires eight steps from Penicillin G (**6**) with a low total yield of 3% via non-stereoselective lactone formation. Thus, the author had developed second generation diastereoselective synthetic route of the unique tricyclic β -lactam core **10** by sulfoxide-directed oxidative lactonization (Figure 1-9).

1st generation route



2nd generation route

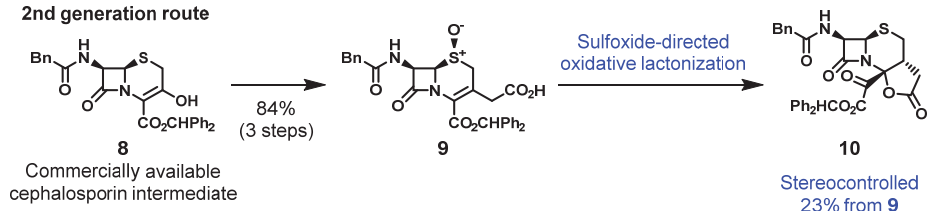


Figure 1-9. Overview of Chapter IV

Chapter V summarizes this thesis.

Reference

- ¹ (a) Centers for Disease Control and Prevention (CDC). *Antibiotic Resistance Threats in the United States 2019*, Atlanta, GA; U.S. Department of Health and Human Services, CDC, 2019. Retrieved from <https://www.cdc.gov/drugresistance/pdf/threats-report/2019-ar-threats-report-508.pdf> (accessed November 22, 2022). (b) (CDC). *Antibiotic Resistance Threats in the United States 2013*, Atlanta, GA; U.S. Department of Health and Human Services, CDC, 2013. Retrieved from <https://www.cdc.gov/drugresistance/pdf/ar-threats-2013-508.pdf> (accessed November 22, 2022).
- ² Singh, G. S. β -Lactams in the New Millennium. Part-I: Monobactams and Carbapenems. *Mini. Rev. Med. Chem.* **2004**, *4*, 69–92.
- ³ World Health Organization. *Global priority list of antibiotic-resistant bacteria to guide research, discovery, and development of new antibiotics*; WHO, February 27, 2017. Retrieved from <https://www.aidsdatahub.org/resource/who-global-priority-list-antibiotic-resistant-bacteria> (accessed November 22, 2022).
- ⁴ Gupta, N.; Limbago, B. M.; Patel, J. B.; Kallen, A. J. Carbapenem-Resistant Enterobacteriaceae: Epidemiology and Prevention. *Clin. Infect. Dis.* **2011**, *53*, 60–67.
- ⁵ Yoshimura, F.; Nikaido, H. Diffusion of β -Lactam Antibiotics Through the Porin Channels of *Escherichia coli* K-12. *Antimicrob. Agents Chemother.* **1985**, *27*, 84–92.
- ⁶ González-Bello, C.; Rodríguez, D.; Pernas, M.; Rodríguez, Á.; Colchón, E. β -Lactamase Inhibitors To Restore the Efficacy of Antibiotics against Superbugs. *J. Med. Chem.* **2020**, *63*, 1859–1881.

-
- ⁷ Bush, K.; Bradford, P. A.; Interplay between β -lactamases and new β -lactamase inhibitors. *Nat. Rev. Microbiol.* **2019**, *17*, 295–306.
- ⁸ Ambler, R. P. The structure of β -lactamases. *Philos. Trans. R. Soc., B* **1980**, *289*, 321–331.
- ⁹ (a) Bush, K. Past and Present Perspectives on β -lactamases. *Antimicrob. Agents Chemother.* **2018**, *62*, e01076–18. (b) Tooke, C. L.; Hinchliffe, P.; Bragginton, E. C.; Colenso, C. K.; Hirvonen, V. H. A.; Takebayashi, Y.; Spencer, J. β -Lactamases and β -Lactamase Inhibitors in the 21st Century. *J. Mol. Biol.* **2019**, *431*, 3472–3500.
- ¹⁰ Paterson, D. L.; Bonomo, R. A. Extended-Spectrum β -Lactamases: a Clinical Update. *Clin. Microbiol. Rev.* **2005**, *18*, 657–686.
- ¹¹ Walther-Rasmussen, J.; Høiby, N. Class A carbapenemases. *J. Antimicrob. Chemother.* **2007**, *60*, 470–482.
- ¹² Leonard, D. A.; Bonomo, R. A.; Powers, R. A. Class D β -Lactamases: A Reappraisal after Five Decades. *Acc. Chem. Res.* **2013**, *46*, 2407–2415.
- ¹³ Bebrone, C. Metallo- β -lactamases (Classification, Activity, Genetic, Organization, Structure, Zinc Coordination) and their superfamily. **2007**, *74*, 1686–1701.
- ¹⁴ Wang, D. Y.; Abboud, M. I.; Markoulides, M. S.; Brem, J.; Schofield, C. J. The road to avibactam: the first clinically useful non- β -lactam working somewhat like a β -lactam. *Future Med. Chem.* **2016**, *8*, 1063–1084.
- ¹⁵ Blizzard, T. A.; Chen, H.; Kim, S.; Wu, J.; Young, K.; Park, Y.-W.; Ogawa, A.; Raghoobar, S.; Painter, R. E.; Hairston, N.; Lee, S. H.; Misura, A.; Felcetto, T.; Fitzgerald, P.; Sharma, N.; Lu, J.; Ha, S.; Hickey, E.; Hermes, J.; Hammond, M. L. Side chain SAR of bicyclic β -lactamase inhibitors (BLIs). 1. Discovery of a class C BLI for combination with imipenem. *Bioorg. Med. Chem. Lett.* **2010**, *20*, 918–921.

¹⁶ Shapiro, A. B.; Moussa, S. H.; McLeod, S. M.; Durand-Réville, T.; Miller, A. A. Durlobactam, a new diazabicyclooctane β -lactamase inhibitor for the treatment of *Acinetobacter* infections in combination with sulbactam. *Front. Microbiol.* **2021**, *12*, 709974.

¹⁷ Novelli, A.; Giacomo, D. P.; Rossolini, M. G.; Tumbarello, M. Meropenem/vaborbactam: a next generation β -lactam β -lactamase inhibitor combination. *Expert Rev. Anti-Infect. Ther.* **2020**, *18*, 643–655.

¹⁸ (a) Nelson, K.; Hemarajata, P.; Sun, D. et al. Resistance to Ceftazidime-Avibactam Is Due to Transposition of KPC in a Porin-Deficient Strain of *Klebsiella pneumoniae* with Increased Efflux Activity. *Antimicrob. Agents Chemother.* **2017**, *61*, e00989–e1017. (b) Shen, Z.; Ding, B.; Ye, M.; Wang, P.; Bi, Y.; Wu, S.; Xu, X.; Guo, Q.; Wang, M. High ceftazidime hydrolysis activity and porin OmpK35 deficiency contribute to the decreased susceptibility to ceftazidime/avibactam in KPC-producing *Klebsiella pneumoniae*. *J. Antimicrob. Chemother.* **2017**, *72*, 1930–1936. (c) Lomovskaya, O.; Sun, D.; Rubio-Aparicio, D.; Nelson, K.; Tsivkovski, R.; Griffith, D. C.; Dudley, M. N. Vaborbactam: Spectrum of Beta-Lactamase Inhibition and Impact of Resistance Mechanisms on Activity in *Enterobacteriaceae*. *Antimicrob. Agents Chemother.* **2017**, *61*, 1–15.

¹⁹ (a) Sato, T.; Ito, A.; Ishioka, Y.; Matsumoto, S.; Rokushima, M.; Kazmierczak, K. M.; Hackel, M.; Sahm, D. F.; Yamano, Y. *Escherichia coli* strains possessing a four amino acid YRIN insertion in PBP3 identified as part of the SIDERO-WT-2014 surveillance study. *JAC-Antimicrob. Resist.* **2020**, *2*, dlaa081. (b) Alm, R. A.; Johnstone, M. R.; Lahiri, S. D. Characterization of *Escherichia coli* NDM isolates with decreased susceptibility to aztreonam/avibactam: role of a novel insertion in PBP3. *J. Antimicrob. Chemother.* **2015**, *70*, 1420–1428.

²⁰ (a) Harada, S.; Tsubotani, S.; Hida, T.; Ono, H.; Okazaki, H. Structure of lactivicin, an antibiotic having a new nucleus and similar biological activities to β -lactam antibiotics. *Tetrahedron Lett.* **1986**, *27*, 6229–6232. (b) Nozaki, Y.; Katayama, N.; Ono, H.; Tsubotani, S.; Harada, S.; Okazaki, H.; Nakao, Y. Binding of a non- β -lactam antibiotic to penicillin-binding proteins. *Nature* **1987**, *325*, 179–180. (c) Tamura, N.; Matsushita, Y.; Kawano, Y.; Yoshioka, K. Synthesis and Antibacterial Activity of Lactivicin Derivatives. *Chem. Pharm. Bull.* **1990**, *38*, 116–122.

²¹ Morimoto, A.; Noguchi, N.; Chou, N. Tricyclic cepham compounds, their production and use. EP253337 A2. Jan 20, 1988.

Chapter II Discovery of a Tricyclic β -lactam Sulfoxide Core

II-1. Introduction

Antimicrobial resistance (AMR) has become a significant worldwide public health issue. The United States CDC and the WHO have sent out alerts about the urgent need for new treatment options for infection due to carbapenem-resistant Enterobacterales (CREs).¹ One of the key resistant mechanisms is the production of carbapenem-hydrolyzing enzymes, carbapenemases, which include serine-type β -lactamase (Class A and D based on the Ambler classification²), such as KPC and OXA-48, and metallo-type β -lactamase (MBL; Class B), such as NDM and VIM. The risk of mortality due to carbapenemase-producing CRE infections is higher than that due to non-carbapenemase-producing CRE infections.³ Since 2015, some combinations of β -lactam and β -lactamase inhibitor (BL/BLI) such as AVYCAZ® (ceftazidime, CAZ, **3**/avibactam, AVI, **4**)⁴ and VABOMERE® (meropenem, MER, **5**/vaborbactam, VAB, **6**)⁵ have been approved by authorities of some countries. In these combinations, the β -lactamase inhibitor hinders hydrolysis and inactivation by β -lactamases to rescue the activity of the β -lactam antibiotic. The BL/BLI strategy is one way of responding to the need of finding effective treatments, however, it does not offer sufficient antibacterial activities against MBL-producing strains and may offer only limited coverage against CREs in the future if the pathogens develop an excess of β -lactamases and/or inhibitor-resistant-phenotype β -lactamases.⁶

Therefore, the author would like to resolve the problem of CREs by using a single molecule of β -lactam, without the β -lactamase inhibitor, as a different from using the BL/BLI strategy. And to reach this goal, he needed to discover a new β -lactam agent,

which is not easily recognized and hydrolyzed by various classes of β -lactamases and can provide sufficient antibacterial activities against CREs without a BLI. Lacticivins (LTVs), which have a unique ring structure consisting of a cycloserine linked to a γ -lactone ring, were reported by Takeda Pharmaceutical Company in the 1980's.⁷ They also reported on tricyclic β -lactam analogues, in which cycloserine had been converted to a β -lactam ring. Since the late 2000's, the antibacterial activities of LTVs against various β -lactamase producers have been reported,⁸ however, further research was not conducted on these tricyclic β -lactam analogues. Since he was interested in the antibacterial activities of the LTVs and the tricyclic β -lactam analogues, especially those acting against β -lactamase producers, the reported compound **1**^{7,8} and **2a**⁹ were evaluated the antibacterial activities, and started exploratory research of compounds with potent activities against several problematic β -lactamase producers (Figure 2-1).

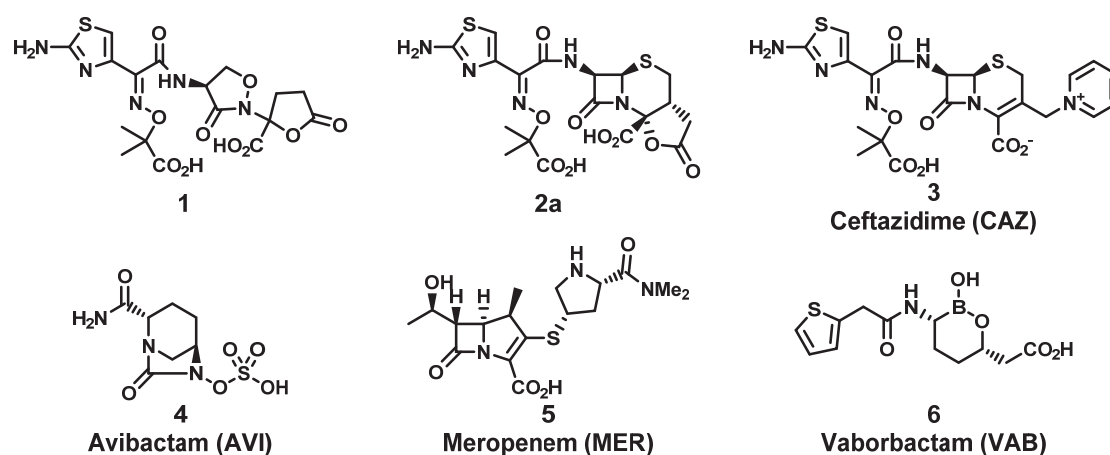
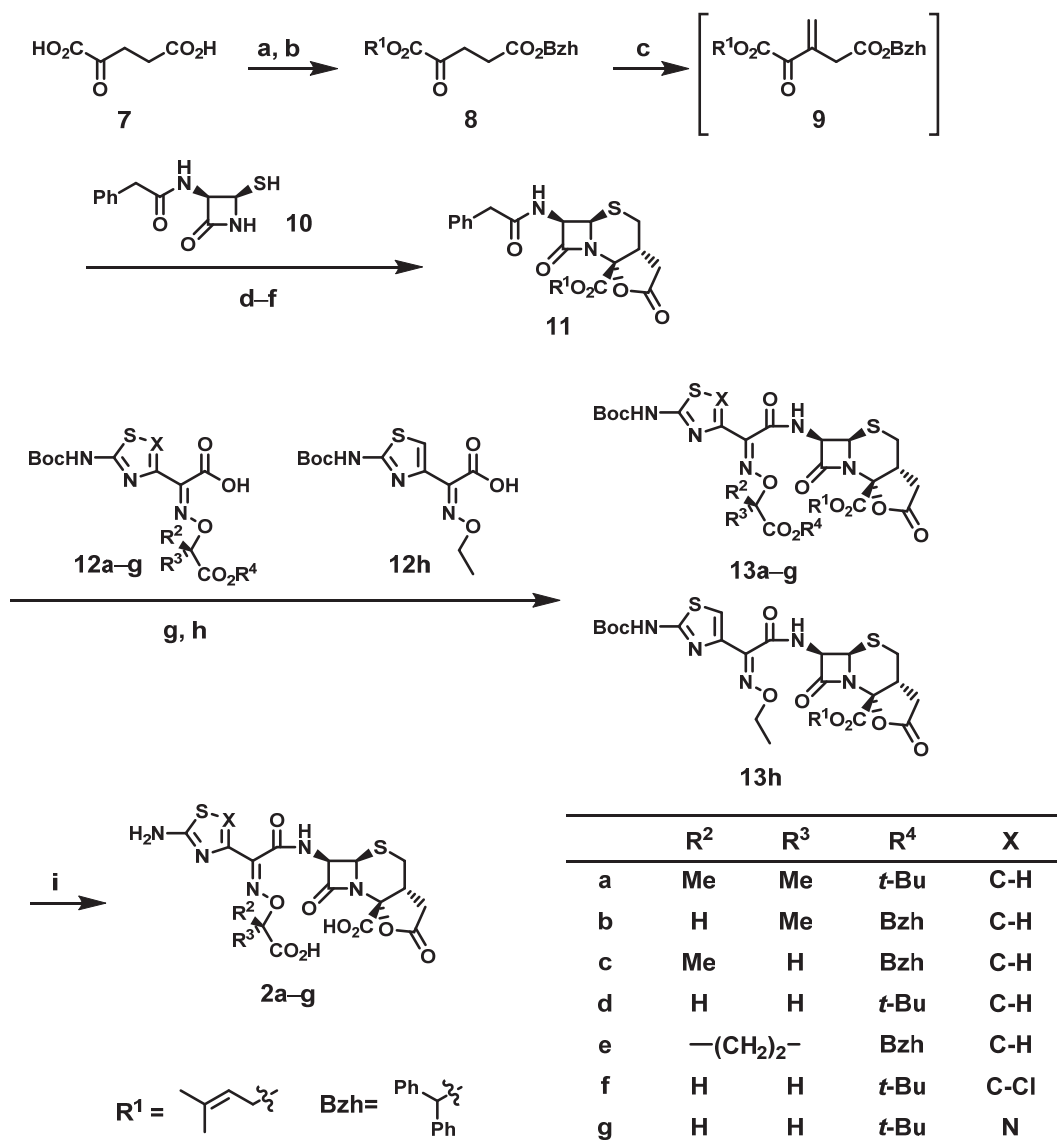


Figure 2-1. Structures of Compounds **1**, **2a** and Approved BL/BLIs

II-2. Synthesis of Tricyclic β -lactams

Scheme 2-1 shows the synthesis of compound **2a** and its derivatives.



Reagents and conditions: (a) 1-Bromo-3-methyl-2-butene, C_2NH , DMF, 60°C; (b) Diphenyldiazomethane, THF, rt; (c) *N,N,N',N'*-Tetramethyldiaminomethane, Ac_2O , AcOH, CH_2Cl_2 , rt; (d) **10**, HMPA, rt; (e) TFA, CH_2Cl_2 , -10 °C; (f) EDC HCl, CH_2Cl_2 , rt; (g) PCl_5 , Py, CH_2Cl_2 , -30 °C; (h) **12a-h**, MsCl, Et_3N , Py, $\text{CH}_2\text{Cl}_2/\text{DMA}$, 0 °C; (i) AlCl_3 , Anisole, CH_2Cl_2 , -40 °C.

Scheme 2-1. Synthesis of Tricyclic β -lactams **2a-g**

An exomethylene group was introduced to the protected keto-acid intermediate **8** to give compound **9**, which was then coupled with compound **10** and cyclized to make the key intermediate **11**. The structure of **11** was confirmed by single crystal X-ray crystallography (Figure 2-2). The phenylacetyl group was removed from the amino group followed by introduction of several aminothiazole side chains **12a–h** and removal of all protective groups to create target compounds **2a–g**.

The sulfur of compounds **13b–e, g** and **h** was oxidized to obtain sulfoxides **14b–e, g, h** and **14d'** and sulfone **15d**. The stereochemistry of the sulfoxides was determined based on single crystal X-ray crystallography of **16d'** (Figure 2-2) and the reported ratio of two isomeric sulfoxides (9:1).¹⁰ Removal of all protective groups created target compounds **16b–e, g, h, 16d'** and **17d** (Scheme 2-2).

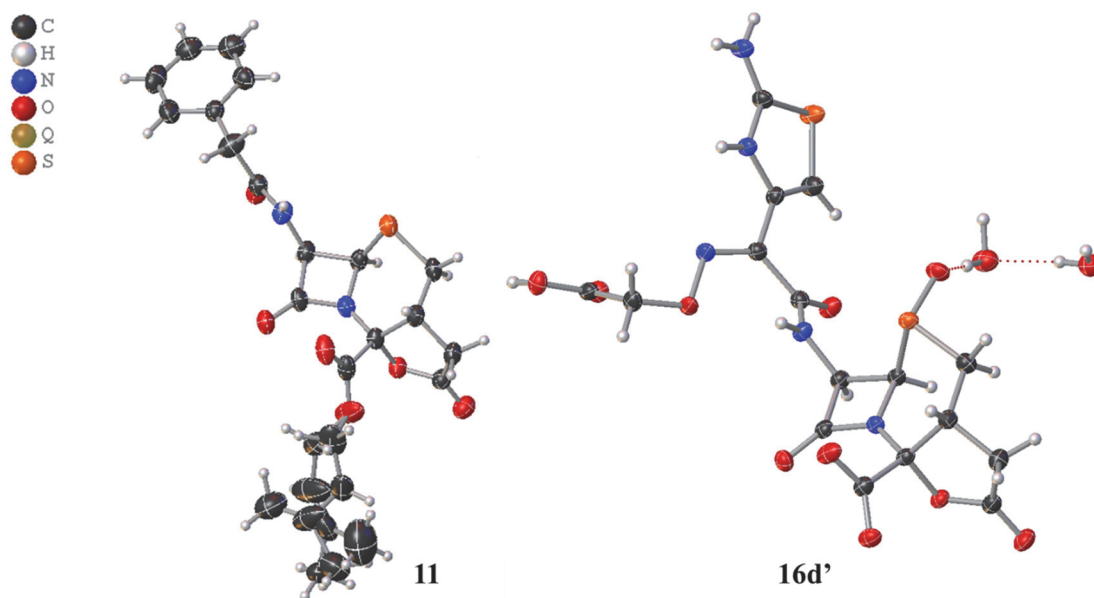
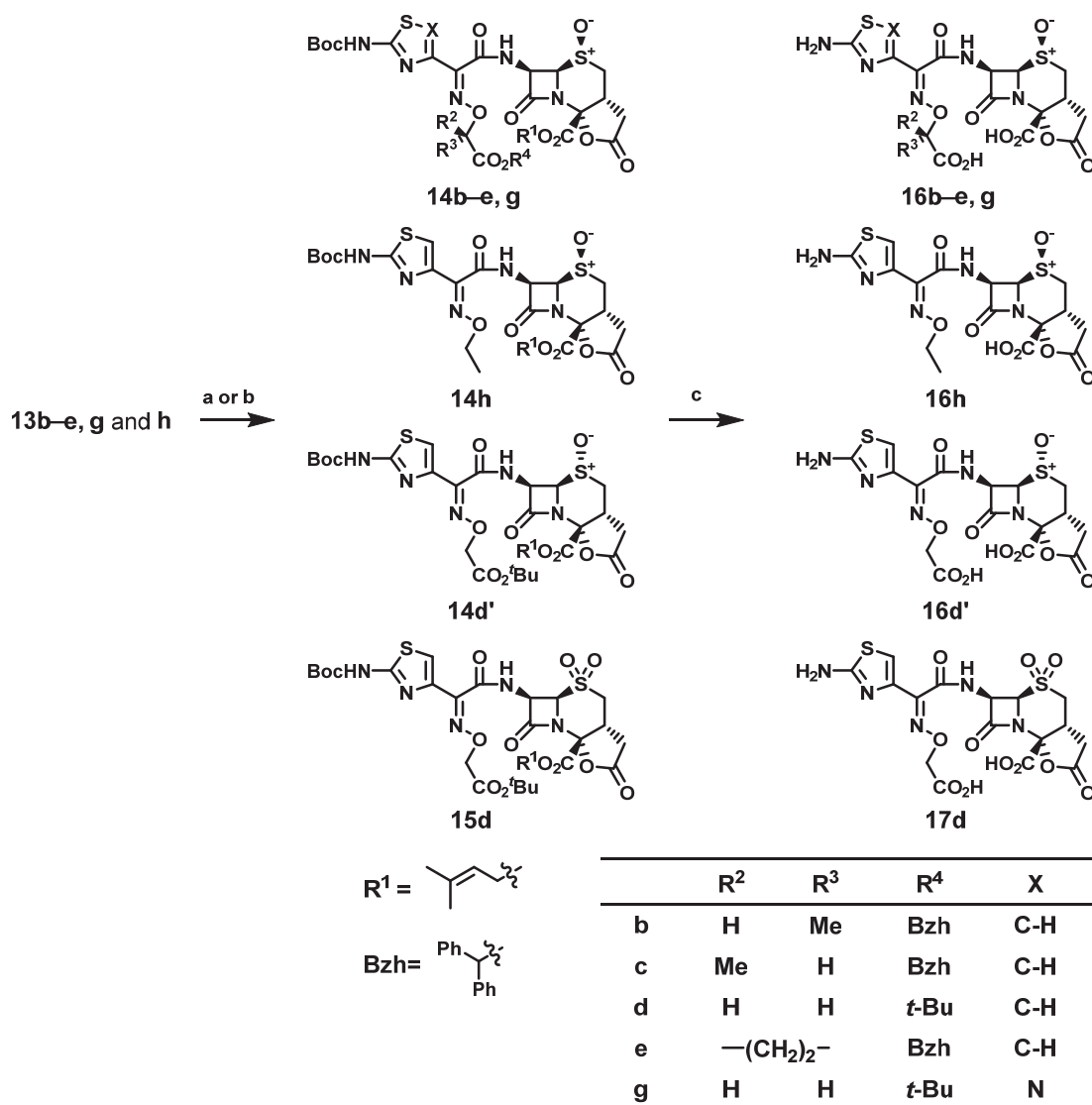


Figure 2-2. Molecular Structure of **11** and **16d'**; Thermal ellipsoids are set at 30% probability



Reagents and conditions: (a) for **14b–e, g, h** and **14d'** AcOOH, MeCN/DMA, 0 °C; (b) for **15d** *m*-CPBA, CH₂Cl₂, 0 °C; (c) AlCl₃, Anisole, CH₂Cl₂, –40 °C.

Scheme 2-2. Synthesis of Tricyclic β -lactams **16b–e, g, h, 16d'** and **17d**

II-3. Identification of Sulfoxide-Introduced Tricyclic β -lactam

Lactivicins (LTVs) have demonstrated their potent antibacterial activities against various kinds of β -lactamase-producing *Escherichia coli* recombinant strains over the

past decade.⁸ LTV lead optimization studies reported by Takeda Pharmaceutical Company described several potent compounds, including compound **1**.⁷ Some potent analogues of LTV had also been reported^{9,11} and tricyclic β -lactam derivatives exhibited the most potent activities among them, but there were no further reports on these derivatives. Consequently, the author first evaluated the potent LTV derivative **1** and the tricyclic β -lactam derivative **2a**⁹ with the same aminothiazole side chain as **1** for antibacterial activities against various kinds of β -lactamase producers. First, to assess the relative β -lactamase susceptibility of these lactivicin analogs, the minimum inhibitory concentrations (MICs) of compound **1**, **2a** and Ceftazidime **3** against various kinds of β -lactamase-producing *E. coli* recombinant strains were determined (Table 2-1).

Table 2-1. *In Vitro* Antibacterial Activities (MIC, $\mu\text{g}/\text{mL}$) of Isogenic Libraries of *E. coli* BL21(DE3) Expressing β -lactamases

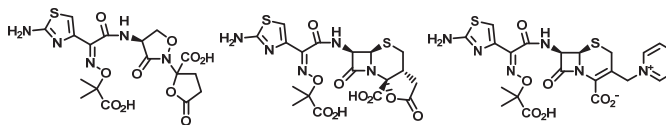
β -lactamase expressed (Ambler classification)	1	2a	3 Ceftazidime (CAZ)
/pET9a (empty vector)	0.063	0.5	0.063
/pET9a::CTX-M-15 (class A)	0.063	0.5	0.25
/pET9a::NDM-1 (class B)	0.25	0.5	>16
/pET9a::AmpC (class C)	2	1	0.25
/pET9a::OXA-48 (class D)	0.063	0.5	0.063

E. coli BL21(DE3) was used as a host strain and the strains transformed by each of the seven β -lactamases carrying pET9a plasmids were used.¹² Ceftazidime **3** as a cephalosporin control was susceptible to the recombinant strains producing CTX-M-15 (class A β -lactamase), NDM-1 (class B β -lactamase) and AmpC (class C β -lactamase). The ratios of MIC values against the β -lactamase-producing strain/host strain for LTV

derivative **1** was 4-fold for the NDM-1 producer and 32-fold for the AmpC producer. On the other hand, the ratios of MIC values for the tricyclic β -lactam derivative **2a** was less than 2-fold for all the tested strains. These results suggest that this tricyclic β -lactam derivative **2a** has an advantage over the LTV derivative **1** regarding class B and C β -lactamase susceptibility in this panel.

Next, the antibacterial activities of these compounds against clinical isolates were evaluated to investigate how the antibacterial activities against β -lactamase-producing *E. coli* recombinant strains were transferred to the clinical isolates (Table 2-2).

Table 2-2. *In Vitro* Antibacterial Activities (MIC, $\mu\text{g}/\text{mL}$) of Clinical Isolates

Strain	Phenotype (Ambler classification)			
		1	2a	3 Ceftazidime
<i>E. coli</i> NIHJ JC-2	Susceptible	0.25	0.5	0.25
<i>E. coli</i> SR34100	CTX-M-15 (class A)	4	1	>32
<i>E. cloacae</i> SR01875	NDM-1 (class B)	1	0.5	>32
<i>E. cloacae</i> SR36276	AmpC (class C)	>32	16	>32
<i>K. pneumoniae</i> SR08787 OXA-48 (class D)		1	2	1

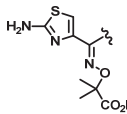
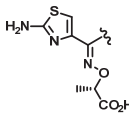
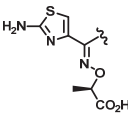
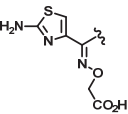
Although compound **1** showed potent activity against the CTX-M-15 producer in the evaluation of *E. coli* recombinant strains, it showed a high MIC value for the clinically isolated *E. coli* SR34100 (CTX-M-15 producer).

In contrast, compound **2a** exhibited moderate activity against *E. coli* SR34100 reflecting the result of the susceptibility to the recombinant strain. However, compound **2a** did not show potent activity against *Enterobacter cloacae* SR36276 (AmpC producer), although it had been shown to have potent activity against an AmpC producer in the evaluation of *E. coli* recombinant strains. These results might have occurred because the transformants

were not developed to match the wild type expression levels of β -lactamases, but they do indicate that the tricyclic β -lactam derivative **2a** has good activity against class A, B and D β -lactamase producers but not the class C β -lactamase producer. As there are multiple β -lactamase producers, including class C β -lactamase in CRE, this prompted the pursuit of the search for a novel tricyclic β -lactam that could overcome class C β -lactamase producers while maintaining activities against other classes of β -lactamase producers.

First, the aminothiazole side chains were converted to improve antibacterial activity against class C β -lactamase producers, because aminothiazole side chains have been reported to affect antibacterial activities against class C β -lactamase producers in cephalosporins.¹³

Table 2-3. *In Vitro* Antibacterial Activities (MIC, $\mu\text{g/mL}$) of Compounds **2a–g**

Strain	Phenotype (Ambler classification)	R=			
					
<i>E. coli</i> NIHJ JC-2	Susceptible	0.5	0.125	0.125	0.063
<i>E. coli</i> SR34100	CTX-M-15 (class A)	1	0.5	0.5	0.25
<i>K. pneumoniae</i> SR01343	KPC-2 (class A)	1	0.25	0.5	0.125
<i>E. cloacae</i> SR01875	NDM-1 (class B)	0.5	0.25	0.25	0.125
<i>E. cloacae</i> SR36276	AmpC (class C)	16	16	16	8
<i>K. pneumoniae</i> SR08787	OXA-48 (class D)	2	0.5	1	1

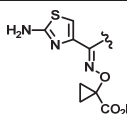
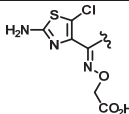
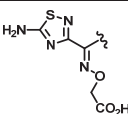
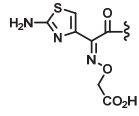
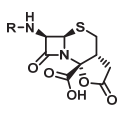
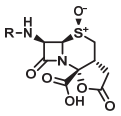
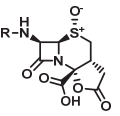
Strain	Phenotype (Ambler classification)	R=		
				
<i>E. coli</i> NIHJ JC-2	Susceptible	0.125	1	0.125
<i>E. coli</i> SR34100	CTX-M-15 (class A)	0.25	4	0.25
<i>K. pneumoniae</i> SR01343	KPC-2 (class A)	0.5	4	0.125
<i>E. cloacae</i> SR01875	NDM-1 (class B)	0.25	2	0.5
<i>E. cloacae</i> SR36276	AmpC (class C)	8	8	4
<i>K. pneumoniae</i> SR08787	OXA-48 (class D)	1	16	1

Table 2-3 shows the effect of various aminothiazole side chains on MICs of tricyclic β -lactam derivatives. The antibacterial activities of mono-methyl substituted **2b** and **2c** against all tested strains, except *E. cloacae* SR36276 (AmpC producer), were better than those of **2a**. The antibacterial activities of **2d**, which has no substituents at the α -position of the carboxyl group, were tested against several strains and found to be superior to **2a–c**, but the activity against *E. cloacae* SR36276 was only slightly improved. A cyclopropyl group was introduced at the α -position (**2e**) in anticipation of a further improvement of the antibacterial activity against *E. cloacae* SR36276, but unfortunately none was noted. Compound **2f** substituted with chloroaminothiazole unexpectedly did not show improvement in antibacterial activity against *E. cloacae* SR36276 although this modification had been reported to be effective in improving activity against class C β -lactamase producers in the case of cephalosporins. Comparing **2g** with **2d**, which was converted from aminothiazole to aminothiadiazole, showed that the antibacterial activity against *E. cloacae* SR36276 (AmpC producer) was slightly improved, but the antibacterial activity against *E. cloacae* SR01875 (NDM-1 producer) was significantly decreased. By converting the aminothiazole side chains, compound **2d** was found to exhibit potent antibacterial activities against the tested strains except for *E. cloacae* SR36276 (AmpC producer). However, unlike the case of cephalosporins, the antibacterial activity against AmpC (class C β -lactamase) producer could not be improved.

Next, conversions of the cepham ring, a characteristic of tricyclic β -lactams were tried. Oxidation of the sulfur at the C-1 position, a transformation known for cephalosporins was attempted (Table 2-4). Fortunately, stereoselective oxidation of sulfur to sulfoxide greatly improved the activity against *E. cloacae* SR36276 (AmpC producer) (**16d**). Compound **16d** overcame the AmpC producer while maintaining activities against class

A, B and D β -lactamase producers and had the desired properties. Further oxidation of the sulfoxide to sulfone resulted in a slight loss of antibacterial activities (**17d**), but compound **17d** still retained better antibacterial activity against *E. cloacae* SR36276 than compound **2d**.

Table 2-4. *In Vitro* Antibacterial Activities (MIC, $\mu\text{g/mL}$) of Compounds **2d** and **16d**–**17d**

Strain	Phenotype (Ambler classification)	R=			
					
		2d	16d	16d'	17d
<i>E. coli</i> NIHJJC-2	Susceptible	0.063	0.063	0.25	0.25
<i>E. coli</i> SR34100	CTX-M-15 (class A)	0.25	0.125	1	1
<i>K. pneumoniae</i> SR01343	KPC-2 (class A)	0.125	0.063	0.5	0.5
<i>E. cloacae</i> SR01875	NDM-1 (class B)	0.125	0.063	2	0.25
<i>E. cloacae</i> SR36276	AmpC (class C)	8	0.063	>32	1
<i>K. pneumoniae</i> SR08787	OXA-48 (class D)	1	0.25	0.5	0.5

II-4. Molecular Modelling for Tricyclic β -lactam

He considered that the improvement of antibacterial activities by conversion of sulfide to sulfoxide **16d** and sulfone **17d** might be associated with interactions between the tricyclic β -lactams and AmpC.¹⁴ The carboxylic acid and the amide moiety are known to interact with key amino acids located at the surface of the active site for β -lactamase protein, such as an interaction between Cephalothin and AmpC (Figure 2-3).¹⁵

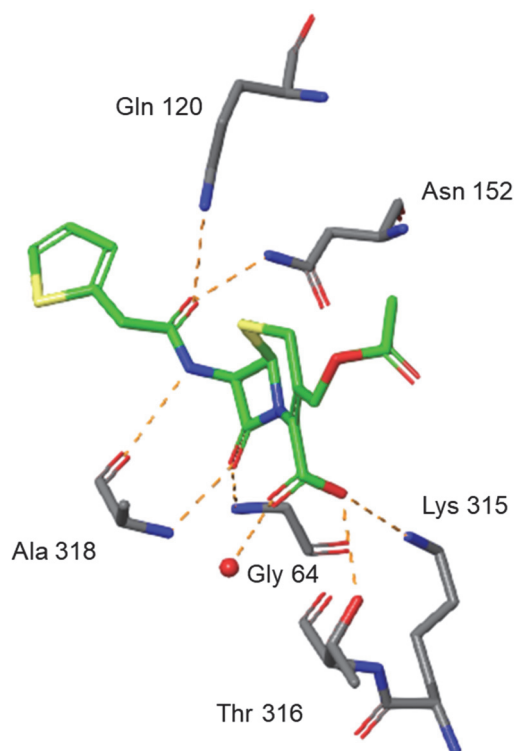


Figure 2-3. Key Interactions Observed between Cephalothin and AmpC(S64G) from X-ray Crystal Structure (1KVL)¹⁵

Therefore, in order to verify the effect of these conversions on the amide moiety and carboxylic acid, the respective energetically stable conformations of these compounds were calculated. The calculation for the aminothiazole side chain was performed for a simple acetyl group in order to focus on the conformational difference around the scaffolds. Conformational searches were carried out using the standard conditions of the Schrödinger Macromodel version 12.1.¹⁶ The calculation results showed that an intramolecular hydrogen bond was formed between the amide moiety and the sulfoxide (**16d-Ac**) or sulfone (**17d-Ac**), whereas the orientation of the amide moiety was significantly different from the others (Figure 2-4).

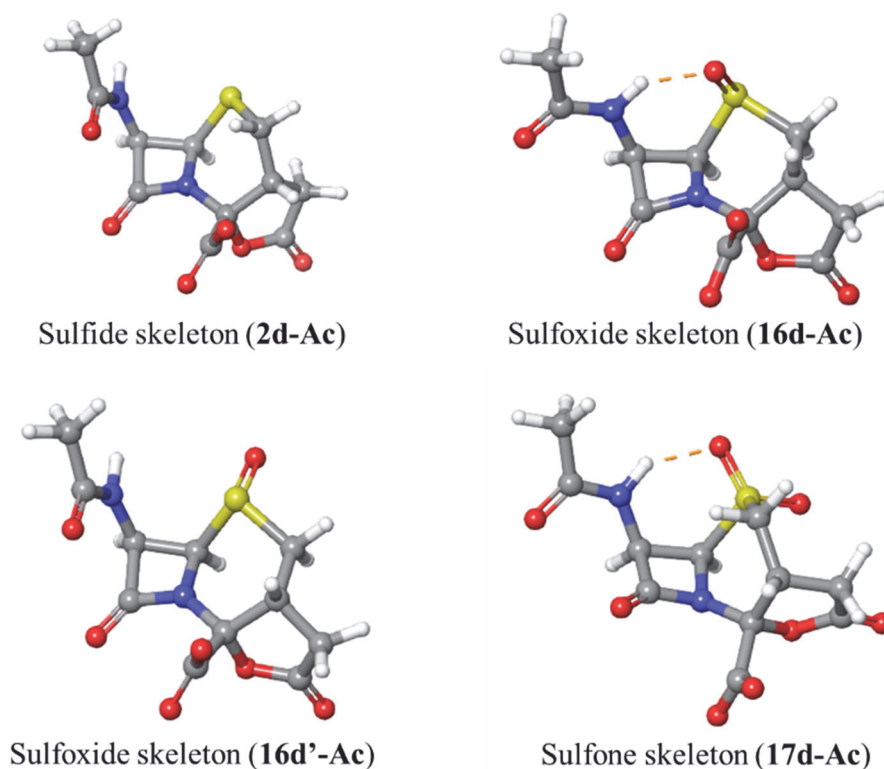


Figure 2-4. Most Stable Conformations and Intramolecular Hydrogen Bonds of the Sulfide, Sulfoxide, and Sulfone Skeletons

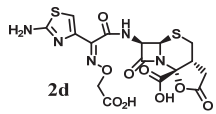
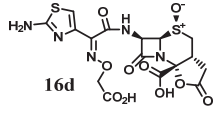
These results suggest that the formation of an intramolecular hydrogen bond could prevent the interaction of the amide moiety with Gln 120, Asn 152, and Ala 318, consequently reducing the affinity between **16d** or **17d** and AmpC and thus improving the activity against *E. cloacae* SR36276.

II-5. Affinity of Tricyclic β -lactam to Class C β -lactamase

To verify this hypothesis that the formation of the intramolecular hydrogen bond caused by oxidation to sulfoxide reduced the affinity for AmpC, an enzymatic assay was performed on compound **16d** which showed very potent antibacterial activity against

AmpC producers, and compound **2d** for comparison (Table 2-5).

Table 2-5. Affinity for CMY-2 and *In Vitro* Antibacterial Activities (MIC, $\mu\text{g/mL}$) of Compounds **2d** and **16d**

	<i>K_i</i> (μM)	MIC ($\mu\text{g/mL}$)	
	CMY-2 (class C)	<i>K. pneumoniae</i> ATCC13883 (susceptible)	<i>E. cloacae</i> SR36276 AmpC (classC)
 2d	0.4	0.125	8
 16d	>60	0.125	0.25

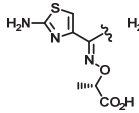
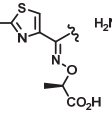
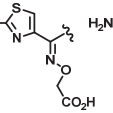
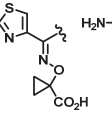
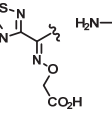
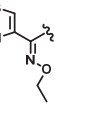
The affinity of compounds **2d** and **16d** for CMY-2 (Class C β -lactamase)¹⁷ is estimated from the apparent inhibition constant (*K_i*) of nitrocefin hydrolysis.¹⁸ Since the *K_i* of **16d** is much larger than that of **2d**, **16d** is less readily recognized by CMY-2 than **2d** and thus escapes hydrolysis by CMY-2. While **16d** avoids hydrolysis by CMY-2, **16d** still has a potent antibacterial activity with the MIC of 0.125 $\mu\text{g/mL}$ against *Klebsiella pneumoniae* ATCC13883, which is almost the same MICs of **2d** and CAZ **3** (0.125 and 0.25 $\mu\text{g/mL}$, respectively). These results suggest that the avoidance of hydrolysis by Class C β -lactamase while maintaining potent antibacterial activity is the main reason for the improved antibacterial activity of **16d** against *E. cloacae* SR36276 (Class C β -lactamase producer).

II-6. Structure-Activity Relationship of Sulfoxide-Introduced Tricyclic β -lactam

Since the antibacterial activity against class C β -lactamase producers was improved by introducing a sulfoxide, he applied a sulfoxide to compounds **2b–e**, **g**, which exhibited

antibacterial activities similar to those of **2d** against four β -lactamase-producers except the class C β -lactamase producer in Table 2-3. This was done in order to identify the best molecule in the series (Table 2-6).

Table 2-6. *In Vitro* Antibacterial Activities (MIC, $\mu\text{g/mL}$) of Compounds **16b–e, g,** and **h**

Strain	Phenotype (Ambler classification)	R=					
							
<i>E. coli</i> NIHJ JC-2	Susceptible	0.25	0.125	0.063	0.25	1	0.25
<i>E. coli</i> SR34100	CTX-M-15 (class A)	1	0.5	0.125	0.5	8	0.5
<i>K. pneumoniae</i> SR01343	KPC-2 (class A)	0.5	0.25	0.063	0.5	1	0.5
<i>E. cloacae</i> SR01875	NDM-1 (class B)	0.5	0.125	0.063	0.25	2	0.5
<i>E. cloacae</i> SR36276	AmpC (class C)	0.25	0.25	0.063	0.25	1	1
<i>K. pneumoniae</i> SR08787	OXA-48 (class D)	1	0.5	0.25	0.5	4	4

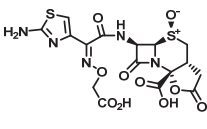
Among the compounds **16b–e**, compound **16d** still showed the most potent activities transferred after the boost by the sulfoxide. Unfortunately, the antibacterial activities of compound **16g**, which was converted from an aminothiazole to an aminothiadiazole, were significantly decreased. Cephalosporins having an aminothiazole side chain without a carboxylic acid in the oxime moiety are commonly well known,¹³ but this time the antibacterial activity of the corresponding sulfoxide derivative (**16h**) was not very potent. These results indicate that the effect on antibacterial activities by introduction of a sulfoxide depends on the side chains, with the carboxyl group being significant.

II-7. Evaluation of *In vitro* Antibacterial Activity

As compound **16d** exhibited potent antibacterial activities against all tested β -lactamase producers without BLI, its antibacterial activities were compared with those of known

BL/BLI (Table 2-7).

Table 2-7. *In Vitro* Antibacterial Activities (MIC, $\mu\text{g/mL}$) of Compounds **16d** and Known BL/BLIs

Strain	Phenotype (Ambler classification)	 16d	CAZ (3)	MER (5)	ATM (18)
			+ AVI (4 , 4 $\mu\text{g/mL}$)	+ VAB (6 , 8 $\mu\text{g/mL}$)	+ AVI (4 , 4 $\mu\text{g/mL}$)
<i>E. coli</i> NIHJ JC-2	Susceptible	0.063	0.25	<0.031	0.125
<i>E. coli</i> SR34100	CTX-M-15 (class A)	0.25	1	<0.031	0.25
<i>K. pneumoniae</i> SR01343	KPC-2 (class A)	0.125	1	<0.031	0.5
<i>E. cloacae</i> SR200039	PER-2 (class A)	0.25	>32	Not tested	>32
<i>E. cloacae</i> SR01875	NDM-1 (class B)	0.125	>32	16	0.25
<i>E. cloacae</i> SR36276	AmpC (class C)	0.125	1	<0.031	1
<i>K. pneumoniae</i> SR08787	OXA-48 (class D)	0.125	0.25	1	0.25

Among them, AVYCAZ® (**3** and **4**) and VABOMERE® (**5** and **6**) showed insufficient activities against PER-2 and NDM-1 producers. Aztreonam/avibactam (ATM **18** and **4**) showed potent activity against the NDM-1 producer but insufficient activity against the PER-2 producer. However, compound **16d** showed potent activities against all tested strains including carbapenemase-producers, indicating that it has potent activities against strains resistant to recently marketed compounds or those under development. To further verify the potential of compound **16d**, expanded panels of clinically isolated carbapenemase-producing strains were tested to compare the antibacterial activities of compound **16d** against KPC-, NDM-, VIM-, and OXA-48-like-producing Enterobacterales to those of BL/BLIs (Table 2-8).

Table 2-8. *In Vitro* Activity Against Various Carbapenemase-Producing Enterobacterales

Enterobacterales organism (Number of strains)	Test compound	MIC ($\mu\text{g/mL}$)		
		Range	MIC ₅₀	MIC ₉₀
KPC-producing strains (14) ^a	Compound 16d	0.25–0.5	0.25	0.5
	CAZ 3 /AVI 4	0.5–>64	4	>64
	ATM 18 /AVI 4	0.25–1	0.5	1
NDM-producing strains (22) ^b	Compound 16d	0.125–1	0.25	1
	CAZ 3 /AVI 4	>64	>64	>64
	ATM 18 /AVI 4	≤ 0.031 –1	0.25	1
VIM-producing strains (25) ^c	Compound 16d	0.125–1	0.25	1
	CAZ 3 /AVI 4	16–>64	>64	>64
	ATM 18 /AVI 4	0.063–2	0.25	2
OXA-48-like-producing strains (12) ^d	Compound 16d	0.063–1	0.125	0.25
	CAZ 3 /AVI 4	0.063–16	0.125	4
	ATM 18 /AVI 4	≤ 0.031 –1	0.063	0.25

a: 12 strains of *K. pneumoniae* and 2 strains of *E. aerogenes* (9 strains of KPC-2 producer and 5 strains of KPC-3 producer).

b: 12 strains of *K. pneumoniae* and 10 strains of *E. cloacae* (19 strains of NDM-1 producer, 2 strains of NDM-6 producer and 1 strain of NDM-7 producer).

c: 10 strains of *E. cloacae*, 5 strains of *K. pneumoniae*, 4 strains of *C. freundii*, 3 strains of *S. marcescens*, 1 strain of *K. oxytoca*, 1 strain of *E. coli*, and 1 strain of *C. amalonaticus* (23 strains of VIM-1 producer, 1 strain of VIM-5 producer, and 1 strain of VIM-19 producer).

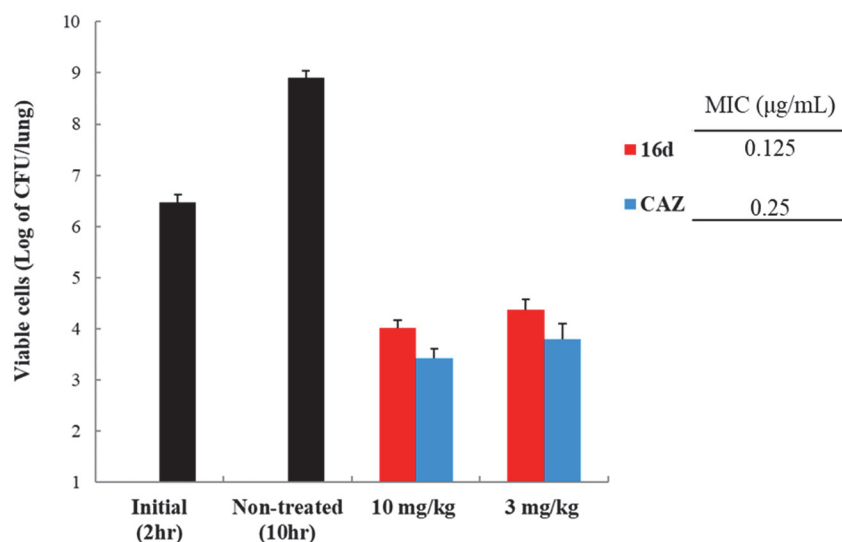
d: 12 strains of *K. pneumoniae*.

Against all four types of carbapenemase-producing Enterobacterales tested, compound **16d** inhibited the bacterial growth at ≤ 1 $\mu\text{g/mL}$ with the range of $\text{MIC}_{90\text{s}}$ being from 0.125 to 0.25 $\mu\text{g/mL}$, while $\text{MIC}_{90\text{s}}$ of AVYCAZ® (**3** and **4**) were > 64 $\mu\text{g/mL}$ against KPC, NDM and VIM producers and 4 $\mu\text{g/mL}$ against OXA-48-like producers. The range of $\text{MIC}_{90\text{s}}$ for ATM/AVI (**18** and **4**) was from 0.25 to 2 $\mu\text{g/mL}$ against those four sets of carbapenemase-producers, being comparable or slightly inferior to compound **16d**. These results indicate that compound **16d** would offer a superior clinical outcome to those competitors against problematic pathogens such as CRE.

II-8. Evaluation of Therapeutic Efficacy

To verify that **16d** exerts a therapeutic effect that reflects its potent *in vitro* antibacterial activities in clinical use, the therapeutic efficacy of compound **16d** and CAZ **3** as a clinical standard was examined using cyclophosphamide-induced neutropenic mouse model of lung infections (Figure 2-5).

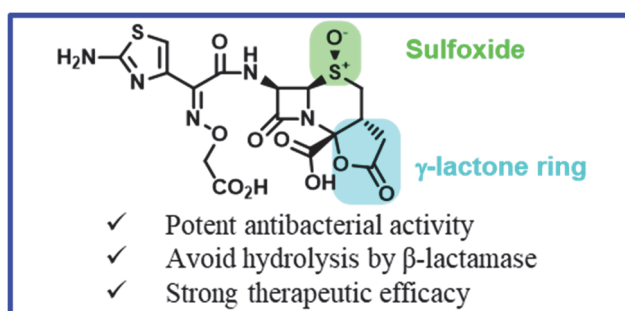
The change in bacterial density was calculated as the difference in \log_{10} CFU from the antibiotic-treated mice after 10 h from the level in the 0 h control animals. The bacterial density increased by 2.44- \log_{10} CFU in control animals at 10 h. Compound **16d** produced a 2.46- \log_{10} CFU reduction at 10 mg/kg and a 2.11- \log_{10} CFU reduction at 3 mg/kg. These results are similar to that of CAZ **3** with 3.05- \log_{10} CFU reduction at 10 mg/kg and 2.67- \log_{10} CFU reduction at 3 mg/kg. This finding indicates that **16d** shows a strong bactericidal effect reflected by its *in vitro* antibacterial activity similar to that of CAZ **3** and consequently **16d** will show sufficient exposure and therapeutic performance in clinical use.



Animal: Jcl:ICR mice, male; neutropenia rendered with cyclophosphamide; n=5.
 Infecting pathogen: *K. pneumoniae* ATCC13883
 Infection: intra-nasal inoculation with 5% gastric mucin (2×10^6 CFU/mouse).
 Administration: subcutaneous injection 2, 5 and 8 hours after infection.
 Evaluation: viable bacteria in lungs 10 hours after infection

Figure 2-5. Therapeutic Efficacy in Neutropenic Mouse Lung Infection Model

II-9. Conclusion



Starting from a reported tricyclic β -lactam including a γ -lactone ring (**2a**), the author succeeded in obtaining a novel scaffold which shows potent antibacterial activity against class C β -lactamase producers while maintaining antibacterial activities against class A, B and D β -lactamase producers. Introduction of a sulfoxide to the core structure containing a γ -lactone ring was the key to obtaining potent antibacterial activities against

several problematic β -lactamase producers without BLI. He identified the novel tricyclic β -lactam **16d** that shows potent activities against Enterobacterales including CREs as well as strains resistant to BL/BLIs on the market or under development. Evaluation of antibacterial activities against clinical isolates shows that **16d** exhibited lower MIC₉₀ values than those of the already approved BL/BLI and also shows a potent therapeutic efficacy in the neutropenic mouse lung infection model. These results demonstrate that the reported tricyclic β -lactam scaffold deserves further study in the search for new antimicrobial agents against CREs.

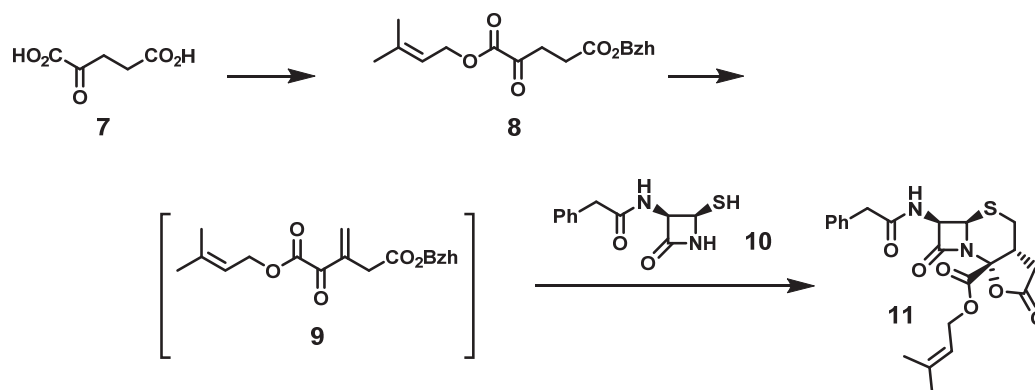
Experimental

Unless otherwise noted, reactions were performed under a nitrogen atmosphere. Solvents and commercial reagents were used without purification. Ceftazidime **3**, Aztreonam **18** and compound **7** were purchased from Tokyo Chemical Industry Co., Ltd. Avibactam **4** was purchased from Shanghai Haoyuan Chemexpress Co., Ltd. Meropenem **5** was purchased from FUJIFILM Wako Pure Chemical Corporation. Vaborbactam **6** was purchased from MedChemExpress LLC. The synthesis of compound **12a**, **12b**, and **12f** has been already reported.¹³ Compound **1**,⁷ **10**,^{9,19} **12c**,²⁰ **12d**,²¹ **12e**,²² **12g**,²³ and **12h**²⁴ were synthesized by the reported method. ¹H and ¹³C NMR spectra were recorded on a Bruker AV400 spectrometer. Chemical shifts (δ) are reported in parts per million (ppm) from tetramethylsilane (in CDCl₃ and DMSO-*d*₆), sodium 2,2-dimethyl-2-silapentane-5-sulfonate (in D₂O) or the solvent residual peak (in DMSO-*d*₆ δ 2.50 and D₂O δ 4.79) as an internal reference. Analytical thin-layer chromatography was run on silica gel F254 precoated plates. Visualization of the developed chromatogram was done using fluorescence quenching or Vaughn's reagent. Flash column chromatography was

carried out on an automated purification system using Yamazen or Fuji Silysia prepacked silica gel columns. Reverse phase column chromatography was performed using HP20SS and octadecylsilyl silica gel (Yamazen Ultra Pack). High-resolution mass spectral data were acquired on Orbitrap Q Exactive Plus (ESI). Low-resolution mass spectral data were collected on a Waters ZQ mass detector (ESI), a Shimadzu LCMS-8030 (ESI), or a Shimadzu LCMS-2020 (ESI). Elemental analysis was performed using a Micro Corder JM11 (J-Science Lab Co., Ltd.) analyzer.

All studies with animals were approved by the Institutional Animal Care and Use Committee of Shionogi & Co., Ltd.

Synthesis of key intermediate 11



Step1. Synthesis of 5-benzhydryl 1-(3-methylbut-2-en-1-yl) 2-oxopentanedioate (8)

A solution of compound 7 (43.8 g, 300 mmol) in DMF (307 mL) was warmed to 60 °C. Dicyclohexylamine (59.6 mL, 300 mmol) and 1-bromo-3-methyl-2-butene (38.1 mL, 300 mmol) were added to the solution. The mixture was stirred at 60 °C for 1 h. The precipitates were removed by filtration. Water was added to the filtrate, followed by extraction with ethyl acetate. The organic layer was washed with water and brine in this order and then dried over anhydrous magnesium sulfate. The solvent was evaporated

under reduced pressure. Under ice cooling, diphenyldiazomethane (64.1 g, 330 mmol) was added to a solution of the obtained residue in tetrahydrofuran (321 mL). The mixture was stirred at room temperature for 7 h. The mixture was left standing at room temperature for 2 days. Next, the solvent was evaporated under reduced pressure. The obtained crude product was purified by silica gel column chromatography (hexane–ethyl acetate) to afford compound **8** (104 g, yield 91%).

^1H NMR (400 MHz, CDCl_3): δ 7.33–7.27 (10H, m), 6.87 (1H, s), 5.40–5.35 (1H, m), 4.73 (2H, d, $J = 7.5$ Hz), 3.18 (2H, t, $J = 6.5$ Hz), 2.78 (2H, t, $J = 6.5$ Hz), 1.76 (3H, s), 1.73 (3H, d, $J = 0.6$ Hz).

^{13}C NMR $\{^1\text{H}\}$ (100 MHz, CDCl_3): δ 192.5, 171.1, 160.5, 141.0, 139.9, 128.5, 128.0, 127.1, 117.3, 77.5, 63.3, 34.3, 27.8, 25.8, 18.1.

MS (ESI) m/z : $[\text{M} + \text{H}_2\text{O} + \text{H}]^+$ calcd for $\text{C}_{23}\text{H}_{27}\text{O}_6$ 399; found 399.

Step 2. Synthesis of 5-benzhydryl 1-(3-methylbut-2-en-1-yl) 3-methylene-2-oxopentanedioate (9)

To a solution of compound **8** (104 g, 273 mmol) in dichloromethane (520 mL), N,N,N',N' -tetramethyldiaminomethane (149 mL, 1093 mmol) was added. Under ice cooling, acetic anhydride (129 mL, 1367 mL) and acetic acid (109 mL, 1914 mmol) were added to the mixture, which was stirred at room temperature for 1 h. Next, the solvent was evaporated under reduced pressure and water was added to the residue, followed by extraction with ethyl acetate. The organic layer was washed with water and then dried

over anhydrous magnesium sulfate. The solvent was evaporated under reduced pressure. The obtained residue was purified by column chromatography (hexane–ethyl acetate) to afford compound **9** (79 g, 74%) as a crude mixture. **9** was used in the next step without further purification.

MS (ESI) m/z : $[M + H_2O + H]^+$ calcd for $C_{24}H_{27}O_6$ 411; found 411.

Step 3. Synthesis of 3-methylbut-2-en-1-yl (3aR,5aR,6R,8aR)-2,7-dioxo-6-(2-phenylacetamido)hexahydro-7H,8aH-azeto[2,1-b]furo[2,3-d][1,3]thiazine-8a-carboxylate (11)

To a solution of compound **9** (10.0 g, 25.5 mmol) in acetone (100 mL), compound **10** (6.02 g, 25.5 mmol) and hexamethylphosphoric triamide (15.5 mL, 89 mmol) were added. The mixture was stirred at room temperature for 1 h. Water was added to the mixture, followed by extraction with ethyl acetate. The organic layer was washed with water and brine in this order and then dried over anhydrous magnesium sulfate. The solvent was evaporated under reduced pressure. The obtained residue was purified by column chromatography (hexane–ethyl acetate) to afford the crude intermediate (2.1 g).

Under nitrogen atmosphere, a solution of the crude intermediate (6.80 g, 10.8 mmol) in dichloromethane (34 mL) was cooled to $-10\text{ }^\circ\text{C}$. A solution of TFA (34 mL, 441 mmol) in dichloromethane (34 mL) was added dropwise to the solution. The mixture was stirred at $-10\text{ }^\circ\text{C}$ for 30 min. Water was added to the reaction mixture, followed by extraction with dichloromethane. The organic layer was washed with water and brine in this order and then dried over anhydrous magnesium sulfate. The solvent was evaporated. A solution of the obtained residue in dichloromethane (50 mL) was cooled to $0\text{ }^\circ\text{C}$. EDC

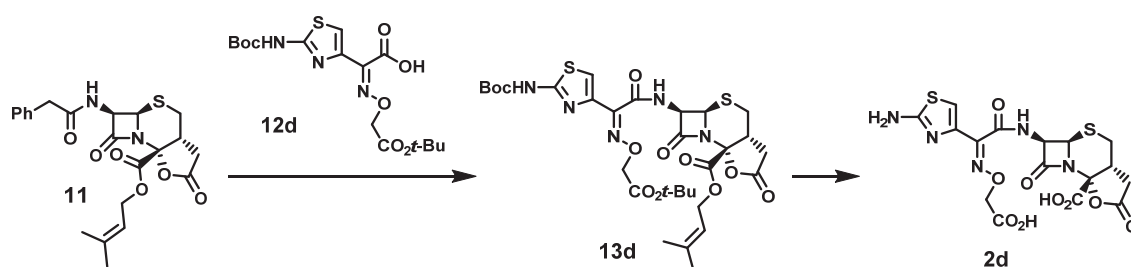
hydrochloride (4.15 g, 21.6 mmol) was added to the solution. The mixture was stirred at room temperature for 1 h. Water was added to the mixture, followed by extraction with dichloromethane. The organic layer was washed with dilute hydrochloric acid and brine in this order and then dried over anhydrous magnesium sulfate. The solvent was evaporated under reduced pressure. The obtained residue was purified by column chromatography (hexane–ethyl acetate) to afford compound **11** (4.0 g, 83%).

^1H NMR (400 MHz, CDCl_3): δ 7.39–7.26 (5H, m), 6.20 (1H, d, $J = 8.8$ Hz), 5.53 (1H, dd, $J = 8.8, 4.7$ Hz), 5.36 (1H, t, $J = 7.4$ Hz), 4.97 (1H, d, $J = 4.7$ Hz), 4.83–4.73 (2H, m), 3.67 (1H, d, $J = 16.2$ Hz), 3.62 (1H, d, $J = 16.2$ Hz), 3.25–3.19 (1H, m), 2.95 (1H, dd, $J = 14.4, 4.4$ Hz), 2.75 (1H, dd, $J = 18.1, 8.3$ Hz), 2.67–2.60 (2H, m), 1.77 (3H, s), 1.71 (3H, s).

^{13}C NMR $\{^1\text{H}\}$ (100 MHz, CDCl_3): δ 171.5, 171.0, 164.7, 163.8, 141.3, 133.7, 129.5, 129.2, 127.7, 116.9, 86.9, 64.8, 60.2, 55.9, 43.3, 35.3, 33.0, 26.9, 25.8, 18.1.

MS (ESI) m/z : $[\text{M} + \text{H}]^+$ calcd for $\text{C}_{22}\text{H}_{25}\text{N}_2\text{O}_6\text{S}$ 445; found 445.

Synthesis of compound **2d**



Step 1. Synthesis of 3-methylbut-2-en-1-yl (3aR,5aR,6R,8aR)-6-((Z)-2-((2-(tert-butoxy)-2-oxoethoxy)imino)-2-(2-((tert-butoxycarbonyl)amino)thiazol-4-yl)acetamido)-2,7-dioxohexahydro-7H,8aH-azeto[2,1-b]furo[2,3-d][1,3]thiazine-8a-carboxylate (13d)

A suspension of phosphorus pentachloride (1.25 g, 6.00 mmol) in dichloromethane (13.3 mL) was cooled to $-40\text{ }^{\circ}\text{C}$. Next, pyridine (0.969 mL, 12.0 mmol) was added, and subsequently, compound **11** (1.33 g, 3.00 mmol) was added to the suspension. Under ice cooling, the mixture was stirred for 1 h. This mixture was then cooled to $-78\text{ }^{\circ}\text{C}$ and ethanol (13.3 mL) was added. After stirring at $-30\text{ }^{\circ}\text{C}$ for 30 min, an aqueous solution of sodium hydrogen carbonate was added to the reaction mixture, followed by extraction with dichloromethane. The organic layer was washed with water and brine in this order and dried over magnesium sulfate. Inorganic matter was removed by filtration. Next, the filtrate was concentrated to approximately 10 mL under reduced pressure to afford a dichloromethane solution (solution A). A solution of compound **12d** (682 mg, 1.70 mmol) in DMA (4.9 mL) was cooled to $-20\text{ }^{\circ}\text{C}$. Next, triethylamine (0.291 mL, 2.10 mmol) and methanesulfonyl chloride (0.148 mL, 1.90 mmol) were added to the solution. The mixture was stirred at $-20\text{ }^{\circ}\text{C}$ for 1 h to afford solution B.

Dichloromethane (5 mL) was added to half the amount of solution A (approximately 5 mL, corresponding to 1.50 mmol). Under ice cooling, pyridine (0.121 mL, 1.50 mmol) and solution B were added to the mixture. Under ice cooling, the mixture was stirred for 1 h. Next, an aqueous solution of dilute hydrochloric acid was added to the mixture, followed by extraction with ethyl acetate. The organic layer was washed with a saturated aqueous solution of sodium bicarbonate, water, and brine in this order and dried over anhydrous magnesium sulfate, which was subsequently filtered off. The filtrate was

concentrated under reduced pressure, and the residue was subjected to silica gel column chromatography, followed by elution with hexane–ethyl acetate. Fractions containing the desired compound were concentrated under reduced pressure to afford compound **13d** (0.44 g, yield 41%) as a crude mixture. **13d** was used in the next step without further purification.

MS (ESI) m/z : $[M + H]^+$ calcd for $C_{30}H_{40}N_5O_{11}S_2$ 710; found 710.

Step 2. Synthesis of (3*aR*,5*aR*,6*R*,8*aR*)-6-((*Z*)-2-(2-aminothiazol-4-yl)-2-((carboxymethoxy)imino)acetamido)-2,7-dioxohexahydro-7*H*,8*aH*-azeto[2,1-*b*]furo[2,3-*d*][1,3]thiazine-8*a*-carboxylic acid (2d**)**

Compound **13d** (0.24 g, 0.298 mmol) was dissolved in dichloromethane (2.4 mL) followed by cooling to $-40\text{ }^\circ\text{C}$. Next, anisole (0.26 mL, 2.39 mmol) and a 2 mol/L solution of aluminum chloride in nitromethane (1.19 mL, 2.39 mmol) were added in this order to the solution. The mixture was stirred at $0\text{ }^\circ\text{C}$ for 20 min. The reaction mixture was dissolved in water, 2 mol/L hydrochloric acid, and acetonitrile. This solution was washed with diisopropyl ether. HP20SS resin was added to the aqueous layer. Acetonitrile was evaporated under reduced pressure. The obtained mixed solution was subjected to HP20SS column chromatography, followed by elution with water–acetonitrile. Fractions containing the desired compounds were concentrated under reduced pressure. The residue was freeze-dried to afford compound **2d** (0.05 g, yield 35%) as a white powder.

^1H NMR (400 MHz, D_2O): δ 7.22 (1H, s), 5.57 (1H, d, $J = 4.5$ Hz), 5.27 (1H, d, $J = 4.5$ Hz), 3.18–3.11 (2H, m), 2.94–2.80 (2H, m), 2.72 (1H, d, $J = 18.4$ Hz).

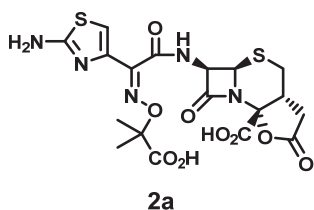
^{13}C NMR $\{^1\text{H}\}$ (100 MHz, D_2O): δ 179.8, 177.7, 173.7, 172.4, 166.4, 164.9, 147.6, 135.3, 115.5, 91.7, 75.2, 62.9, 59.2, 39.6, 36.2, 29.8.

Anal.: $\text{C}_{16}\text{H}_{15}\text{N}_5\text{O}_9\text{S}_2(\text{H}_2\text{O})_{2.6}$.

Calc.: C, 36.1; H, 3.8; N, 13.2; S, 12.05 (%).

Found: C, 36.0; H, 3.8; N, 13.4; S, 11.9 (%).

Compounds **2a–c**, **e–g** were prepared from compound **11** and compounds **12a–c**, **e–g** by a similar procedure as that described for **2d**.



(3aR,5aR,6R,8aR)-6-((Z)-2-(2-aminothiazol-4-yl)-2-(((2-carboxypropan-2-yl)oxy)imino)acetamido)-2,7-dioxohexahydro-7H,8aH-azeto[2,1-b]furo[2,3-d][1,3]thiazine-8a-carboxylic acid (2a)

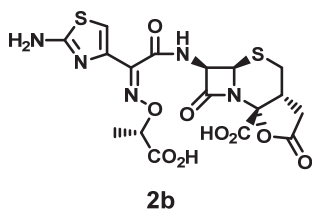
^1H NMR (400 MHz, D_2O): δ 7.04 (1H, s), 5.60 (1H, d, $J = 4.5\text{Hz}$), 5.28 (1H, d, $J = 4.5\text{Hz}$), 3.19–3.15 (2H, m), 2.95–2.84 (2H, m), 2.69 (1H, d, $J = 17.7\text{Hz}$), 1.51 (3H, s), 1.49 (3H, s).

^{13}C NMR $\{^1\text{H}\}$ (100 MHz, $\text{DMSO}-d_6$): δ 174.8, 173.0, 168.4, 166.1, 162.8, 162.7, 149.3, 142.6, 109.7, 86.1, 81.6, 59.6, 55.9, 35.6, 32.6, 26.5, 24.1, 23.8.

Anal.: C₁₈H₁₉N₅O₉S₂(H₂O)_{4.2}.

Calc.: C, 36.7; H, 4.7; N, 11.9; S, 10.9 (%).

Found: C, 36.6; H, 4.4; N, 12.1; S, 10.6 (%).



(3aR,5aR,6R,8aR)-6-((Z)-2-(2-aminothiazol-4-yl)-2-(((S)-1-carboxyethoxy)imino)acetamido)-2,7-dioxohexahydro-7H,8aH-azeto[2,1-b]furo[2,3-d][1,3]thiazine-8a-carboxylic acid (2b)

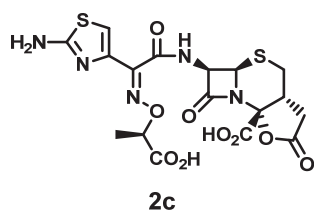
¹H NMR (400 MHz, D₂O): δ 7.18 (1H, s), 5.59 (1H, d, *J* = 4.5 Hz), 5.28 (1H, d, *J* = 4.5 Hz), 4.82 (1H, d, *J* = 6.8 Hz), 3.19–3.10 (2H, m), 2.94–2.81 (2H, m), 2.71 (1H, d, *J* = 18.7 Hz), 1.51 (3H, d, *J* = 7.1 Hz).

¹³C NMR {¹H} (Na salt) (100 MHz, D₂O): δ 183.3, 179.8, 173.7, 172.3, 167.7, 166.6, 150.6, 143.5, 116.2, 91.8, 84.1, 62.5, 59.3, 39.4, 36.3, 29.8, 19.6.

Anal.: C₁₇H₁₇N₅O₉S₂(H₂O)_{3.1}.

Calc.: C, 36.8; H, 4.2; N, 12.6; S, 11.55 (%).

Found: C, 36.65; H, 4.1; N, 12.9; S, 11.4 (%).



(3aR,5aR,6R,8aR)-6-((Z)-2-(2-aminothiazol-4-yl)-2-(((R)-1-carboxyethoxy)imino)acetamido)-2,7-dioxohexahydro-7H,8aH-azeto[2,1-b]furo[2,3-d][1,3]thiazine-8a-carboxylic acid (2c)

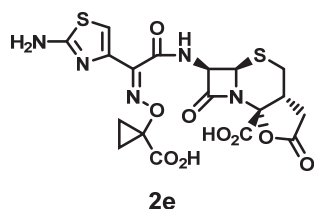
^1H NMR (400 MHz, D_2O): δ 7.18 (1H, s), 5.57 (1H, d, $J = 4.5$ Hz), 5.27 (1H, d, $J = 4.5$ Hz), 3.19–3.12 (2H, m), 2.94–2.80 (2H, m), 2.71 (1H, d, $J = 18.4$ Hz), 1.51 (3H, d, $J = 7.1$ Hz).

^{13}C NMR $\{^1\text{H}\}$ (Na salt) (100 MHz, D_2O): δ 183.2, 179.8, 173.7, 172.3, 167.7, 166.6, 150.6, 143.3, 116.2, 91.8, 84.1, 62.7, 59.5, 39.4, 36.3, 29.8, 19.7.

Anal.: $\text{C}_{17}\text{H}_{17}\text{N}_5\text{O}_9\text{S}_2(\text{H}_2\text{O})_3$.

Calc.: C, 36.9; H, 4.2; N, 12.65; S, 11.6 (%).

Found: C, 36.8; H, 4.0; N, 12.7; S, 11.5 (%).



(3aR,5aR,6R,8aR)-6-((Z)-2-(2-aminothiazol-4-yl)-2-(((1R)-1-carboxycyclopropoxy)imino)acetamido)-2,7-dioxohexahydro-7H,8aH-azeto[2,1-b]furo[2,3-d][1,3]thiazine-8a-carboxylic acid (2e)

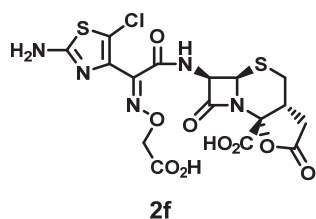
^1H NMR (Na salt) (400 MHz, D_2O): δ 7.11 (1H, s), 5.58 (1H, d, $J = 4.6$ Hz), 5.27 (1H, d, $J = 4.6$ Hz), 3.19–3.12 (2H, m), 2.96–2.80 (2H, m), 2.70 (1H, d, $J = 18.8$ Hz), 1.41–1.26 (4H, m).

^{13}C NMR $\{^1\text{H}\}$ (Na salt) (100 MHz, D_2O): δ 182.6, 179.7, 173.7, 172.4, 167.5, 166.6, 151.7, 143.1, 116.7, 91.8, 68.1, 62.5, 59.5, 39.4, 36.4, 29.8, 18.0.

Anal.: $\text{C}_{18}\text{H}_{15}\text{N}_5\text{Na}_2\text{O}_9\text{S}_2(\text{H}_2\text{O})_2$.

Calc.: C, 36.55; H, 3.2; N, 11.8; Na, 7.8; S, 10.8 (%).

Found: C, 36.4; H, 3.3; N, 12.1; Na, 7.95; S, 10.6 (%).



(3aR,5aR,6R,8aR)-6-((Z)-2-(2-amino-5-chlorothiazol-4-yl)-2-((carboxymethoxy)imino)acetamido)-2,7-dioxohexahydro-7H,8aH-azeto[2,1-b]furo[2,3-d][1,3]thiazine-8a-carboxylic acid (2f)

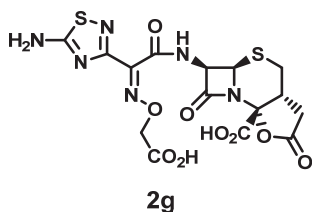
^1H NMR (400 MHz, D_2O): δ 5.63 (1H, d, $J = 4.3$ Hz), 5.27 (1H, d, $J = 4.3$ Hz), 4.66 (2H, s), 3.15–3.07 (2H, m), 2.94–2.79 (2H, m), 2.62 (1H, d, $J = 18.7$ Hz).

^{13}C NMR $\{^1\text{H}\}$ (Na salt) (100 MHz, D_2O): δ 179.8, 179.7, 172.4, 169.8, 166.9, 166.8, 149.7, 137.9, 118.9, 91.7, 76.0, 62.2, 59.6, 39.5, 36.6, 30.0.

Anal.: C₁₆H₁₄ClN₅O₉S₂(H₂O)_{3.3}.

Calc.: C, 33.2; H, 3.6; Cl, 6.1; N, 12.1; S, 11.1 (%).

Found: C, 33.2; H, 3.4; Cl, 6.1; N, 12.2; S, 11.0 (%).



(3aR,5aR,6R,8aR)-6-((Z)-2-(5-amino-1,2,4-thiadiazol-3-yl)-2-

**((carboxymethoxy)imino)acetamido)-2,7-dioxohexahydro-7H,8aH-azeto[2,1-
b]furo[2,3-d][1,3]thiazine-8a-carboxylic acid (2g)**

¹H NMR (400 MHz, D₂O): δ 5.64 (1H, d, *J* = 4.5 Hz), 5.28 (1H, d, *J* = 4.5 Hz), 4.88 (2H, s), 3.19–3.05 (2H, m), 2.94–2.79 (2H, m), 2.64 (1H, d, *J* = 18.2 Hz).

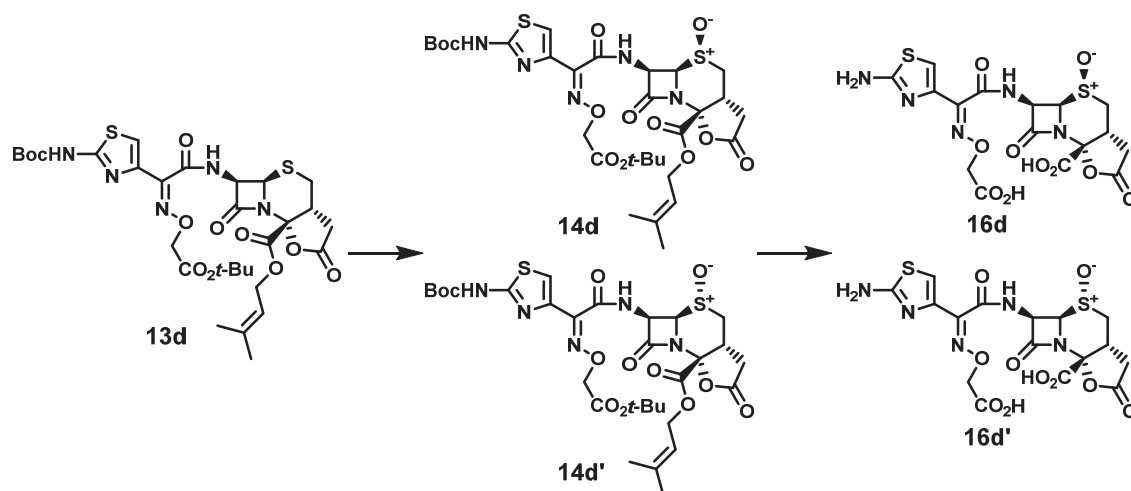
¹³C NMR {¹H} (100 MHz, D₂O): δ 187.5, 179.7, 172.4, 166.7, 166.1, 163.4, 150.7, 119.3, 91.6, 74.5, 62.4, 59.8, 39.6, 36.6, 30.0.

Anal.: C₁₅H₁₄N₆O₉S₂(H₂O)_{4.4}.

Calc.: C, 32.2; H, 4.0; N, 15.0; S, 11.4 (%).

Found: C, 32.25; H, 3.8; N, 14.9; S, 11.2 (%).

Synthesis of compounds 16d and 16d'



Step 1. Synthesis of a mixture of 3-methylbut-2-en-1-yl (3a*R*,5*S*,5a*R*,6*R*,8a*R*)-6-((*Z*)-2-((2-(*tert*-butoxy)-2-oxoethoxy)imino)-2-(2-((*tert*-butoxycarbonyl)amino)thiazol-4-yl)acetamido)-2,7-dioxohexahydro-7*H*,8a*H*-azeto[2,1-*b*]furo[2,3-*d*][1,3]thiazine-8a-carboxylate 5-oxide (14d) and 3-methylbut-2-en-1-yl (3a*R*,5*R*,5a*R*,6*R*,8a*R*)-6-((*Z*)-2-((2-(*tert*-butoxy)-2-oxoethoxy)imino)-2-(2-((*tert*-butoxycarbonyl)amino)thiazol-4-yl)acetamido)-2,7-dioxohexahydro-7*H*,8a*H*-azeto[2,1-*b*]furo[2,3-*d*][1,3]thiazine-8a-carboxylate 5-oxide (14d')

Compound **13d** (0.75 g, 1.06 mmol) was dissolved in acetonitrile (4 mL) and DMA (4 mL). The solution was cooled to $-20\text{ }^{\circ}\text{C}$. Next, 37% peracetic acid solution (0.20 mL, 1.11 mmol) was added to the solution. Under ice cooling, the mixture was stirred for 1 h. The reaction mixture was then separated into aqueous and organic layers by the addition of 10% aqueous solution of sodium sulfite and ethyl acetate. The organic layer was washed with water, a saturated aqueous solution of sodium bicarbonate and brine in this order, and then dried over magnesium sulfate, which was subsequently filtered off. Next, the filtrate was concentrated under reduced pressure. The residue was subjected to silica gel column chromatography, followed by elution with hexane–ethyl acetate. Fractions

containing the desired compound were concentrated under reduced pressure to afford a mixture of compound **14d** + **14d'** (0.64 g, yield 84%) as an isomeric mixture of sulfoxide (5:1).

¹H NMR (400 MHz, CDCl₃): δ 9.18 (0.2H, d, *J* = 7.0 Hz), 8.41 (1.0H, d, *J* = 9.3 Hz), 8.12 (1.0H, s), 7.34 (0.8H, s), 7.32 (0.2H, s), 5.97 (1.0H, dd, *J* = 9.2, 4.8 Hz), 5.39 (1.2H, t, *J* = 7.3 Hz), 5.23–5.20 (0.2H, m), 4.91–4.62 (6.0H, m), 3.81–3.72 (1.0H, m), 3.64 (0.2H, dd, *J* = 14.7, 3.6 Hz), 3.57–3.51 (0.2H, m), 3.42 (1.0H, dd, *J* = 14.5, 5.0 Hz), 3.20 (0.2H, dd, *J* = 14.7, 5.8 Hz), 2.96 (1.0H, dd, *J* = 17.8, 7.7 Hz), 2.86 (0.2H, dd, *J* = 18.5, 9.3 Hz), 2.47–2.38 (2.0H, m), 1.74 (7.2H, t, *J* = 10.0 Hz), 1.54 (10.8H, s), 1.48–1.45 (10.8H, m).

MS (ESI) *m/z*: [M + H]⁺ calcd for C₃₀H₄₀N₅O₁₂S₂ 726; found 726.

Step 2. Synthesis of compounds (3aR,5S,5aR,6R,8aR)-6-((Z)-2-(2-aminothiazol-4-yl)-2-((carboxymethoxy)imino)acetamido)-2,7-dioxohexahydro-7H,8aH-azeto[2,1-b]furo[2,3-d][1,3]thiazine-8a-carboxylic acid 5-oxide (16d) and (3aR,5R,5aR,6R,8aR)-6-((Z)-2-(2-aminothiazol-4-yl)-2-((carboxymethoxy)imino)acetamido)-2,7-dioxohexahydro-7H,8aH-azeto[2,1-b]furo[2,3-d][1,3]thiazine-8a-carboxylic acid 5-oxide (16d')

A mixture of compound **14d** + **14d'** (0.64 g, 0.882 mmol) was dissolved in dichloromethane (10 mL). The solution was cooled to –40 °C, then anisole (1.16 mL, 10.6 mmol) and a 2 mol/L solution of aluminum chloride in nitromethane (5.29 mL, 10.6 mmol) were added in this order. The mixture was stirred at –30 °C for 30 min. The reaction mixture was dissolved in water, 2 mol/L hydrochloric acid, and acetonitrile. This

solution was washed with diisopropyl ether. HP20SS resin was added to the aqueous layer. Acetonitrile was evaporated under reduced pressure. The obtained mixed solution was subjected to HP20SS column chromatography, followed by elution with water–acetonitrile. Fractions containing the desired compounds were concentrated under reduced pressure. The residue was freeze-dried to afford compound **16d** and compound **16d'** as white powders.

Yield amount: compound **16d**: 273 mg (yield 57%).

compound **16d'**: 57.6 mg (yield 12%).

Compound **16d**

^1H NMR (Na salt) (400 MHz, D_2O): δ 7.07 (1H, s), 5.89 (1H, d, $J = 4.8$ Hz), 5.01 (1H, d, $J = 4.8$ Hz), 4.59 (2H, d, $J = 1.1$ Hz), 3.66–3.52 (2H, m), 3.07 (1H, dd, $J = 18.4, 7.8$ Hz), 2.82 (1H, dd, $J = 14.6, 12.6$ Hz), 2.57 (1H, d, $J = 18.4$ Hz).

^{13}C NMR $\{^1\text{H}\}$ (Na salt) (100 MHz, D_2O): δ 179.9, 178.5, 173.8, 171.1, 167.5, 166.2, 150.9, 143.1, 116.2, 90.7, 76.0, 68.3, 62.0, 46.1, 36.7, 32.0.

Anal.: $\text{C}_{16}\text{H}_{15}\text{N}_5\text{O}_{10}\text{S}_2(\text{H}_2\text{O})_{2.3}$.

Calc.: C, 35.4; H, 3.6; N, 12.9; S, 11.8 (%).

Found: C, 35.4; H, 3.6; N, 13.1; S, 11.8 (%).

Compound **16d'**

^1H NMR (400 MHz, $\text{DMSO}-d_6$): δ 9.87 (1H, d, $J = 7.9$ Hz), 7.27 (2H, s), 6.85 (1H, s),

5.59 (1H, dd, $J = 7.9, 4.6$ Hz), 4.90 (1H, d, $J = 4.6$ Hz), 4.58 (2H, s), 3.02–2.87 (2H, m).

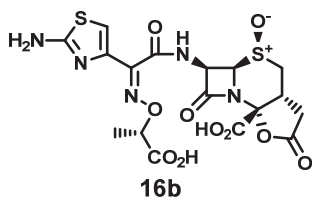
^{13}C NMR $\{^1\text{H}\}$ (100 MHz, DMSO): δ 172.7, 170.7, 168.4, 165.4, 162.7, 161.9, 149.1, 142.2, 110.9, 84.4, 73.6, 70.7, 60.5, 46.7, 37.3, 32.5.

Anal.: $\text{C}_{16}\text{H}_{15}\text{N}_5\text{O}_{10}\text{S}_2(\text{H}_2\text{O})_{2.1}$.

Calc.: C, 35.6; H, 3.6; N, 13.0; S, 11.9 (%).

Found: C, 35.7; H, 3.7; N, 13.2; S, 11.7 (%).

Compounds **16b**, **c**, **e**, **g**, **h** were prepared from compound **13b**, **c**, **e**, **g**, **h** by a procedure similar to that described for **16d**.



(3aR,5S,5aR,6R,8aR)-6-((Z)-2-(2-aminothiazol-4-yl)-2-(((S)-1-carboxyethoxy)imino)acetamido)-2,7-dioxohexahydro-7H,8aH-azeto[2,1-b]furo[2,3-d][1,3]thiazine-8a-carboxylic acid 5-oxide (16b)

^1H NMR (400 MHz, D_2O): δ 7.24 (1H, s), 5.92 (1H, d, $J = 4.8$ Hz), 5.02 (1H, d, $J = 4.8$ Hz), 4.96 (1H, q, $J = 7.2$ Hz), 3.63 (1H, dd, $J = 14.7, 5.2$ Hz), 3.57–3.51 (1H, m), 3.07 (1H, dd, $J = 18.3, 7.8$ Hz), 2.83 (1H, dd, $J = 14.7, 12.5$ Hz), 2.56 (1H, d, $J = 18.3$ Hz), 1.58 (3H, d, $J = 7.2$ Hz).

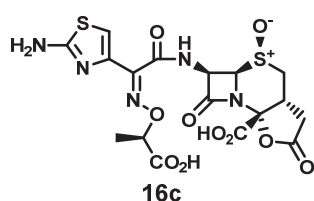
^{13}C NMR $\{^1\text{H}\}$ (100 MHz, D_2O): δ 179.7, 178.5, 173.7, 171.1, 166.2, 164.6, 146.6, 134.2,

115.1, 90.6, 83.1, 68.3, 62.1, 46.1, 36.8, 32.1, 18.9.

Anal.: C₁₇H₁₇N₅O₁₀S₂(H₂O)_{2.5}.

Calc.: C, 36.4; H, 4.0; N, 12.5; S, 11.4 (%).

Found: C, 36.3; H, 3.9; N, 12.6; S, 11.6 (%).



(3aR,5S,5aR,6R,8aR)-6-((Z)-2-(2-aminothiazol-4-yl)-2-(((R)-1-carboxyethoxy)imino)acetamido)-2,7-dioxohexahydro-7H,8aH-azeto[2,1-b]furo[2,3-d][1,3]thiazine-8a-carboxylic acid 5-oxide (16c)

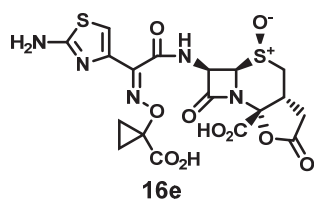
¹H NMR (Na salt) (400 MHz, D₂O): δ 7.05 (1H, s), 5.88 (1H, d, *J* = 4.7 Hz), 5.01 (1H, d, *J* = 4.7 Hz), 4.62 (1H, q, *J* = 6.8 Hz), 3.66–3.53 (2H, m), 3.07 (1H, dd, *J* = 18.3, 7.5 Hz), 2.82 (1H, t, *J* = 13.6 Hz), 2.57 (1H, d, *J* = 18.3 Hz), 1.47 (3H, d, *J* = 6.8 Hz).

¹³C NMR {1H} (Na salt) (100 MHz, D₂O): δ 183.0, 178.5, 173.8, 171.2, 167.6, 166.2, 150.3, 142.8, 115.9, 90.7, 84.0, 68.4, 62.0, 46.1, 36.8, 32.1, 19.5.

Anal.: C₁₇H₁₅N₅O₁₀S₂Na_{1.8}(H₂O)_{4.9}.

Calc.: C, 31.75; H, 3.9; N, 10.9; Na, 6.4; S, 10.0 (%).

Found: C, 31.7; H, 3.8; N, 11.1; Na, 6.3; S, 9.9 (%).



(3aR,5S,5aR,6R,8aR)-6-((Z)-2-(2-aminothiazol-4-yl)-2-((1-carboxycyclopropoxy)imino)acetamido)-2,7-dioxohexahydro-7H,8aH-azeto[2,1-b]furo[2,3-d][1,3]thiazine-8a-carboxylic acid 5-oxide (16e)

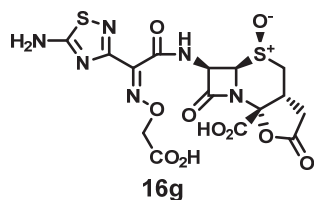
^1H NMR (Na salt) (400 MHz, D_2O): δ 7.08 (1H, s), 5.86 (1H, d, $J = 4.8$ Hz), 5.00 (1H, d, $J = 4.8$ Hz), 3.66–3.52 (2H, m), 3.07 (1H, dd, $J = 18.4, 7.6$ Hz), 2.82 (1H, t, $J = 13.4$ Hz), 2.57 (1H, d, $J = 18.4$ Hz), 1.42–1.26 (4H, m).

^{13}C NMR $\{^1\text{H}\}$ (Na salt) (100 MHz, D_2O): δ 182.4, 178.5, 173.7, 171.1, 167.5, 166.2, 151.5, 143.1, 116.3, 90.7, 68.4, 68.3, 61.9, 46.1, 36.7, 32.0, 17.94, 17.86.

Anal.: $\text{C}_{18}\text{H}_{15}\text{N}_5\text{Na}_2\text{O}_{10}\text{S}_2(\text{H}_2\text{O})_{5.1}$.

Calc.: C, 32.6; H, 3.8; N, 10.6; Na, 6.9; S, 9.7 (%).

Found: C, 32.5; H, 3.8; N, 10.7; Na, 7.1; S, 9.6 (%).



(3aR,5S,5aR,6R,8aR)-6-((Z)-2-(5-amino-1,2,4-thiadiazol-3-yl)-2-((carboxymethoxy)imino)acetamido)-2,7-dioxohexahydro-7H,8aH-azeto[2,1-b]furo[2,3-d][1,3]thiazine-8a-carboxylic acid 5-oxide (16g)

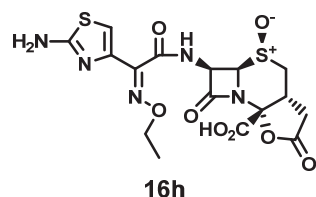
^1H NMR (Na salt) (400 MHz, D_2O): δ 5.93 (1H, d, $J = 4.5$ Hz), 5.01 (1H, d, $J = 4.5$ Hz), 4.67 (2H, t, $J = 16.3$ Hz), 3.65–3.52 (2H, m), 3.07 (1H, dd, $J = 18.4, 7.5$ Hz), 2.81 (1H, t, $J = 13.4$ Hz), 2.57 (1H, d, $J = 18.4$ Hz).

^{13}C NMR $\{^1\text{H}\}$ (Na salt) (100 MHz, D_2O): δ 187.4, 179.4, 178.5, 171.2, 166.5, 166.3, 163.7, 149.6, 90.7, 76.5, 68.5, 61.7, 46.0, 36.7, 32.1.

Anal.: $\text{C}_{15}\text{H}_{12}\text{N}_6\text{O}_{10}\text{Na}_2\text{S}_2(\text{H}_2\text{O})_{3.1}$.

Calc.: C, 29.9; H, 3.05; N, 13.95; Na, 7.6; S, 10.65 (%).

Found: C, 29.9; H, 3.0; N, 14.1; Na, 7.6; S, 10.5 (%).



(3aR,5S,5aR,6R,8aR)-6-((Z)-2-(2-aminothiazol-4-yl)-2-(ethoxyimino)acetamido)-2,7-dioxohexahydro-7H,8aH-azeto[2,1-b]furo[2,3-d][1,3]thiazine-8a-carboxylic acid 5-oxide (16h)

^1H NMR (Na salt) (400 MHz, D_2O): δ 7.03 (1H, s), 5.88 (1H, d, $J = 4.8$ Hz), 5.01 (1H, d, $J = 4.8$ Hz), 4.33–4.25 (2H, m), 3.64 (1H, dd, $J = 14.7, 5.3$ Hz), 3.59–3.52 (1H, m), 3.07 (1H, dd, $J = 18.3, 7.8$ Hz), 2.83 (1H, dd, $J = 14.7, 12.5$ Hz), 2.57 (1H, d, $J = 18.3$ Hz), 1.33 (3H, t, $J = 7.1$ Hz).

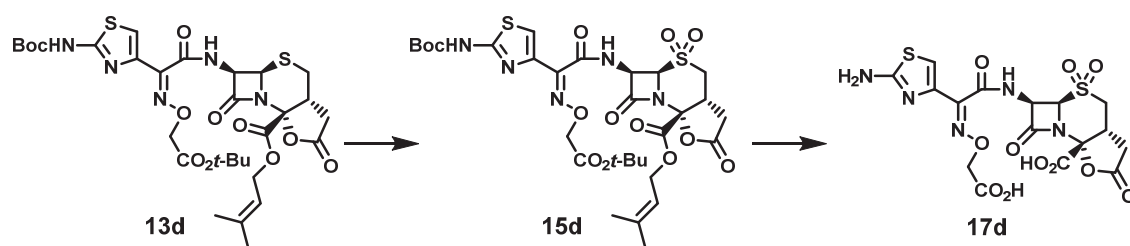
^{13}C NMR $\{^1\text{H}\}$ (Na salt) (100 MHz, D_2O): δ 178.5, 173.8, 171.1, 167.8, 166.1, 150.6, 143.3, 115.8, 90.7, 74.3, 68.3, 62.0, 46.1, 36.7, 32.0, 16.7.

Anal.: C₁₆H₁₆N₅O₈NaS₂(H₂O)₄.

Calc.: C, 34.0; H, 4.3; N, 12.4; Na, 4.1; S, 11.3 (%).

Found: C, 34.0; H, 4.2; N, 12.5; Na, 4.2; S, 11.5 (%).

Synthesis of compound 17d



Step 1. Synthesis of 3-methylbut-2-en-1-yl (3*aR*,5*aR*,6*R*,8*aR*)-6-((*Z*)-2-((2-(*tert*-butoxy)-2-oxoethoxy)imino)-2-(2-((*tert*-butoxycarbonyl)amino)thiazol-4-yl)acetamido)-2,7-dioxohexahydro-7*H*,8*aH*-azeto[2,1-*b*]furo[2,3-*d*][1,3]thiazine-8*a*-carboxylate 5,5-dioxide (15d)

Compound **13d** (0.75 g, 1.06 mmol) was dissolved in dichloromethane (10 mL). Under ice cooling, 70 % *m*-CPBA (0.52 g, 2.11 mmol) was added to the solution with stirring for 1 h. This reaction mixture was then separated into aqueous and organic layers by the addition of a saturated aqueous solution of sodium bicarbonate. The organic layer was washed with water, a saturated aqueous solution of sodium bicarbonate and brine in this order and dried over magnesium sulfate, which was subsequently removed by filtration. Next, the filtrate was concentrated under reduced pressure. The residue was subjected to silica gel column chromatography, followed by elution with hexane–ethyl acetate. Fractions containing the desired compound were concentrated under reduced pressure to afford compound **15d** (0.09 g, yield 12%) as a crude mixture. **15d** was used in the next step without further purification.

MS (ESI) m/z : $[M + H]^+$ calcd for $C_{30}H_{40}N_5O_{13}S_2$ 742; found 742.

Step 2. Synthesis of (3a*R*,5a*R*,6*R*,8a*R*)-6-((*Z*)-2-(2-aminothiazol-4-yl)-2-((carboxymethoxy)imino)acetamido)-2,7-dioxohexahydro-7*H*,8a*H*-azeto[2,1-*b*]furo[2,3-*d*][1,3]thiazine-8a-carboxylic acid 5,5-dioxide (17d)

Compound **17d** was obtained from compound **15d** (0.09 g, 0.121 mmol) by a procedure similar to that described for **2d**.

Yield amount: 20.2 mg (yield 32%)

1H NMR (Na salt) (400 MHz, DMSO- d_6): δ 7.03 (1H, s), 5.93 (1H, d, $J = 4.7$ Hz), 5.39 (1H, d, $J = 4.7$ Hz), 3.91–3.85 (1H, m), 4.55 (2H, s), 3.64 (1H, dd, $J = 15.4, 5.6$ Hz), 3.56–3.49 (1H, m), 3.01 (1H, dd, $J = 18.4, 7.6$ Hz), 2.56 (1H, d, $J = 18.4$ Hz).

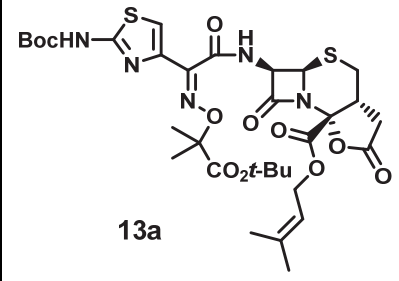
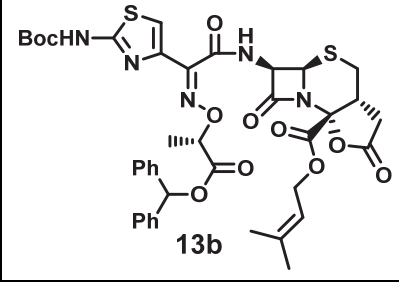
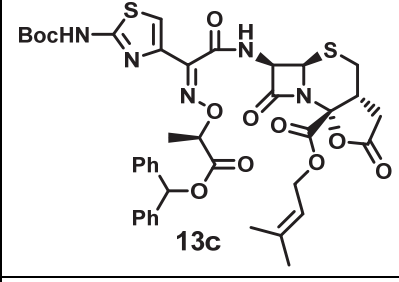
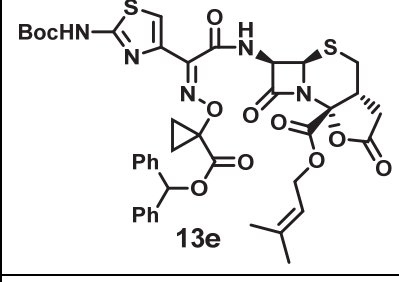
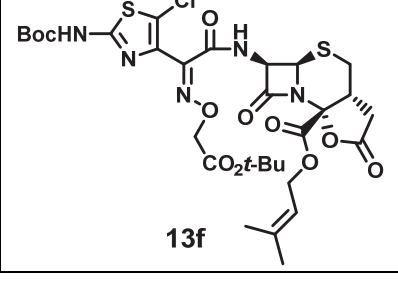
^{13}C NMR $\{^1H\}$ (Na salt) (100 MHz, D $_2$ O): δ 180.1, 177.6, 173.8, 170.6, 167.3, 165.6, 150.5, 142.6, 116.6, 89.7, 75.9, 68.5, 61.7, 52.6, 45.1, 37.2.

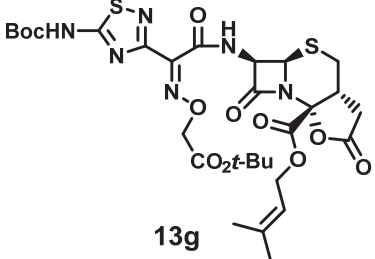
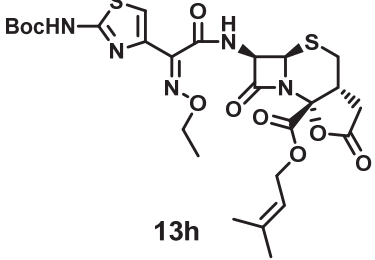
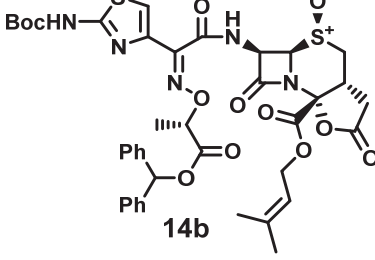
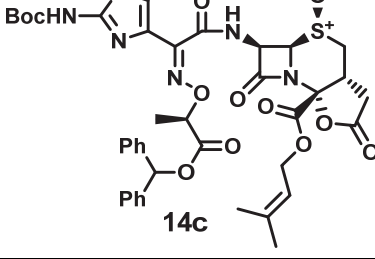
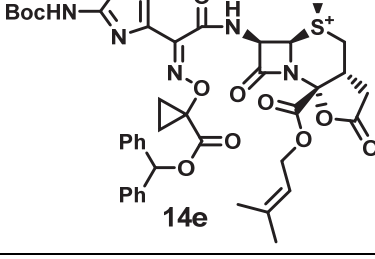
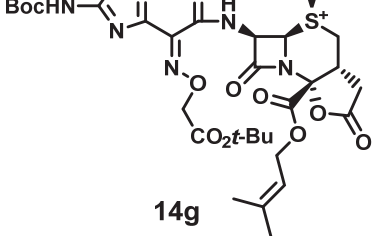
Anal.: $C_{16}H_{13}N_5O_{11}S_2Na_2(H_2O)_4$.

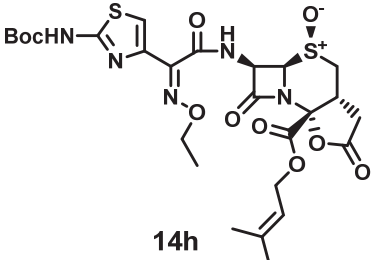
Calc.: C, 30.3; H, 3.3; N, 11.1; S, 10.1; Na, 7.3 (%).

Found: C, 30.6; H, 3.5; N, 11.0; S, 9.8; Na, 7.0 (%).

MS (ESI) Data of 13a–c, e–h, 14b, c, e, g and h

compound	$[M + H]^+$	<i>m/z</i> : calcd	<i>m/z</i> : found
 <p>13a</p>	$C_{32}H_{44}N_5O_{11}S_2$	738	738
 <p>13b</p>	$C_{40}H_{44}N_5O_{11}S_2$	834	834
 <p>13c</p>	$C_{40}H_{44}N_5O_{11}S_2$	834	834
 <p>13e</p>	$C_{41}H_{44}N_5O_{11}S_2$	846	846
 <p>13f</p>	$C_{30}H_{39}ClN_5O_{11}S_2$	744	744

 <p>13g</p>	C ₂₉ H ₃₉ N ₆ O ₁₁ S ₂	711	711
 <p>13h</p>	C ₂₆ H ₃₄ N ₅ O ₉ S ₂	624	624
 <p>14b</p>	C ₄₀ H ₄₄ N ₅ O ₁₂ S ₂	850	850
 <p>14c</p>	C ₄₀ H ₄₄ N ₅ O ₁₂ S ₂	850	850
 <p>14e</p>	C ₄₁ H ₄₄ N ₅ O ₁₂ S ₂	862	862
 <p>14g</p>	C ₂₉ H ₃₉ N ₆ O ₁₂ S ₂	727	727

 <p style="text-align: center;">14h</p>	$C_{26}H_{34}N_5O_{10}S_2$	640	640
---	----------------------------	-----	-----

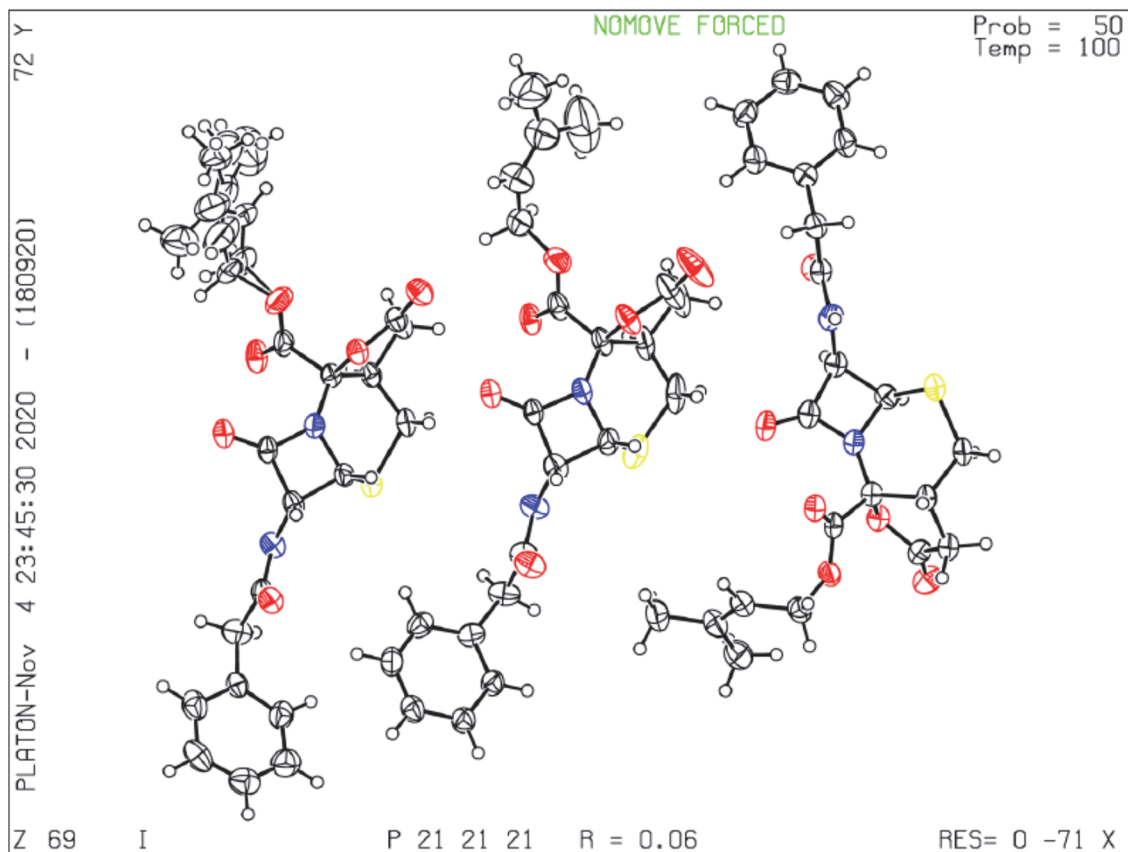
X-ray crystallographic data of compound **11** and **16d'**

X-ray Crystallography: The diffraction data of **11** and **16d'** were collected on an XtaLAB AFC10 (RCD3): quarter-chi single diffractometer. The crystal was kept at 100.0 K during data collection. Using Olex2,1 the structure was solved with the ShelXT2 structure solution program using Intrinsic Phasing and refined with the ShelXL3 refinement package using Least Squares minimization.

Sample Preparation: X-ray quality crystal was prepared by vapor diffusion method using ethanol–water for **11** and acetonitrile–water for **16d'** at room temperature.

Compound 11

CCDC Deposition Number; 2043449



Identification code; X4230r3

Empirical formula; C₆₆H₇₂N₆O₁₈S₃

Formula weight; 1333.47

Temperature; 100 K

Crystal system; orthorhombic

Space group; P2₁2₁2₁

Unit cell dimension;

$$\alpha = 4.96740(10) \text{ \AA} \quad \alpha = 90^\circ$$

$$\beta = 31.4762(9) \text{ \AA} \quad \beta = 90^\circ$$

$$\gamma = 41.1495(7) \text{ \AA} \quad \gamma = 90^\circ$$

Volume; 6433.9(3) Å³

Z; 4

Density (calculated) 1.377 g/cm³

Absorption coefficient; 1.704 μ/mm⁻¹

F(000); 2808.0

Crystal size; 0.19 × 0.06 × 0.01 mm

Radiation; CuKα (λ = 1.54184 Å)

2Θ range for data collection; 5.132 to 148.062 °

Index ranges; -6 ≤ h ≤ 5, -34 ≤ k ≤ 38, -37 ≤ l ≤ 50

Reflections collected; 39918

Independent reflections; 12635 [R_{int} = 0.0805, R_{sigma} = 0.0840]

Data / restraints / parameters; 12635 / 6 / 891

Goodness-of-fit on F²; 1.052

Final R indexes [I ≥ 2σ (I)]; R₁ = 0.0594, wR₂ = 0.1456

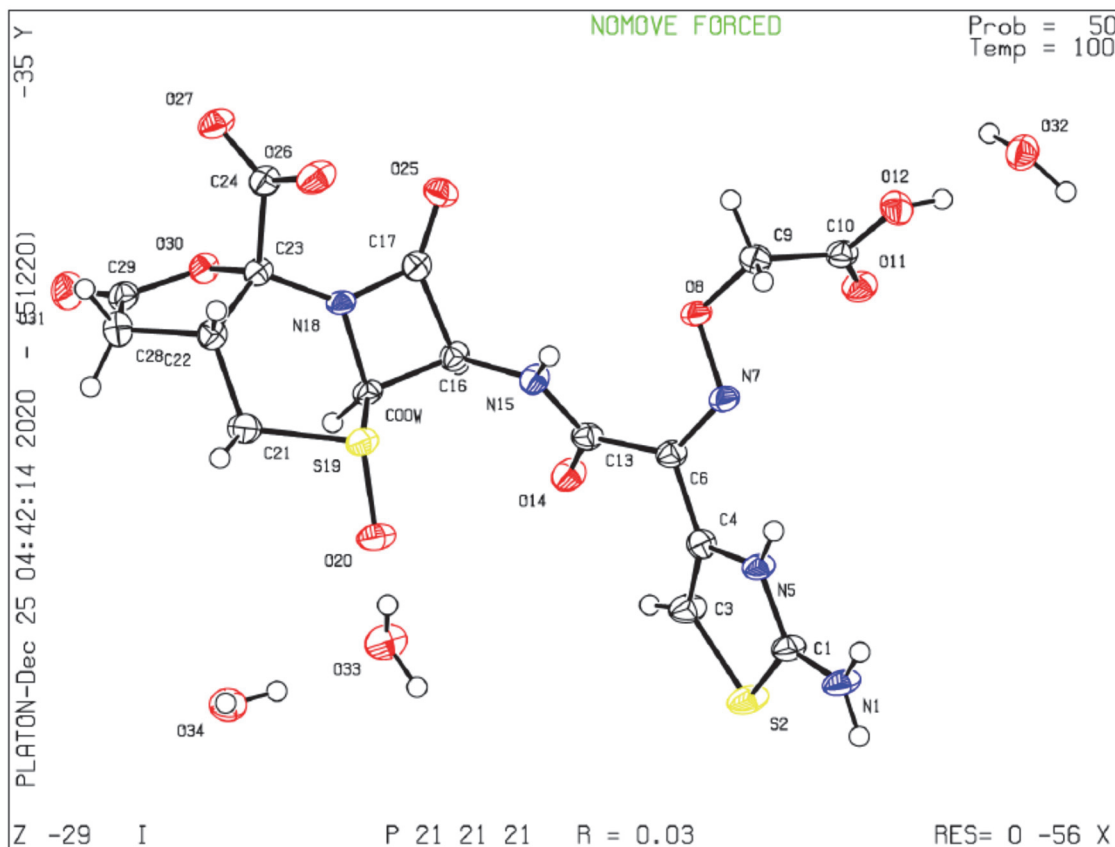
Final R indexes [all data]; R₁ = 0.0851, wR₂ = 0.1656

Largest diff. peak / hole; 0.41 / -0.57 eÅ⁻³

Flack parameter; 0.002(14)

Compound 16d'

CCDC Deposition Number; 2052400



Identification code; X4267

Empirical formula; C₁₆H₂₁N₅O₁₃S₂

Formula weight; 555.50

Temperature; 100 K

Crystal system; orthorhombic

Space group; P2₁2₁2₁

Unit cell dimension;

$$\alpha = 7.62170(10) \text{ \AA} \quad \alpha = 90^\circ$$

$$\beta = 14.3620(2) \text{ \AA} \quad \beta = 90^\circ$$

$$\gamma = 20.5427(3) \text{ \AA} \quad \gamma = 90^\circ$$

Volume; 2248.66(5) Å³

Z; 4

Density (calculated) 1.641 g/cm³

Absorption coefficient; 2.883 μ/mm⁻¹

F(000); 1152.0

Crystal size; 0.13 × 0.07 × 0.02 mm

Radiation; CuKα (λ = 1.54184 Å)

2θ range for data collection; 7.51 to 147.86 °

Index ranges; -8 ≤ h ≤ 9, -17 ≤ k ≤ 17, -24 ≤ l ≤ 25

Reflections collected; 14908

Independent reflections; 4453 [R_{int} = 0.0423, R_{sigma} = 0.0395]

Data / restraints / parameters; 4453 / 2 / 349

Goodness-of-fit on F²; 1.046

Final R indexes [I ≥ 2σ (I)]; R₁ = 0.0333, wR₂ = 0.0842

Final R indexes [all data]; R₁ = 0.0356, wR₂ = 0.0854

Largest diff. peak / hole; 0.37 / -0.35 eÅ⁻³

Flack parameter; 0.005(8)

Evaluation of in vitro antibacterial activity

The minimum inhibitory concentrations (MICs) were determined using the broth microdilution method in accordance with Clinical Laboratory Standards Institute (CLSI) guidelines. Briefly, two-fold serial dilutions of the test compounds were prepared and transferred to a 96-well plate containing Cation-Adjusted Mueller-Hinton broth (CAMHB). The bacterial suspension for the inoculum was prepared based on an optical

density of 625 nm for a final inoculum size of approximately 5×10^4 CFU/well. The 96-well plates were incubated at 35 °C for 16 to 20 h. The MIC endpoint was defined as the lowest concentration of the compound that inhibited bacterial growth as detected by the naked eye.

Conformational analysis

The Macromodel module of the Schrödinger Maestro version 12.1.¹⁶ was used for conformational analysis. OPLS3e was used as a force field for calculation. We carried out the conformational search using mixed torsional/low-mode sampling. The number of separate conformers generated was 1000, with a maximum of 100 unique structures to be saved for each rotatable bond. A 21 kJ/mol energy cutoff was used to remove the higher energy conformers. A conformer was considered redundant and subsequently eliminated if its maximum atom deviation from an already-identified conformer was less than 0.5 Å. All conformers were subjected to further minimization using the Powell – Reeves conjugate gradient (PRCG) method for a maximum of 2500 steps, and because some conformers could not be easily minimized, we used a second minimization step and increased the number of iterations to 2500 to ensure that all conformers were minimized.

Determination of the competitive inhibition constant (K_i)

CMY-2 was prepared as the native form without any affinity tags from E. coli BL21-derived strains with the expression vector of pET9a. The concentration of crude enzyme used was determined by the measurement of hydrolysis of nitrocefin (150 µM), where the change of the absorbance was linearly approximately 0.2 to 0.7 over the 20 min. The competitive inhibition constant (K_i) was determined in the presence of 100 µM nitrocefin

($\Delta\epsilon$ 492 nm = 17400 M⁻¹ cm⁻¹) in reaction buffer (50 mM MOPS (pH 7.0), 50 mM NaCl) at 25 °C with a final substrate concentration of 20 μM to 2.6 mM and the absorbance of nitrocefin was monitored at 492 nm every 3 min for 15 min with a UV-2550 spectrophotometer 93 (Shimadzu, Japan) or U-3010 (Hitachi, Japan). *K_i* values were calculated by method of Waley S.G.¹⁸

Evaluation of therapeutic efficacy in cyclophosphamide-induced neutropenic mouse model of lung infections

The neutropenic mouse lung infections outlined by Koomanachai et al.²⁵ and Drusano et al.²⁶ were tested. Five-week-old, specific-pathogen-free, male Jcl:ICR mice (weight, 17 to 20 g) were obtained from CLEA Japan, Inc. (Tokyo, Japan). Mice were anesthetized by intramuscular injection of a mixture of tiletamine, zolazepam, and xylazine. The mice were infected by intranasal instillation of 0.07 mL of bacterial suspension. The challenge doses ranged from approximately 10⁵ to 10⁶ CFU/lung.

Reference

¹ (a) Centers for Disease Control and Prevention (CDC). *Antibiotic Resistance Threats in the United States 2019*, Atlanta, GA; U.S. Department of Health and Human Services, CDC, 2019. Retrieved from <https://www.cdc.gov/drugresistance/pdf/threats-report/2019-ar-threats-report-508.pdf> (accessed November 22, 2022). (b) World Health Organization. *Global priority list of antibiotic-resistant bacteria to guide research, discovery, and development of new antibiotics*; WHO, February 27, 2017. Retrieved from <https://www.aidsdatahub.org/resource/who-global-priority-list-antibiotic-resistant->

bacteria (accessed November 22, 2022).

² Ambler, R. P. The structure of β -lactamases. *Philos. Trans. R. Soc., B* **1980**, *289*, 321–331.

³ (a) Walsh, T. R. Emerging carbapenemases: a global perspective. *Int. J. Antimicrob. Agents* **2010**, *36*, S8–S14. (b) Guh, A. Y.; Bulens, S. N.; Mu, Y. et al. Epidemiology of Carbapenem-Resistant Enterobacteriaceae in 7 US Communities. 2012–2013. *JAMA*. **2015**, *314*, 1479–1487. (c) Logan, L. K.; Weinstein, R.A. The Epidemiology of Carbapenem-Resistant Enterobacteriaceae: The Impact and Evolution of a Global Menace. *J Infect Dis*. **2017**, *215*, S28–S36. (d) Tamma, P. D.; Goodman, K. E.; Harris, A. D. et al. Comparing the Outcomes of Patients with Carbapenemase-Producing and Non-Carbapenemase-Producing Carbapenem-Resistant *Enterobacteriaceae* Bacteremia. *Clin Infect Dis*. **2017**, *64*, 257–264.

⁴ Wang, D. Y.; Abboud, M. I.; Markoulides, M. S.; Brem, J.; Schofield, C. J. The road to avibactam: the first clinically useful non- β -lactam working somewhat like a β -lactam. *Future Med. Chem*. **2016**, *8*, 1063–1084.

⁵ Novelli, A.; Giacomo, D. P.; Rossolini, M. G.; Tumbarello, M. Meropenem/vaborbactam: a next generation β -lactam β -lactamase inhibitor combination. *Expert Rev. Anti-Infect. Ther*. **2020**, *18*, 643–655.

⁶ Nelson, K.; Hemarajata, P.; Sun, D. et al. Resistance to Ceftazidime-Avibactam Is Due to Transposition of KPC in a Porin-Deficient Strain of *Klebsiella pneumoniae* with Increased Efflux Activity. *Antimicrob. Agents Chemother*. **2017**, *61*, e00989–e1017.

⁷ (a) Harada, S.; Tsubotani, S.; Hida, T.; Ono, H.; Okazaki, H. Structure of lactivicin, an antibiotic having a new nucleus and similar biological activities to β -lactam antibiotics. *Tetrahedron Lett*. **1986**, *27*, 6229–6232. (b) Nozaki, Y.; Katayama, N.; Ono, H.;

Tsubotani, S.; Harada, S.; Okazaki, H.; Nakao, Y. Binding of a non- β -lactam antibiotic to penicillin-binding proteins. *Nature* **1987**, *325*, 179–180. (c) Tamura, N.; Matsushita, Y.; Kawano, Y.; Yoshioka, K.; Synthesis and Antibacterial Activity of Lactivicin Derivatives. *Chem. Pharm. Bull.* **1990**, *38*, 116–122.

⁸ (a) Macheboeuf, P.; Fischer, D. S.; Brown, J. T. et al. Structural and mechanistic basis of penicillin-binding protein inhibition by lactivicins. *Nature Chem. Bio.* **2007**, *3*, 565–569. (b) Starr, J.; Brown, M. F.; Aschenbrenner, L. et al. Siderophore Receptor-Mediated Uptake of Lactivicin Analogues in Gram-Negative Bacteria. *J. Med. Chem.* **2014**, *57*, 3845–3855. (c) Calvopiña, K.; Umland, K. D.; Rydzik, A. M. et al. Sideromimic Modification of Lactivicin Dramatically Increases Potency against Extensively Drug-Resistant *Stenotrophomonas maltophilia* Clinical Isolates. *Antimicrob. Agents Chemother.* **2016**, *60*, 4170–4175.

⁹ Morimoto, A.; Noguchi, N.; Chou, N. Tricyclic cepham compounds, their production and use. EP253337 Jan 20. 1988.

¹⁰ Cooper, R. D. G.; Demarco, P. V.; Murphy, C. F.; Spangle, L. A. Chemistry of Cephalosporin Antibiotics. Part XV1. Configurational and Conformational Analysis of Deacetoxy- Δ 2- and - Δ 3-Cephalosporins and their Corresponding Sulphoxide Isomers by Nuclear Magnetic Resonance. *J. Chem. Soc. C.* **1970**, *2*, 340–344.

¹¹ (a) Morimoto, A.; Chou, N.; Noguchi, N. Tricyclic penam compounds, their production and their use. EP249909. Dec 23, 1987. (b) Allen, N. E.; Hobbs, J. J. N.; Preaton, D. A.; Turner, J. R.; Wu, C. Y. E. Antibacterial properties of the bicyclic pyrazolidinones. *J. Antibiot.* **1990**, *43*, 92–99.

¹² Kohira, N.; Hackel, M. A.; Ishioka, Y. et al. Reduced susceptibility mechanism to cefiderocol, a siderophore cephalosporin, among clinical isolates from a global

surveillance programme (SIDERO-WT-2014). *J. Global Antimicrob. Resist.* **2020**, *22*, 738–741.

¹³ (a) Yamawaki, K.; Nomura, T.; Yasukata, T. et al. A novel series of parenteral cephalosporins exhibiting potent activities against *Pseudomonas aeruginosa* and other Gram-negative pathogens: Synthesis and structure-activity relationships. *Bioorg. Med. Chem.* **2007**, *15*, 6716–6732. (b) Takaya, T.; Takasugi, H.; Masugi, T.; Chiba, T.; Kochi, T.; Takano, T. Structure-activity Relationships of Sodium 7 β -[(*Z*)-2-(2-Amino-4-thiazolyl)-2-(methoxyimino) acetamido]-3-cephem-4-carboxylate (Ceftizoxime) and Its Related Compounds. *Nippon Kagaku Kaishi.* **1981**, *5*, 785–804. (c) Nakayama, E.; Fujimoto, K.; Muramatsu, S. et al. Synthesis and structure-activity relationships of 3-thiazoliummethyl derivatives. *J. Antibiot.* **1991**, *44*, 854–863.

¹⁴ Phelps, D. J.; Carlton, D. D.; Farrell, C. A.; Kessler, R. E. Affinity of Cephalosporins for β -Lactamases as a Factor in Antibacterial Efficacy. *Antimicrob. Agents Chemother.* **1986**, *29*, 845–848.

¹⁵ (a) Beadle, B. M.; Trehan, I.; Focia, P. J.; Shoichet, B. K. Structural Milestones in the Reaction Pathway of an Amide Hydrolase: Substrate, Acyl, and Product Complexes of Cephalothin with AmpC β -Lactamase. *Structure* **2002**, *10*, 413–424. (b) Goldberg, S. D.; Iannuccilli, W.; Nguyen, T.; Ju, J.; Cornish, V. W. Identification of residues critical for catalysis in a class C β -lactamase by combinatorial scanning mutagenesis. *Protein Sci.* **2003**, *12*, 1633–1645.

¹⁶ Schrödinger Release 2020-3: MacroModel, Schrödinger, LLC, New York, NY, 2020. <https://www.schrodinger.com/macromodel>.

¹⁷ (a) Bauernfeind, A.; Stemplinger, I.; Jungwirth, R.; Giamarellou, H. Characterization of the plasmidic β -lactamase CMY-2, which is responsible for cephamycin resistance.

Antimicrob. Agents Chemother. **1996**, *40*, 221–224. (b) Philippon, A.; Arlet, G.; Jacoby, G. A. Plasmid-determined AmpC-type β -lactamases. *Antimicrob. Agents Chemother.* **2002**, *46*, 1–11.

¹⁸ Waley, S. G. A quick method for the determination of inhibition constants. *Biochemistry* **1982**, *205*, 631–633.

¹⁹ Marchand-Brynaert, J.; Ghosez, L.; Cossement, E. Synthesis of 2-oxo-bisnorpenicillin G esters. *Tetrahedron Lett.* **1980**, *21*, 3085–3088.

²⁰ Hisakawa, S.; Hasegawa, Y.; Aoki, T. et al. Preparation of cephem compounds having catechol group as antibacterial agents. WO2011125967. Oct 13, 2011.

²¹ Nishitani, Y.; Yamawaki, K.; Takeoka, Y.; Sugimoto, H.; Hisakawa, S.; Aoki, T. Preparation of cephalosporins having catechol group as antibacterial agents. WO2010050468. May 6, 2010.

²² Reck, F.; Bermingham, A.; Blais, J. et al. Optimization of novel monobactams with activity against carbapenem-resistant Enterobacteriaceae-Identification of LYS228. *Bioorg Med Chem Lett.* **2018**, *28*, 748–755.

²³ Miyake, A.; Yoshimura, Y.; Yamaoka, M.; Nishimura, T.; Hashimoto, N.; Imada, A. Studies on condensed-heterocyclic azolium cephalosporins. IV. Synthesis and antibacterial activity of 7β -[2-(5-amino-1,2,4-thiadiazol-3-yl)-2(Z)-alkoxyiminoacetamido]-3-(condensed-heterocyclic azolium)methylcephalosporins including SCE-2787. *J Antibiot.* **1992**, *45*, 709–720.

²⁴ (a) Matsunaga, T.; Tsuchiya, M. Process for production of alkoxy-carbonylaminothiazole acetic acid derivative. EP 781769. Jul 2, 1997 (b) Yokoo, K.; Yamawaki, K.; Yoshida, Y. et al. Novel broad-spectrum and long-acting parenteral cephalosporins having an acyl cyanamide moiety at the C-3 terminal: Synthesis and

structure-activity relationships. *Eur. J. Med. Chem.* **2016**, *124*, 698–712.

²⁵ Koomanachai, P.; Kim, A.; Nicolau, D. P. Pharmacodynamic evaluation of tigecycline against *Acinetobacter baumannii* in a murine pneumonia model. *J Antimicrob Chemother.* **2009**, *63*, 982–987.

²⁶ Drusano, G. L.; Lodise, T. P.; Melnick, D. et al. Meropenem penetration into epithelial lining fluid in mice and humans and delineation of exposure targets. *Antimicrob Agents Chemother.* **2011**, *55*, 3406–3412.

Chapter III Optimization of Aminothiazole Side Chain

III-1. Introduction

Carbapenem-resistant Enterobacterales (CREs) are a worldwide clinical and public health problem.¹ Carbapenem resistance is usually caused by production of carbapenem-hydrolyzing enzymes, carbapenemases, which include serine-type β -lactamases (classes A and D based on Ambler classification²) such as KPC and OXA-48 and metallo-type β -lactamases (class B) such as NDM and VIM.³ Since 2015, some combinations of β -lactam and β -lactamase inhibitor (BL/BLI) such as AVYCAZ® (ceftazidime, CAZ, **2** and avibactam, AVI, **3**) and VABOMERE® (meropenem, MER, **4** and vaborbactam, VAB, **5**) have been approved in some countries. Furthermore, new BL/BLI combinations currently under clinical development, such as monobactam aztreonam (ATM, **6**) and AVI **3**, have potent activities against class B β -lactamase producing Enterobacterales, where therapeutic options are currently very limited. In these combinations, the BLI hinders hydrolysis and inactivation by β -lactamases to restore the activity of the β -lactam antibiotic. The BL/BLI strategy should be one of the therapeutic options for infections caused by CREs; however, these activities would be lost against clinical isolates with resistance mechanisms other than β -lactamase production. Examples include reduction of the outer membrane permeability caused by porin deficiency with β -lactamase production⁴ and degradation of target affinity by mutations in penicillin-binding proteins (PBPs), such as the insertion of four amino acids into PBP3 (encoded by *ftsI*).⁵

Regarding the relationship between outer membrane permeability and antibacterial activity, it has been reported that β -lactams use porin channels to permeate the outer membrane, and their antibacterial activities are strongly influenced by the rate of

penetration of the outer membrane because β -lactams need to access their target PBPs by crossing the outer membrane of Gram-negative bacteria to enter the periplasmic space. Therefore, the lack of major porins due to mutations or downregulation of the corresponding genes is believed to reduce the permeability of the outer membrane and to affect the antibacterial activities.⁶ Furthermore, it has been reported that reduced outer membrane permeability combined with the production of extended-spectrum β -lactamases (class A) and/or AmpC β -lactamase (class C) can reduce the susceptibility to carbapenems in the clinical isolates of Enterobacterales without carbapenemases.⁷ The insertion of four amino acids (YRIN or YRIK) into PBP3 has been reported to affect the susceptibility of several β -lactams, especially monobactam and cephalosporins,⁵ because they have the highest affinity for PBP3 among the PBPs⁸ and are reported to be enriched among NDM-type carbapenemase (class B) producing strains, especially in India.⁵ Therefore, this four-amino acid insertion in combination with the NDM-type considerably elevates the minimum inhibitory concentrations (MICs) of BL/BLIs. These findings indicate a critical need for new therapeutic options against CREs that have overcome these two resistance mechanisms. In Chapter II, the author identified the novel tricyclic β -lactam **1a** which has a γ -lactone ring and a sulfoxide of the tricyclic core as key structures for exhibiting potent antibacterial activities against several problematic β -lactamase-producing CREs without a BLI (Figure 3-1). During the evaluation of **1a**, two strains with increased MICs were found, and their characterization revealed that they are a porin-deficient strain and a four-amino acid inserted strain. Further modifications of compound **1a** were started with the aim overcoming these resistant mechanisms and improving its antibacterial activities.

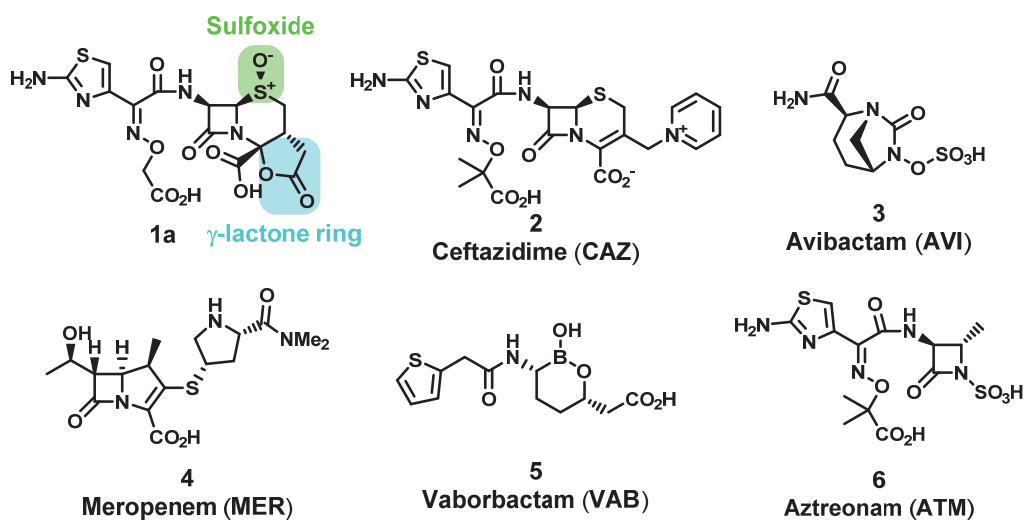
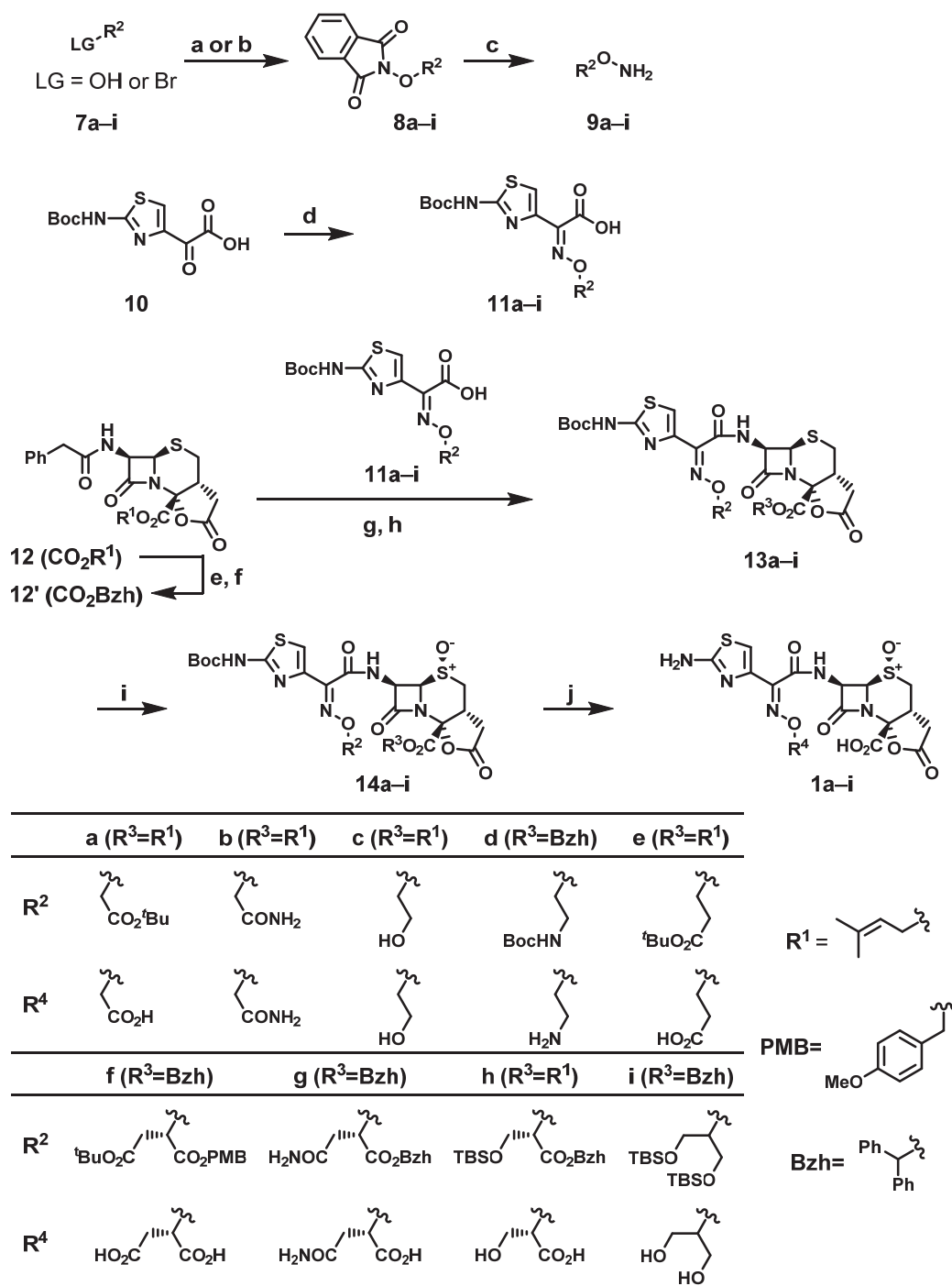


Figure 3-1. Structures of Compounds **1a** and BL/BLIs

III-2. Synthesis of Tricyclic β -lactams

Scheme 3-1 shows the synthesis of compound **1a** and its derivatives.

N-hydroxyphthalimide was alkylated with compounds **7a–i** under the conditions of alkylation or Mitsunobu reaction to afford the corresponding compounds **8a–i**. Treatment of **8a–i** with *N*-methylhydrazine in dichloromethane gave alkoxyamines **9a–i**, which were immediately reacted with α -keto carboxylic acid **10** to afford aminothiazole side chains **11a–i**. Compound **12'** was prepared from compound **12** by hydrogenation followed by protection with the diphenylmethyl group. The aminothiazole side chains **11a–i** were introduced after removing the phenylacetyl group of compounds **12** or **12'** from the amino group and removal of all protective groups to afford target compounds **1a–i**. The structure of the target compounds was confirmed by single crystal X-ray crystallography of **1i** (Figure 3-2).



Reagents and conditions : (a) for LG=Br *N*-hydroxyphthalimide, base (b) for LG=OH *N*-hydroxyphthalimide, Mitsunobu reaction; (c) *N*-methylhydrazine, CH₂Cl₂; (d) **9a-i**, CH₂Cl₂/MeOH; (e) H₂, Pd/C, EtOAc/0.1 mol/L Phosphate buffer (pH=7), rt; (f) Diphenyldiazomethane, THF, rt; (g) PCl₅, Py, CH₂Cl₂, -30 °C; (h) **11a-i**, MsCl, Et₃N, Py, CH₂Cl₂/DMA, 0 °C; (i) AcOOH, MeCN/DMA, 0 °C; (j) AlCl₃, Anisole, CH₂Cl₂, -40 °C.

Scheme 3-1. Synthesis of Tricyclic β -lactams **1a-i**

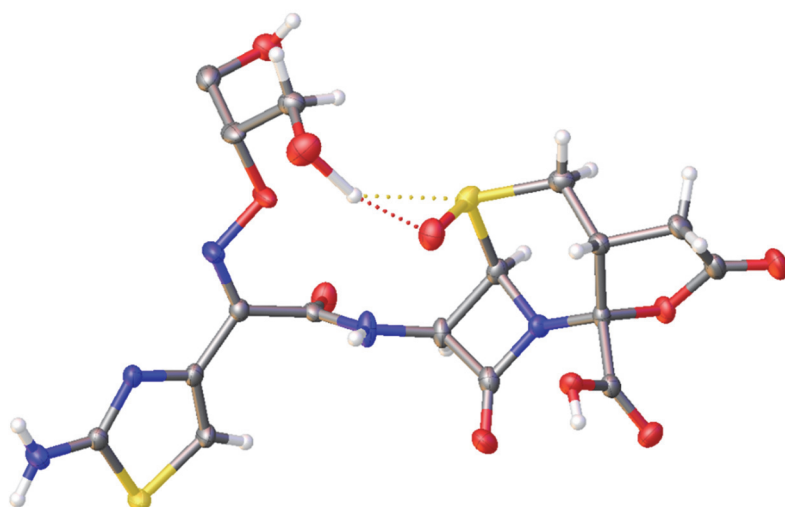


Figure 3-2. Molecular Structure of **1i**; Thermal ellipsoids are set at 30% probability

III-3. Structure-Activity Relationship of Aminothiazole Side Chain

The structure-activity relationships for several analogues with modified alkoxyimino moieties of the aminothiazole side chain are summarized in Table 2-1 by the MICs of six strains including two low susceptible strains described below.

During the evaluation of **1a**, two strains with increased MICs were identified. One was *Klebsiella pneumoniae* NCTC13443 (NDM-1 producer), which is deficient in porin OmpK35, and the other was *Escherichia coli* SR08587 (NDM-1 producer), which has a four-amino acid (YRIN) insertion into PBP3. *E. coli* SR08587 shows an increased MIC of **1a**; however, it has only been found in *E. coli* clinical isolates, and their spread in the future is still unknown.⁵

The author therefore decided to prioritize the improvement of activities against porin-deficient strains. The antibacterial activities of β -lactams have been reported to be strongly influenced by the rate of penetration through the outer membrane.⁹ Therefore, he hypothesized that the high MIC of **1a** against *K. pneumoniae* NCTC13443 is due to a

decrease in the outer membrane permeability caused by a deficiency in porin OmpK35.

Table 3-1. *In Vitro* Antibacterial Activities (MIC, $\mu\text{g/mL}$) of Compounds **1a-i**

Strain	Phenotype (Ambler classification)	R=				
		1a	1b	1c	1d	1e
<i>K. pneumoniae</i> SR01343	KPC-2 (class A)	0.063	0.063	0.125	8	0.25
<i>E. cloacae</i> SR01875	NDM-1 (class B)	0.063	0.063	0.063	8	0.25
<i>E. cloacae</i> SR36276	AmpC (class C)	0.063	0.5	0.25	8	0.25
<i>K. pneumoniae</i> SR08787	OXA-48 (class D)	0.25	0.25	0.5	8	0.5
<i>K. pneumoniae</i> NCTC13443	NDM-1 (class B) Δ OmpK35	1	2	1	16	4
<i>E. coli</i> SR08587	NDM-1 (class B) YRIN-inserted in PBP3	8	8	4	>32	32

Strain	Phenotype (Ambler classification)	R=			
		1f	1g	1h	1i
<i>K. pneumoniae</i> SR01343	KPC-2 (class A)	4	0.5	0.125	0.063
<i>E. cloacae</i> SR01875	NDM-1 (class B)	1	0.5	0.063	0.063
<i>E. cloacae</i> SR36276	AmpC (class C)	1	0.5	<0.031	0.125
<i>K. pneumoniae</i> SR08787	OXA-48 (class D)	4	1	<0.031	0.25
<i>K. pneumoniae</i> NCTC13443	NDM-1 (class B) Δ OmpK35	16	4	1	0.5
<i>E. coli</i> SR08587	NDM-1 (class B) YRIN-inserted in PBP3	>32	32	4	2

Studies on porin channels have shown that β -lactams with two negative charges penetrate more slowly than β -lactams with one negative charge and that β -lactams with exceptionally bulky side chains show much slower penetration rates than expected from their hydrophobicity.¹⁰ Hence, he proposed that converting the carboxylic acid group on the alkoxyimino moiety of compound **1a** into a non-anionic group and/or introducing a non-bulky hydrophilic functional group should improve the permeability of porin and consequently its antibacterial activities against the porin-deficient strains. This strategy

for improving porin permeability should simultaneously improve the antibacterial activities against the four-amino acid inserted strains because it has been reported that the binding of β -lactams, which have a large substituent at the position of the aminothiazole side chain, to PBP3 is hindered by the four-amino acid insertion.⁸

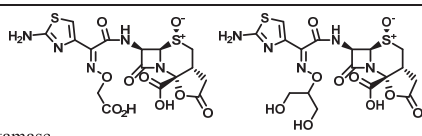
First, the carboxylic acid group at the alkoxyimino moiety of the aminothiazole side chain was converted to amide group **1b**, hydroxy group **1c**, and amino group **1d** to reduce the negative charge of the whole molecule from 2 to 1. Contrary to his expectations, the antibacterial activities of **1b** and **1c** against the two target strains (*K. pneumoniae* NCTC13443 and *E. coli* SR08587) did not improve, and **1d** showed significant reduction of the activities. In addition, the reduced activities of **1e** having an extended carbon chain suggests that carbon chain extension is not suitable for potent antibacterial activities. The combined results indicate that the conversion of the carboxylic acid at the alkoxyimino moiety of the aminothiazole side chain alone would not achieve improved antibacterial activities against the porin-deficient strains. Thus, additional non-bulky hydrophilic functional groups were introduced into the alkoxyimino moiety of **1a** to improve the activities in the next attempt. Introductions of another carboxylic acid group **1f** and an amide group **1g** significantly decreased the antibacterial activities, and introduction of a hydroxy group **1h** did not significantly improve the activities against the two target strains as compared with **1a**. These results indicate that the introduction of additional hydrophilic functional groups alone could not improve the activities. Therefore, the reduction of the negative charge was combined with the introduction of additional hydrophilic functional groups. Comparison of the antibacterial activities of **1f–h** showed that **1h** displayed activities superior to the others. This led to convert the carboxylic acid group of **1h** to a hydroxy group. As expected, compound **1i** showed improved activities against *K.*

pneumoniae NCTC13443 (porin-deficient strain) and, fortunately, against *E. coli* SR08587 (YRIN inserted strain). In addition, the activities of **1i** against *Enterobacter cloacae* SR36276 (class C producer) and *K. pneumoniae* SR08787(class D producer) were slightly lower than those of **1h**, but **1i** exhibited potent antibacterial activities against the other four strains. Therefore, **1i** was the most well-balanced compound with improved activities against the two target strains.

III-4. Assessment of Impact of Porin Deficiency on Antibacterial Activity

To assess the impact of porin deficiency, the MICs of compound **1a**, **1i**, CAZ **2**/AVI **3**, and ATM **6**/AVI **3** against *K. pneumoniae* NVT2001S and its recombinant derivative strains were determined (Table 3-2).⁹

Table 3-2. Antibacterial Activities Against *K. pneumoniae* NVT2001S and Its OmpK35/36-Deletion Strains with or without Carrying β -lactamase

Strain	Knock-out porin	Carrying β -lactamase			CAZ (2) + AVI (3 , 4 μ g/mL)	ATM (6) + AVI (3 , 4 μ g/mL)
			1a	1i		
NVT2001S	Parent	-	0.031	0.031	0.063	0.016
SR-L3006	Δ OmpK35	-	0.125	0.063	0.25	0.125
SR-L3007	Δ OmpK36	-	0.063	0.031	0.125	0.063
SR-L3008	Δ OmpK35 & Δ OmpK36	-	1	0.25	0.5	0.25
SR-L3014	-	pACYC177:: <i>bla</i> _{KPC-2}	0.063	0.031	0.5	0.5
SR 9872	Δ OmpK35 & Δ OmpK36	pACYC177:: <i>bla</i> _{KPC-2}	1	0.25	8	2

The single deletion of either OmpK35 or OmpK36 had no significant impact on the MICs of **1i**. However, double deletion of both genes increased the MICs by 8-fold for **1i**, with an 8-fold increase for CAZ **2**/AVI **3**, 16-fold for ATM **6**/AVI **3**, and 32-fold for **1a**.

When the OmpK35/36-deficient strain produces KPC-2, no significant MIC increase for **1a** or **1i** was exhibited compared to the OmpK35/36-deficient strain without KPC-2 production. On the other hand, the MICs of CAZ **2**/AVI **3** and ATM **6**/AVI **3** were affected by the KPC-2 production, irrespective of OmpK35/36-deficiency. Significant MIC shifts from 0.5 to 8 µg/mL for CAZ **2**/AVI **3** and from 0.25 to 2 µg/mL for ATM **6**/AVI **3** were observed against the OmpK35/36-deficient strain when combined with KPC-2 production. These results suggest that the antibacterial activities of **1i** against CREs are less affected by porin deficiency and hydrolysis by β -lactamases than BL/BLIs such as CAZ **2**/AVI **3** and ATM **6**/AVI **3**.

Table 3-3. *In Vitro* Activity against Porin-Deficient Enterobacterales

Strain	Characteristics	MIC (µg/mL)		
		1i	CAZ (2) /AVI (3)	ATM (6) /AVI (3)
<i>K. pneumoniae</i> NCTC13443	NDM-1, CMY-2 type, CTX-M-15, Δ OmpK35	0.5	>32	>32
<i>K. pneumoniae</i> SR08786	OXA-48, Δ OmpK35	0.25	>32	1
<i>K. pneumoniae</i> SR200062	PER-4, SHV-1, OXA-1, Δ OmpK35	\leq 0.031	>32	>32
<i>K. pneumoniae</i> SR200071	KPC-3, SHV-OSBL, TEM-OSBL, Δ OmpK35	0.125	16	1
<i>E. cloacae</i> SR200030	PER-2, Δ OmpF	0.5	>32	32
<i>C. freundii</i> SR200027	VEB-5, CTX-M-15, TEM-1, SHV-1, CMY-98-like, Δ OmpF	0.063	>32	16

Next, to investigate how the antibacterial activities against *K. pneumoniae* NVT2001S recombinant strains are transferred to the clinical isolates, the antibacterial activities of **1i** and BL/BLIs against clinically isolated strains with the porin deficiency where the MICs of CAZ **2**/AVI **3** were greater than or equal to 16 µg/mL were evaluated (Table 3-3).

ATM **6**/AVI **3** also showed high MIC values (≥ 16 $\mu\text{g/mL}$) except *K. pneumoniae* SR08786 and SR200071 (MICs = 1 $\mu\text{g/mL}$). However, **1i** showed potent activities against all porin-deficient strains (MICs ≤ 0.5 $\mu\text{g/mL}$). As these results show that **1i** has an advantage in antibacterial activities against clinical isolates with the porin deficiency.

III-5. Verification of Antibacterial Activity against Four-Amino-Acid Inserted Strains

To verify the antibacterial activities of **1i** against clinical isolates with a four-amino acid insertion, another resistance mechanism, the antibacterial activities of **1i** and ATM **6**/AVI **3** were evaluated against clinically isolated strains with the four-amino acid insertion and NDM-1 production (Table 3-4).

Table 3-4. *In Vitro* Activity against Four-Amino-Acid Inserted *E. coli*

Strain	Characteristics	MIC ($\mu\text{g/mL}$)	
		1i	ATM (6)/AVI (3)
<i>E. coli</i> SR08587	NDM-1, YRIN-inserted in PBP3	2	4
<i>E. coli</i> SR01463	NDM-1, YRIN-inserted in PBP3	2	8
<i>E. coli</i> SR08586	NDM-1, YRIK-inserted in PBP3	4	16
<i>E. coli</i> SR01442	NDM-1, ΔOmpF , YRIK-inserted in PBP3	4	16
<i>E. coli</i> SR200040	NDM-1, YRIK-inserted in PBP3	4	32

ATM **6**/AVI **3** showed high MIC values (≥ 16 $\mu\text{g/mL}$) except *E. coli* SR08587 and SR01463 (4 and 8 $\mu\text{g/mL}$, respectively). However, **1i** showed 2–8 fold improved activities over ATM **6**/AVI **3** against all four-amino acid inserted strains which include *E.*

coli SR01442 with both porin deficiency and four-amino acid insertion. These results indicate that **1i** has an advantage in antibacterial activities against clinical isolates with the four-amino acid insertion in addition to the porin deficiency.

III-6. Evaluation of *In Vitro* Antibacterial Activity

To further verify the potential of compound **1i**, expanded panels of clinically isolated carbapenemase-producing strains collected between 2014 and 2016 from various countries¹¹ were tested and the antibacterial activities of **1i** were compared with those of BL/BLIs (Table 3-5).

Against all four types (KPC, NDM, VIM, and OXA-48-like) of CREs tested, **1i** inhibited bacterial growth at ≤ 1 $\mu\text{g/mL}$ with the range of MIC_{90s} being from 0.125 to 0.5 $\mu\text{g/mL}$, while MIC_{90s} of CAZ **2**/AVI **3** were >64 $\mu\text{g/mL}$ against KPC, NDM, and VIM producers and 4 $\mu\text{g/mL}$ against OXA-48-like producers. The range of MIC_{90s} for ATM **6**/AVI **3** was from 0.25 to 1 $\mu\text{g/mL}$ against KPC-, NDM-, and OXA-48-like producers, being comparable or slightly inferior to compound **1i**. However, the MIC₉₀ of ATM **6**/AVI **3** was 2 $\mu\text{g/mL}$ against VIM producers, which was 4-fold that of **1i**. These results demonstrate that compound **1i** could be expected to exhibit more potent antibacterial activity against CREs than BL/BLIs.

Table 3-5. *In Vitro* Activity against Various Carbapenemase-Producing Enterobacterales

Enterobacterales (Number of strains)	Test compound	MIC ($\mu\text{g/mL}$)	
		Range	MIC ₉₀
KPC-producing strains (49) ^a	Compound 1i	≤ 0.031 –1	0.5
	CAZ (2)/AVI (3)	0.125–>64	>64
	ATM (6)/AVI (3)	≤ 0.031 –2	1
NDM-producing strains (22) ^b	Compound 1i	0.063–1	0.5
	CAZ (2)/AVI (3)	>64	>64
	ATM (6)/AVI (3)	≤ 0.031 –1	1
VIM-producing strains (25) ^c	Compound 1i	0.125–0.5	0.5
	CAZ (2)/AVI (3)	16–>64	>64
	ATM (6)/AVI (3)	0.063–2	2
OXA-48-like-producing strains (12) ^d	Compound 1i	0.063–1	0.125
	CAZ (2)/AVI (3)	0.063–16	4
	ATM (6)/AVI (3)	≤ 0.031 –1	0.25

a: 33 strains of *K. pneumoniae*, 5 strains of *Klebsiella oxytoca*, 5 strains of *Serratia marcescens*, 2 strains of *E. coli*, 2 strains of *Enterobacter aerogenes*, 1 strain of *E. cloacae*, and 1 strain of *Citrobacter freundii*, (29 strains of KPC-2 producer, 13 strains of KPC-3 producer, 1 strain of KPC-6 producer, 1 strain of KPC-18 producer, and 5 subtype unidentified strains).

b: 12 strains of *K. pneumoniae* and 10 strains of *E. cloacae* (19 strains of NDM-1 producer, 2 strains of NDM-6 producer, and 1 strain of NDM-7 producer).

c: 10 strains of *E. cloacae*, 5 strains of *K. pneumoniae*, 4 strains of *Citrobacter freundii*, 3 strains of *Serratia marcescens*, 1 strain of *Klebsiella oxytoca*, 1 strain of *E. coli*, and 1 strain of *C. amalonaticus* (23 strains of VIM-1 producer, 1 strain of VIM-5 producer, and 1 strain of VIM-19 producer).

d: 12 strains of *K. pneumoniae*.

III-7. Evaluation of Therapeutic Efficacy

To verify that compound **1i** exerts a therapeutic effect that reflects its potent in vitro antibacterial activities in clinical use, the therapeutic efficacies of **1i**, CAZ **2**/AVI **3**, and ATM **6**/ AVI **3** were examined using a cyclophosphamide-induced neutropenic mouse model of lung infections caused by KPC producing *K. pneumoniae* VA-391 (Figure 3-3).

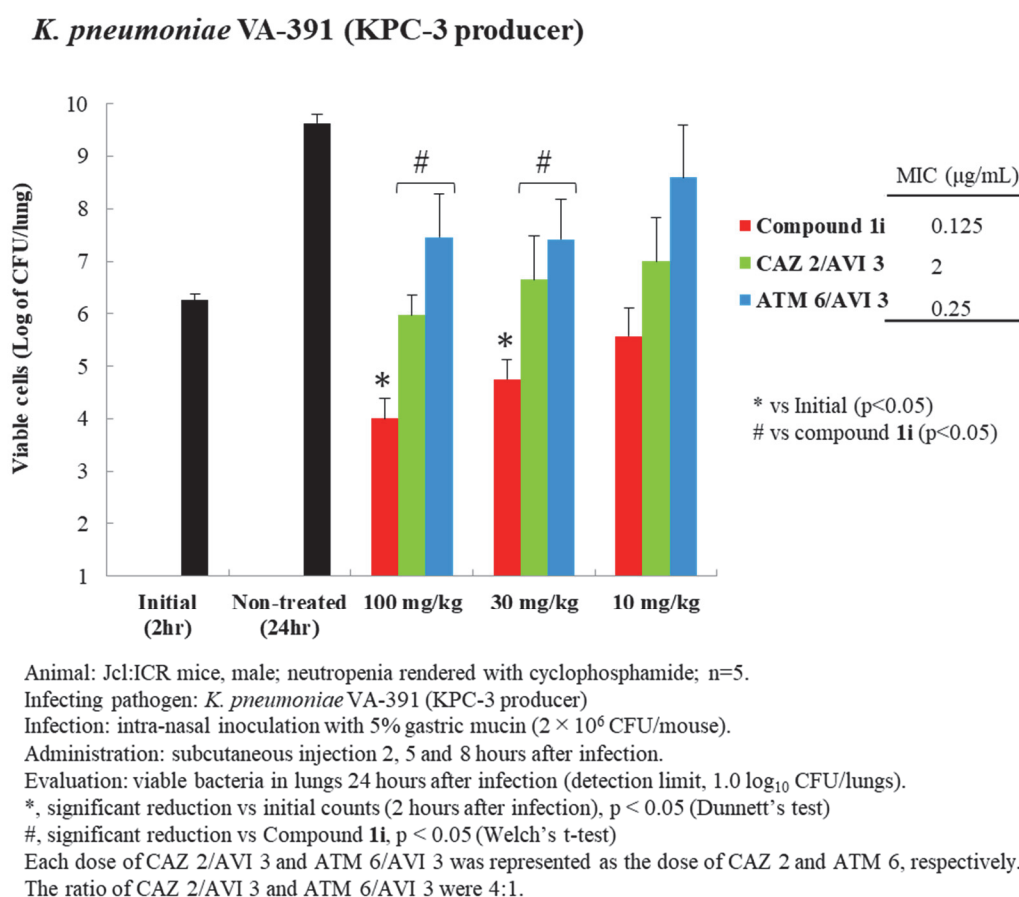


Figure 3-3. Therapeutic Efficacy in Neutropenic Mouse Lung Infection Model

The change in bacterial density was calculated as the difference in \log_{10} CFU from the antibiotic-treated mice after 24 h from the level in the 0 h control animals. **1i** showed

dose-dependent bactericidal efficacy with the reflection of its low MIC and achieved 2- \log_{10} CFU reductions from the initial counts at 100 mg/kg/dose, which is significantly superior to BL/BLIs at the same doses ($p < 0.05$). These results indicate that **1i** shows a strong bactericidal effect reflected by its *in vitro* antibacterial activity and consequently should offer a superior clinical outcome to BL/BLIs against problematic pathogens such as CRE.

III-8. Validation of Frequency of Spontaneously Resistant Mutants

Because **1i** showed strong therapeutic efficacy in the neutropenic mouse lung infection model, the frequency of spontaneous resistant mutants was validated to predict the possibility of resistant strains emerging during therapy (Table 3-6).¹²

Table 3-6. Frequency of Resistant Mutants against Six Enterobacterales ^a

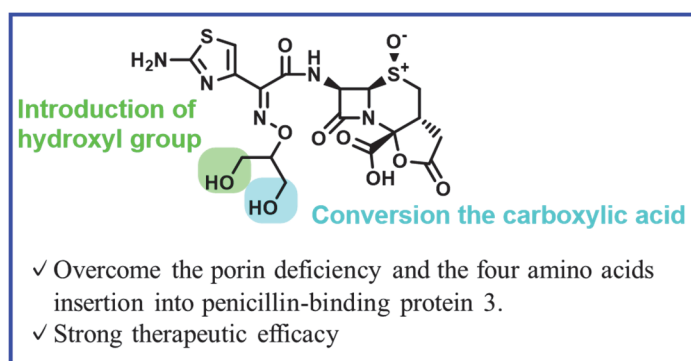
Test strain	Frequency of resistant mutants (MIC, $\mu\text{g/mL}$)	
	Compound 1i	CAZ (2)/AVI (3)
<i>E. coli</i> NIHJ JC-2	1.21×10^{-9} (0.031)	$< 9.39 \times 10^{-10}$ (0.125)
<i>K. pneumoniae</i> ATCC13883	$< 5.99 \times 10^{-10}$ (0.031)	$< 9.43 \times 10^{-10}$ (0.25)
<i>E. cloacae</i> SR36271 (AmpC)	$< 5.01 \times 10^{-10}$ (0.031)	NT
<i>E. coli</i> SR21266 (CTX-M-14)	$< 8.55 \times 10^{-10}$ (0.063)	$< 8.55 \times 10^{-10}$ (0.125)
<i>K. pneumoniae</i> SR01343 (KPC-2)	$< 1.05 \times 10^{-9}$ (0.125)	4.76×10^{-9} (1)
<i>K. pneumoniae</i> SR01453 (NDM-1)	$< 1.45 \times 10^{-9}$ (0.125)	$< 1.45 \times 10^{-9}$ ^b (0.125)

a: The bacterial inoculum was approximately 10^9 CFU. The number of mutant strains on MHA containing 10-fold MIC of each compound was counted. AVI **3**, fixed concentration of 4 $\mu\text{g/mL}$. NT, not tested.

b: ATM **6** was used instead of CAZ **2**.

The frequencies for **1i** against these test strains were $<1.05 \times 10^{-9}$, which are similar to those of the already approved CAZ **2**/AVI **3** or ATM **6**/AVI **3** under development. These results obviate the concern of spontaneous resistance mutations in the clinical use of **1i**.

III-9. Conclusion



This chapter describes the discovery of compound **1i** that overcomes the reduction of outer membrane permeability caused by porin deficiency with β -lactamase production and the insertion of four amino acids into PBP3, which significantly increases the MICs of BL/BLIs. Introduction of a hydrophilic functional group, a hydroxyl group, into the alkoxyimino moiety of the aminothiazole side chain and conversion of the carboxylic acid into another hydroxyl group to reduce the negative charge of the whole molecule from 2 to 1 are the keys to overcoming the porin deficiency. In addition, **1i** shows 2- to 8-fold improved antibacterial activities over ATM **6**/AVI **3** against clinical isolates with four-amino acid insertion and NDM-1 production. Therefore, this conversion is also effective for overcoming the four-amino acid insertion into PBP3. **1i** also shows strong therapeutic efficacy that is significantly superior to BL/BLIs in the neutropenic mouse lung infection model and a low frequency of the production of spontaneous resistant mutants, which is similar to the already approved CAZ **2**/AVI **3** (AVYCAZ®). These results demonstrate that **1i** is a promising drug candidate for infections caused by CREs including those with

reduced outer membrane permeability and the four-amino acid insertion into PBP3, in addition to β -lactamase production.

Experimental

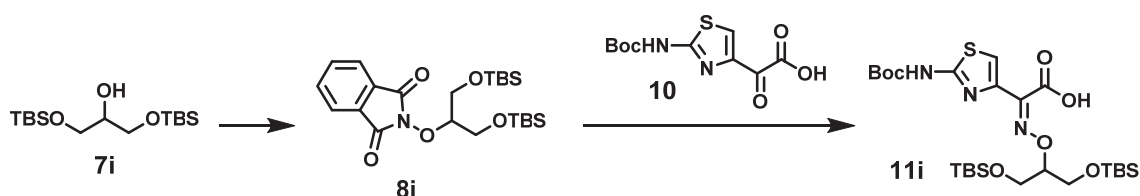
Unless otherwise noted, reactions were performed under a nitrogen atmosphere. Solvents and commercial reagents were used without purification. Ceftazidime **2** and aztreonam **6** were purchased from Tokyo Chemical Industry Co., Ltd. Avibactam **3** was purchased from Shanghai Haoyuan Chemexpress Co., Ltd. Meropenem **4** was purchased from FUJIFILM Wako Pure Chemical Corporation. Vaborbactam **5** was purchased from MedChemExpress LLC. All of these purchased antibiotics had a purity >98%. Compounds **7i**,¹³ **8b**,¹⁴ **8c**,¹⁵ **8d**,¹⁶ **8e**,¹⁷ **8f**,¹⁸ **8h**,¹⁹ and **11g**²⁰ were synthesized by the reported methods. ¹H and ¹³C NMR spectra were recorded on a Bruker AV400 spectrometer. Chemical shifts (δ) are reported in parts per million (ppm) from tetramethylsilane (in CDCl₃ and DMSO-*d*₆), sodium 2,2-dimethyl-2-silapentane-5-sulfonate (in D₂O) or the solvent residual peak (in DMSO-*d*₆ δ 2.50 and D₂O δ 4.79) as an internal reference. Analytical thin-layer chromatography was run on silica gel F254 precoated plates. Visualization of the developed chromatogram was done using fluorescence quenching or Vaughn's reagent. Flash column chromatography was carried out on an automated purification system using Yamazen or Fuji Silysia prepacked silica gel columns. Reverse phase column chromatography was performed using HP20SS and octadecylsilyl silica gel (Yamazen Ultra Pack). High-resolution mass spectral data were acquired on Orbitrap Q Exactive Plus (ESI). Low-resolution mass spectral data were collected on a Waters ZQ mass detector (ESI), a Shimadzu LCMS-8030 (ESI), or a Shimadzu LCMS-2020 (ESI). Elemental analysis was performed using a Micro Corder

JM11 (J-Science Lab Co., Ltd.) analyzer.

Strains were obtained from the American Type Culture Collection (Manassa, VA) and the National Collection of Type Cultures (Salisbury, United Kingdom). Clinical strains were kindly provided by the Bicêtre Hospital (Le Kremlin-Bicêtre, France), Dr. Koh Tse Hsien in Singapore General Hospital (Singapore), International Health Management Associates (Schaumburg, USA), and Dr. Robert A. Bonomo in Case Western Reserve University (Ohio, USA). Other test strains were obtained from various hospitals, mainly in Japan. *K. pneumoniae* NVT2001S and its OmpK35 and/or OmpK36 deletion mutants were kindly provided by the National Health Research Institutes of Taiwan.

All studies with animals were approved by the Institutional Animal Care and Use Committee of Shionogi & Co., Ltd.

Synthesis of Aminothiazole Side Chain 11i



Step 1. Synthesis of 2-((2,2,3,3,9,9,10,10-octamethyl-4,8-dioxo-3,9-disilaundecan-6-yl)oxy)isoindoline-1,3-dione (8i)

To a solution of compound **7i** (3.13 g, 9.8 mmol) in tetrahydrofuran (31 mL), *N*-hydroxyphthalimide (1.91 g, 11.7 mmol) and triphenylphosphine (3.07 g, 11.7 mmol) were added. Next, 1.9 mol/L solution of DIAD in toluene was added dropwise under ice cooling. The mixture was stirred at room temperature for 1 h and then concentrated under reduced pressure. Methanol was added to the residue. The resulting solid was collected by filtration and dried under reduced pressure to afford **8i** (3.07 g, yield 67%) as a white

solid.

^1H NMR (400 MHz, CDCl_3): δ 7.81 (2H, dd, $J = 5.5, 3.1$ Hz), 7.72 (2H, dd, $J = 5.5, 3.1$ Hz), 4.38–4.33 (1H, m), 3.93 (4H, ddd, $J = 14.6, 9.5, 3.3$ Hz), 0.81 (18H, s), 0.02 (6H, s), 0.00 (6H, s).

^{13}C NMR $\{^1\text{H}\}$ (100 MHz, CDCl_3): δ 163.67, 134.20, 129.21, 123.35, 88.20, 61.76, 25.75, 18.21, $-5.55, -5.58$.

HRMS (ESI) m/z : $[\text{M} + \text{H}]^+$ calcd for $\text{C}_{23}\text{H}_{39}\text{NO}_5\text{Si}_2$, 466.2440; found, 466.2437.

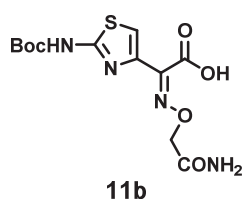
Step 2. Synthesis of (*Z*)-2-(2-((*tert*-Butoxycarbonyl)amino)thiazol-4-yl)-5-(((*tert*-Butyldimethylsilyl)oxy)methyl)-8,8,9,9-tetramethyl-4,7-dioxa-3-aza-8-siladec-2-enoic Acid (11i**)**

To a solution of compound **8i** (3.07 g, 6.6 mmol) in dichloromethane (30 mL), methylhydrazine (0.383 mL, 7.2 mmol) was added at -30 °C. Under ice cooling, the mixture was stirred for 30 min. The resulting insoluble material was removed by filtration. Compound **10** (1.79 g, 6.6 mmol) was added to the filtrate. The mixture was stirred at room temperature for 2 h and then concentrated under reduced pressure. Dilute hydrochloric acid was added to the residue, followed by extraction with ethyl acetate. The organic layer was washed with water and brine in this order and dried over anhydrous magnesium sulfate. After filtration, the filtrate was concentrated under reduced pressure. The residue was dissolved in diisopropyl ether. Next, triethylamine (1.1 mL, 7.9 mmol) was added to the solution. The resulting solid was collected by filtration and dried under reduced pressure to afford **11i** (1.79 g, yield 39%) as a white solid. **11i** was used in the

next step without further purification.

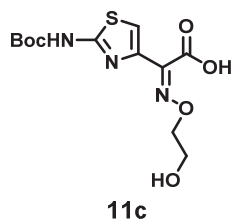
MS (ESI) m/z : $[M + H]^+$ calcd for $C_{25}H_{47}N_3O_7SSi_2$, 590; found, 590.

Aminothiazole side chains **11b–f, h** were prepared from compounds **8b–f, h** by a procedure similar to that described for **11i**.



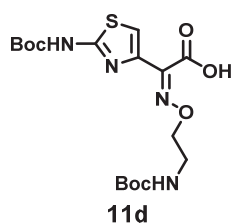
(Z)-2-((2-Amino-2-oxoethoxy)imino)-2-((tert-butoxycarbonyl)amino)thiazol-4-yl)acetic Acid (11b)

MS (ESI) m/z : $[M + H]^+$ calcd for $C_{12}H_{16}N_4O_6S$, 345; found, 345.



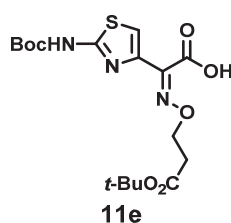
(Z)-2-((2-((tert-Butoxycarbonyl)amino)thiazol-4-yl)-2-((2-hydroxyethoxy)imino)acetic Acid (11c)

MS (ESI) m/z : $[M + H]^+$ calcd for $C_{12}H_{17}N_3O_6S$, 332; found, 332.



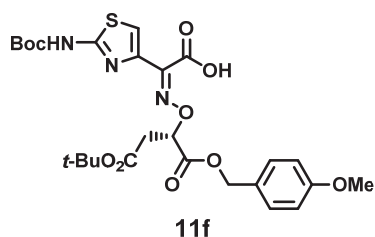
(Z)-2-(2-((*tert*-Butoxycarbonyl)amino)thiazol-4-yl)-10,10-dimethyl-8-oxo-4,9-dioxo-3,7-diazaundec-2-enoic Acid (11d)

MS (ESI) m/z : $[M + H]^+$ calcd for $C_{17}H_{26}N_4O_7S$, 431; found, 431.



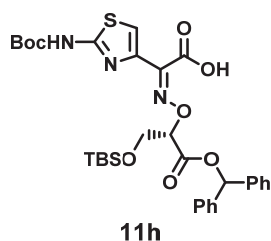
(Z)-2-((3-(*tert*-Butoxy)-3-oxopropoxy)imino)-2-(2-((*tert*-butoxycarbonyl)amino)thiazol-4-yl)acetic Acid (11e)

MS (ESI) m/z : $[M + H]^+$ calcd for $C_{17}H_{25}N_3O_7S$, 416; found, 416.



(*S,Z*)-2-(((4-(*tert*-Butoxy)-1-((4-methoxybenzyl)oxy)-1,4-dioxobutan-2-yl)oxy)imino)-2-(2-((*tert*-butoxycarbonyl)amino)thiazol-4-yl)acetic Acid (11f)

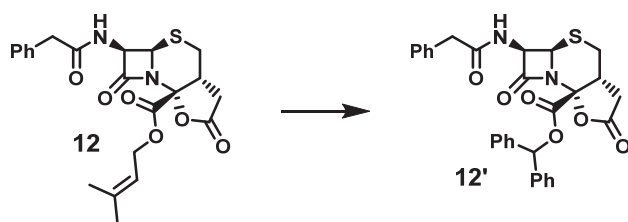
MS (ESI) m/z : $[M + H]^+$ calcd for $C_{26}H_{33}N_3O_{10}S$, 580; found, 580.



(*S,Z*)-5-((Benzhydryloxy)carbonyl)-2-(2-((*tert*-butoxycarbonyl)amino)thiazol-4-yl)-8,8,9,9-tetramethyl-4,7-dioxa-3-aza-8-siladec-2-enoic Acid (11h)

MS (ESI) m/z : $[M + H]^+$ calcd for $C_{32}H_{41}N_3O_8SSi$, 656; found, 656.

Synthesis of Compound 12'



Compound **12** (31.5 g, 70.9 mmol) was dissolved in tetrahydrofuran (320 mL), and then 5% palladium carbon (15.1 g, 7.09 mmol) was added to the solution. Under a hydrogen atmosphere, the mixture was stirred at room temperature for 4 h and 30 min. The catalyst was removed by filtration through Celite. Next, 5% palladium carbon (15.1 g, 7.09 mmol) was added again to the filtrate. Under a hydrogen atmosphere, the mixture was stirred at room temperature for 1 h. The catalyst was removed by filtration through Celite. Diphenyldiazomethane (15.1 g, 78.0 mmol) was added to the filtrate. The mixture was stirred at room temperature for 1 h. The solvent was evaporated. Ethyl acetate and diisopropyl ether were added to the residue. The resulting solid was collected by filtration and dried to afford **12'** (27.5 g, yield 71%) as a white solid.

1H NMR (400 MHz, $CDCl_3$): δ 7.38–7.26 (14H, m), 7.25 (1H, s), 6.93 (1H, s), 6.21 (1H, d, $J = 8.7$ Hz), 5.52 (1H, dd, $J = 8.7, 4.8$ Hz), 4.98 (1H, d, $J = 4.8$ Hz), 3.63 (2H, dd, $J =$

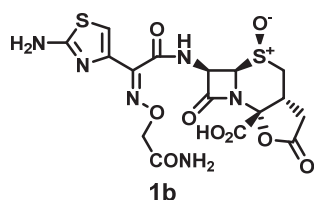
20.7, 16.1 Hz), 3.13–3.08 (1H, m), 2.90 (1H, dd, $J = 14.5, 4.5$ Hz), 2.60 (1H, dd, $J = 14.5, 9.6$ Hz), 2.52 (2H, t, $J = 3.1$ Hz).

^{13}C NMR $\{^1\text{H}\}$ (100 MHz, CDCl_3): δ 171.43, 170.97, 164.13, 163.69, 138.76, 138.18, 133.70, 129.48, 129.17, 128.75, 128.55, 128.51, 128.45, 127.74, 127.62, 127.01, 86.89, 80.88, 60.23, 56.29, 43.32, 35.63, 33.17, 27.01.

HRMS (ESI) m/z : $[\text{M} + \text{H}]^+$ calcd for $\text{C}_{30}\text{H}_{27}\text{N}_2\text{O}_6\text{S}$, 543.1584; found, 543.1581.

Synthesis of Compounds 1b–i

Compounds **1b–i** were synthesized using compound **12** or **12'** and aminothiazole side chain **11b–i** in the same manner as already reported in Chapter II.



(3a*R*,5*S*,5a*R*,6*R*,8a*R*)-6-((*Z*)-2-((2-Amino-2-oxoethoxy)imino)-2-(2-aminothiazol-4-yl)acetamido)-2,7-dioxohexahydro-7*H*,8a*H*-azeto[2,1-*b*]furo[2,3-*d*][1,3]thiazine-8a-carboxylic Acid 5-Oxide (**1b**)

^1H NMR (Na salt) (400 MHz, D_2O): δ 7.13 (1H, s), 5.88 (1H, d, $J = 4.8$ Hz), 5.02 (1H, d, $J = 4.8$ Hz), 4.76–4.70 (2H, m), 3.66–3.52 (2H, m), 3.07 (1H, dd, $J = 18.3, 7.8$ Hz), 2.83 (1H, dd, $J = 14.5, 12.6$ Hz), 2.57 (1H, d, $J = 18.3$ Hz).

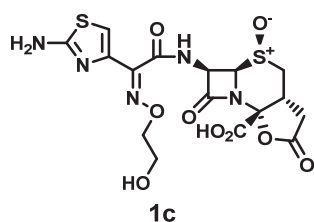
^{13}C NMR $\{^1\text{H}\}$ (Na salt) (100 MHz, D_2O): δ 178.46, 177.46, 173.91, 171.08, 167.02,

165.91, 152.55, 142.60, 117.42, 90.62, 75.61, 68.17, 62.12, 46.12, 36.70, 32.00.

Anal.: C₁₆H₁₅N₆O₉S₂Na(H₂O)_{3.8}.

Calcd: C, 32.52; H, 3.86; N, 14.22; S, 10.85; Na, 3.89 (%).

Found: C, 32.57; H, 3.92; N, 14.35; S, 10.65; Na, 3.94 (%).



(3aR,5S,5aR,6R,8aR)-6-((Z)-2-(2-Aminothiazol-4-yl)-2-((2-hydroxyethoxy)imino)acetamido)-2,7-dioxohexahydro-7H,8aH-azeto[2,1-b]furo[2,3-d][1,3]thiazine-8a-carboxylic Acid 5-Oxide (1c)

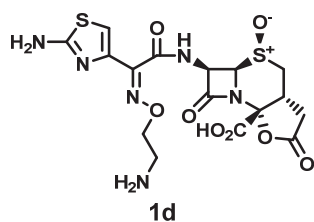
¹H NMR (Na salt) (400 MHz, D₂O): δ 7.04 (1H, s), 5.88 (1H, d, *J* = 4.6 Hz), 5.01 (1H, d, *J* = 4.6 Hz), 4.35–4.33 (2H, m), 3.90–3.88 (2H, m), 3.64 (1H, dd, *J* = 14.7, 5.1 Hz), 3.58–3.52 (1H, m), 3.07 (1H, dd, *J* = 18.4, 7.7 Hz), 2.85–2.78 (1H, m), 2.56 (1H, d, *J* = 18.4 Hz).

¹³C NMR {¹H}(Na salt) (100 MHz, D₂O): δ 178.48, 173.84, 171.09, 167.60, 166.09, 150.84, 143.14, 116.09, 90.64, 79.29, 68.29, 62.94, 62.08, 46.13, 36.72, 32.02.

Anal.: C₁₆H₁₆N₅O₉S₂Na(H₂O)_{4.3}.

Calcd: C, 32.74; H, 4.23; N, 11.93; S, 10.93; Na, 3.92 (%).

Found: C, 32.90; H, 4.16; N, 12.09; S, 10.75; Na, 3.92 (%).



(3aR,5S,5aR,6R,8aR)-6-((Z)-2-((2-Aminoethoxy)imino)-2-(2-aminothiazol-4-yl)acetamido)-2,7-dioxohexahydro-7H,8aH-azeto[2,1-b]furo[2,3-d][1,3]thiazine-8a-carboxylic Acid 5-Oxide (1d)

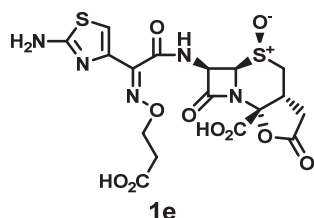
^1H NMR (400 MHz, D_2O): δ 7.08 (1H, s), 5.87 (1H, d, $J = 4.8$ Hz), 5.02 (1H, d, $J = 4.8$ Hz), 4.53–4.45 (2H, m), 3.65 (1H, dd, $J = 14.8, 5.1$ Hz), 3.58–3.52 (1H, m), 3.47–3.36 (2H, m), 3.07 (1H, dd, $J = 18.3, 7.8$ Hz), 2.84 (1H, dd, $J = 14.8, 12.9$ Hz), 2.57 (1H, d, $J = 18.3$ Hz).

^{13}C NMR $\{^1\text{H}\}$ (100 MHz, D_2O): δ 178.43, 174.00, 171.12, 167.15, 166.10, 151.75, 142.84, 117.08, 90.57, 73.91, 68.22, 62.20, 46.13, 41.68, 36.68, 32.03.

Anal.: $\text{C}_{16}\text{H}_{18}\text{N}_6\text{O}_8\text{S}_2(\text{H}_2\text{O})_{3.4}$.

Calcd: C, 35.09; H, 4.56; N, 15.34; S, 11.71 (%).

Found: C, 35.06; H, 4.51; N, 15.46; S, 11.79 (%).



(3aR,5S,5aR,6R,8aR)-6-((Z)-2-(2-Aminothiazol-4-yl)-2-((2-carboxyethoxy)imino)acetamido)-2,7-dioxohexahydro-7H,8aH-azeto[2,1-

***b*[furo[2,3-*d*][1,3]thiazine-8a-carboxylic Acid 5-Oxide (1e)**

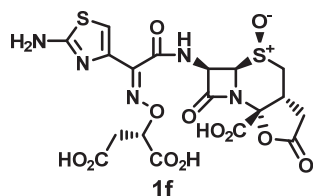
^1H NMR (Na salt) (400 MHz, D_2O): δ 7.03 (1H, s), 5.86 (1H, d, $J = 4.8$ Hz), 5.00 (1H, d, $J = 4.8$ Hz), 4.47–4.43 (2H, m), 3.64 (1H, dd, $J = 14.7, 5.3$ Hz), 3.58–3.52 (1H, m), 3.07 (1H, dd, $J = 18.3, 7.8$ Hz), 2.82 (1H, dd, $J = 14.7, 12.5$ Hz), 2.68 (2H, t, $J = 6.5$ Hz), 2.57 (1H, d, $J = 18.3$ Hz).

^{13}C NMR $\{^1\text{H}\}$ (Na salt) (100 MHz, D_2O): δ 181.87, 178.52, 173.80, 171.13, 167.61, 166.15, 150.65, 143.06, 115.91, 90.70, 75.01, 68.31, 61.94, 46.08, 39.40, 36.73, 32.05.

Anal.: $\text{C}_{17}\text{H}_{15.2}\text{N}_5\text{O}_{10}\text{S}_2\text{Na}_{1.8}(\text{H}_2\text{O})_{3.9}$.

Calcd: C, 32.65; H, 3.71; N, 11.20; S, 10.25; Na, 6.62 (%).

Found: C, 32.61; H, 3.86; N, 11.44; S, 10.07; Na, 6.52 (%).



(*S*)-2-((((*Z*)-1-(2-Aminothiazol-4-yl)-2-(((3*aR*,5*S*,5*aR*,6*R*,8*aR*)-8a-carboxy-5-oxido-2,7-dioxohexahydro-4*H*,7*H*-azeto[2,1-*b*]furo[2,3-*d*][1,3]thiazin-6-yl)amino)-2-oxoethylidene)amino)oxy)succinic Acid (1f)

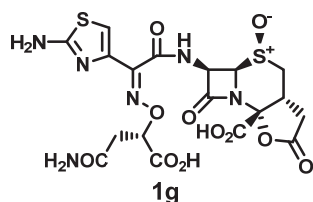
^1H NMR (Na salt) (400 MHz, D_2O): δ 7.05 (1H, s), 5.89 (1H, d, $J = 4.8$ Hz), 5.00 (1H, d, $J = 4.8$ Hz), 4.96 (1H, dd, $J = 10.0, 3.6$ Hz), 3.63 (1H, dd, $J = 14.6, 5.3$ Hz), 3.58–3.52 (1H, m), 3.06 (1H, dd, $J = 18.3, 7.7$ Hz), 2.84–2.74 (2H, m), 2.66 (1H, dd, $J = 16.1, 9.9$ Hz), 2.57 (1H, d, $J = 18.3$ Hz).

^{13}C NMR $\{^1\text{H}\}$ (Na salt) (100 MHz, D_2O): δ 181.36, 180.60, 178.54, 173.75, 171.13, 167.50, 166.32, 150.36, 143.11, 115.98, 90.75, 85.48, 68.25, 61.86, 45.98, 41.98, 36.75, 32.06.

Anal.: $\text{C}_{18}\text{H}_{14.3}\text{N}_5\text{O}_{12}\text{S}_2\text{Na}_{2.7}(\text{H}_2\text{O})_{4.5}$.

Calcd.: C, 30.89; H, 3.36; N, 10.01; S, 9.16; Na, 8.87 (%).

Found: C, 30.77; H, 3.34; N, 10.20; S, 8.98; Na, 8.99 (%).



(3a*R*,5*S*,5a*R*,6*R*,8a*R*)-6-((*Z*)-2-(((*S*)-3-Amino-1-carboxy-3-oxopropoxy)imino)-2-(2-aminothiazol-4-yl)acetamido)-2,7-dioxohexahydro-7*H*,8a*H*-azeto[2,1-*b*]furo[2,3-*d*][1,3]thiazine-8a-carboxylic Acid 5-Oxide (1g)

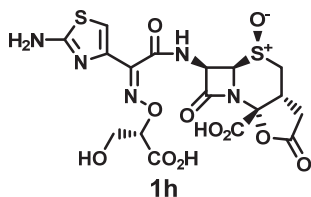
^1H NMR (400 MHz, D_2O): δ 7.23 (1H, s), 5.88 (1H, d, $J = 4.9$ Hz), 5.08 (1H, t, $J = 6.8$ Hz), 5.00 (1H, d, $J = 4.9$ Hz), 3.63 (1H, dd, $J = 14.7, 5.1$ Hz), 3.57–3.51 (1H, m), 3.06 (1H, dd, $J = 18.3, 7.9$ Hz), 2.91 (2H, t, $J = 8.3$ Hz), 2.81 (1H, t, $J = 13.6$ Hz), 2.55 (1H, d, $J = 18.3$ Hz).

^{13}C NMR $\{^1\text{H}\}$ (100 MHz, D_2O): δ 178.47, 177.57, 177.30, 173.65, 171.09, 166.10, 164.20, 146.77, 133.96, 115.45, 90.59, 83.43, 68.14, 62.21, 46.14, 39.77, 36.78, 32.07.

Anal.: C₁₈H₁₈N₆O₁₁S₂(H₂O)_{3.5}.

Calcd: C, 34.78; H, 4.05; N, 13.52; S, 10.32 (%).

Found: C, 34.91; H, 3.96; N, 13.73; S, 10.08 (%).



(3aR,5S,5aR,6R,8aR)-6-((Z)-2-(2-Aminothiazol-4-yl)-2-(((S)-1-carboxy-2-hydroxyethoxy)imino)acetamido)-2,7-dioxohexahydro-7H,8aH-azeto[2,1-b]furo[2,3-d][1,3]thiazine-8a-carboxylic Acid 5-Oxide (1h)

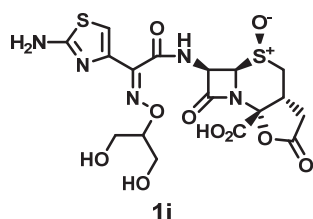
¹H NMR (Na salt) (400 MHz, D₂O): δ 7.06 (1H, s), 5.90 (1H, d, *J* = 4.6 Hz), 5.03 (1H, d, *J* = 4.6 Hz), 4.75–4.73 (1H, m), 4.02–3.94 (2H, m), 3.65 (1H, dd, *J* = 14.7, 5.1 Hz), 3.59–3.52 (1H, m), 3.07 (1H, dd, *J* = 18.3, 7.7 Hz), 2.82 (1H, t, *J* = 13.7 Hz), 2.57 (1H, d, *J* = 18.3 Hz).

¹³C NMR {¹H}(Na salt) (100 MHz, D₂O): δ 179.07, 178.48, 173.75, 171.07, 167.57, 166.17, 150.62, 143.31, 116.06, 90.64, 89.47, 68.30, 64.70, 62.06, 46.07, 36.72, 32.01.

Anal.: C₁₇H₁₅N₅O₁₁S₂Na₂(H₂O)_{2.5}.

Calcd: C, 32.91; H, 3.25; N, 11.29; S, 10.33; Na, 7.41 (%).

Found: C, 32.91; H, 3.30; N, 11.31; S, 10.19; Na, 7.39 (%).



(3aR,5S,5aR,6R,8aR)-6-((Z)-2-(2-Aminothiazol-4-yl)-2-(((1,3-dihydroxypropan-2-yl)oxy)imino)acetamido)-2,7-dioxohexahydro-7H,8aH-azeto[2,1-b]furo[2,3-d][1,3]thiazine-8a-carboxylic Acid 5-Oxide (1i)

^1H NMR (Na salt) (400 MHz, D_2O): δ 7.05 (1H, s), 5.90 (1H, d, $J = 4.8$ Hz), 5.03 (1H, d, $J = 4.8$ Hz), 4.47-4.41 (1H, m), 3.86 (4H, t, $J = 5.1$ Hz), 3.65 (1H, dd, $J = 14.8, 5.3$ Hz), 3.59–3.52 (1H, m), 3.07 (1H, dd, $J = 18.3, 7.8$ Hz), 2.84 (1H, dd, $J = 14.6, 12.6$ Hz), 2.57 (1H, d, $J = 18.3$ Hz).

^{13}C NMR $\{^1\text{H}\}$ (Na salt) (100 MHz, D_2O): δ 178.46, 173.87, 171.05, 167.67, 166.10, 150.89, 143.23, 116.10, 90.62, 88.97, 68.33, 63.40, 63.30, 62.06, 46.10, 36.71, 32.01.

Anal.: $\text{C}_{17}\text{H}_{18}\text{N}_5\text{O}_{10}\text{S}_2\text{Na}(\text{H}_2\text{O})_{1.8}$.

Calcd: C, 35.70; H, 3.81; N, 12.25; S, 11.21; Na, 4.02 (%).

Found: C, 35.55; H, 3.80; N, 12.40; S, 11.07; Na, 4.07 (%).

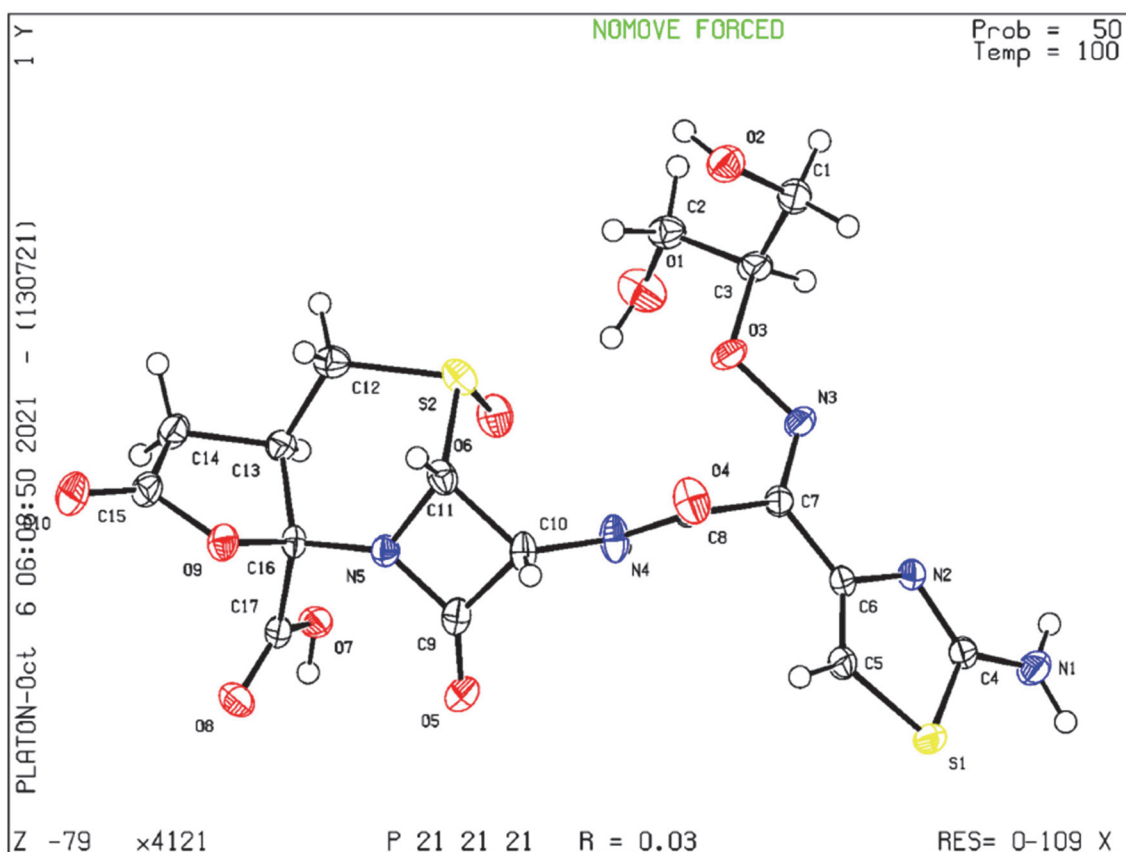
X-ray crystallographic data of compound 1i

X-ray Crystallography: The diffraction data of **1i** were collected on an XtaLAB AFC10 (RCD3): quarter-chi single diffractometer. The crystal was kept at 100.0 K during data collection. Using Olex2,1 the structure was solved with the ShelXT2 structure solution program using Intrinsic Phasing and refined with the ShelXL3 refinement package using Least Squares minimization.

Sample Preparation: X-ray quality crystal was prepared by vapor diffusion method using acetone–water at room temperature.

Compound 1i

CCDC Deposition Number; 2114100



Identification code; X4121

Empirical formula; C₁₇H₁₉N₅O₁₀S₂

Formula weight; 517.49

Temperature; 100 K

Crystal system; orthorhombic

Space group; P2₁2₁2₁

Unit cell dimension;

$\alpha = 9.20570(10) \text{ \AA}$ $\alpha = 90^\circ$

$\beta = 14.1061(2) \text{ \AA}$ $\beta = 90^\circ$

$\gamma = 16.0407(2) \text{ \AA}$ $\gamma = 90^\circ$

Volume; 2082.99(5) \AA^3

Z; 4

Density (calculated) 1.650 g/cm^3

Absorption coefficient; 2.955 μ/mm^{-1}

F(000); 1072.0

Crystal size; 0.12 \times 0.03 \times 0.02 mm

Radiation; CuK α ($\lambda = 1.54184 \text{ \AA}$)

2 Θ range for data collection; 8.348 to 144.496 $^\circ$

Index ranges; $-11 \leq h \leq 10$, $-14 \leq k \leq 17$, $-19 \leq l \leq 18$

Reflections collected; 11262

Independent reflections; 4012 [$R_{\text{int}} = 0.0225$, $R_{\text{sigma}} = 0.0262$]

Data / restraints / parameters; 4012 / 0 / 310

Goodness-of-fit on F^2 ; 1.078

Final R indexes [$I \geq 2\sigma(I)$]; $R_1 = 0.0335$, $wR_2 = 0.0921$

Final R indexes [all data]; $R_1 = 0.0354$, $wR_2 = 0.0931$

Largest diff. peak / hole; 1.06 / -0.30 e\AA^{-3}

Flack parameter; 0.003(7)

Evaluation of *In Vitro* Antibacterial Activity

The MICs were determined using the broth microdilution method in accordance with

Clinical Laboratory Standards Institute guidelines. Briefly, two-fold serial dilutions of the test compounds were prepared and transferred to a 96-well plate containing Cation-Adjusted Mueller–Hinton broth. The bacterial suspension for the inoculum was prepared based on an optical density of 625 nm for a final inoculum size of approximately 5×10^4 CFU/well. The 96-well plates were incubated at 35 °C for 16 to 20 h. The MIC endpoint was defined as the lowest concentration of the compound that inhibited bacterial growth as detected by the naked eye.

Spontaneous Mutation Frequency Study

The frequency of spontaneous resistant mutants following overnight culture on CAMHA containing 10-fold MIC of each compound was examined. The number of CFUs recovered was counted, and this value was compared to the parental bacterial density (6.9×10^8 to 2.5×10^9 CFU) to generate the frequency of mutation.

Evaluation of Therapeutic Efficacy in the Cyclophosphamide-Induced Neutropenic Mouse Model of Lung Infections

The neutropenic mouse lung infections outlined by Koomanachai et al.²¹ and Drusano et al.²² were tested. Five-week-old, specific-pathogen-free, male Jcl:ICR mice (weight, 17 to 20 g) were obtained from CLEA Japan, Inc. (Tokyo, Japan). The mice were anesthetized by intramuscular injection of a mixture of tiletamine, zolazepam, and xylazine. The mice were infected by intranasal instillation of 0.07 ml of bacterial suspension. The challenge doses ranged from approximately 10^5 to 10^6 CFU/lung.

Reference

-
- ¹ (a) Centers for Disease Control and Prevention (CDC). *Antibiotic Resistance Threats in the United States 2019*, Atlanta, GA; U.S. Department of Health and Human Services, CDC, 2019. Retrieved from <https://www.cdc.gov/drugresistance/pdf/threats-report/2019-ar-threats-report-508.pdf> (accessed November 22, 2022). (b) World Health Organization. *Global priority list of antibiotic-resistant bacteria to guide research, discovery, and development of new antibiotics*; WHO, February 27, 2017. Retrieved from <https://www.aidsdatahub.org/resource/who-global-priority-list-antibiotic-resistant-bacteria> (accessed November 22, 2022).
- ² Ambler, R. P. The structure of β -lactamases. *Philos. Trans. R. Soc., B* **1980**, 289, 321–331.
- ³ (a) Nordmann, P.; Dortet, L.; Poirel, L. Carbapenem resistance in *Enterobacteriaceae*: here is the storm! *Trends Mol. Med.* **2012**, 18, 263–272. (b) van Duin, D.; Doi, Y. The global epidemiology of carbapenemase-producing *Enterobacteriaceae*. *Virulence* **2017**, 8, 460–469.
- ⁴ (a) Shen, Z.; Ding, B.; Ye, M.; Wang, P.; Bi, Y.; Wu, S.; Xu, X.; Guo, Q.; Wang, M. High ceftazidime hydrolysis activity and porin OmpK35 deficiency contribute to the decreased susceptibility to ceftazidime/avibactam in KPC-producing *Klebsiella pneumoniae*. *J. Antimicrob. Chemother.* **2017**, 72, 1930–1936. (b) Lomovskaya, O.; Sun, D.; Rubio-Aparicio, D.; Nelson, K.; Tsivkovski, R.; Griffith, D. C.; Dudley, M. N. Vaborbactam: Spectrum of Beta-Lactamase Inhibition and Impact of Resistance Mechanisms on Activity in *Enterobacteriaceae*. *Antimicrob. Agents Chemother.* **2017**, 61, 1–15.
- ⁵ (a) Sato, T.; Ito, A.; Ishioka, Y.; Matsumoto, S.; Rokushima, M.; Kazmierczak, K. M.;

Hackel, M.; Sahm, D. F.; Yamano, Y. *Escherichia coli* strains possessing a four amino acid YRIN insertion in PBP3 identified as part of the SIDERO-WT-2014 surveillance study. *JAC-Antimicrob. Resist.* **2020**, *2*, dlaa081. (b) Alm, R. A.; Johnstone, M. R.; Lahiri, S. D. Characterization of *Escherichia coli* NDM isolates with decreased susceptibility to aztreonam/avibactam: role of a novel insertion in PBP3. *J. Antimicrob. Chemother.* **2015**, *70*, 1420–1428.

⁶ (a) Pagès, J.-M.; James, C. E.; Winterhalter, M. The porin and the permeating antibiotic: a selective diffusion barrier in Gram-negative bacteria. *Nat. Rev. Microbiol.* **2008**, *6*, 893–903. (b) James, C. E.; Mahendran, K. R.; Molitor, A.; Bolla, J.-M.; Bessonov, A. N.; Winterhalter, M.; Pagès, J.-M. How β -Lactam Antibiotics Enter Bacteria: A Dialogue with the Porins. *PLoS One* **2009**, *4*, No. e5453. (c) Martínez-Martínez, L.; Pascual, A.; Hernández-Allés, S.; Alvarez-Díaz, D.; Suárez, A. I.; Tran, J.; Benedí, V. J.; Jacoby, G. A. Roles of β -Lactamases and Porins in Activities of Carbapenems and Cephalosporins against *Klebsiella pneumoniae*. *Antimicrob. Agents Chemother.* **1999**, *43*, 1669–1673.

⁷ Goodman, K.; Simner, P.; Tamma, P.; Milstone, A. Infection control implications of heterogeneous resistance mechanisms in carbapenem-resistant Enterobacteriaceae (CRE). *Expert Rev. Anti-Infect. Ther.* **2016**, *14*, 95–108.

⁸ Davies, T. A.; Page, M. G. P.; Shang, W.; Andrew, T.; Kania, M.; Bush, K. Binding of Ceftobiprole and Comparators to the Penicillin-Binding Proteins of *Escherichia coli*, *Pseudomonas aeruginosa*, *Staphylococcus aureus*, and *Streptococcus pneumoniae*. *Antimicrob. Agents Chemother.* **2007**, *51*, 2621–2624.

⁹ (a) Tsai, Y.-K.; Fung, C.-P.; Lin, J.-C.; Chen, J.-H.; Chang, F.-Y.; Chen, T.-L.; Siu, L. K. *Klebsiella pneumoniae* outer membrane porins OmpK35 and OmpK36 play roles in both antimicrobial resistance and virulence. *Antimicrob. Agents Chemother.* **2011**, *55*,

1485–1493. (b) Ito, A.; Sato, T.; Ota, M.; Takemura, M.; Nishikawa, T.; Toba, S.; Kohira, N.; Miyagawa, S.; Ishibashi, N.; Matsumoto, S.; Nakamura, R.; Tsuji, M.; Yamano, Y. In vitro antibacterial properties of cefiderocol, a novel siderophore cephalosporin, against Gram-negative bacteria. *Antimicrob. Agents Chemother.* 2018, 62, e01454–17. (c) Tsai, Y.-K.; Liou, C.-H.; Fung, C.-P.; Lin, J.-C.; Siu, L. K. Single or in combination antimicrobial resistance mechanisms of *Klebsiella pneumoniae* contribute to varied susceptibility to different carbapenems. *PLoS One* 2013, 8, No. e79640.

¹⁰ (a) Yoshimura, F.; Nikaido, H. Diffusion of beta-lactam antibiotics through the porin channels of *Escherichia coli* K-12. *Antimicrob. Agents Chemother.* **1985**, 27, 84–92. (b) Nikaido, H.; Rosenberg, E. Y.; Foulds, J. Porin channels in *Escherichia coli*: studies with beta-lactams in intact cells. *J. Bacteriol.* **1983**, 153, 232–240.

¹¹ (a) Yamano, Y. In Vitro Activity of Cefiderocol Against a Broad Range of Clinically Important Gram-negative Bacteria. *Clin. Infect. Dis.* **2019**, 69, S544–S551. (b) Hackel, M. A.; Tsuji, M.; Yamano, Y.; Echols, R.; Karlowsky, J. A.; Sahm, D. F. In vitro activity of the siderophore cephalosporin, cefiderocol, against carbapenem-nonsusceptible and multidrugresistant isolates of Gram-negative bacilli collected worldwide in 2014 to 2016. *Antimicrob. Agents Chemother.* **2018**, 62, e01968–e02007.

¹² Martinez, J. L.; Baquero, F. Mutation frequencies and antibiotic resistance. *Antimicrob. Agents Chemother.* **2000**, 44, 1771–1777.

¹³ Baszczyński, O.; Jansa, P.; Dračinský, M.; Klepetářová, B.; Holý, A.; Votruba, I.; Clercq, E. d.; Balzarini, J.; Janeba, Z. Synthesis and antiviral activity of N⁹-[3-fluoro-2-(phosphonomethoxy)propyl] analogues derived from N⁶-substituted adenines and 2,6-diaminopurines. *Bioorg. Med. Chem.* **2011**, 19, 2114–2124.

-
- ¹⁴ Horiguchi, Y.; Imoto, H.; Wolf, M. A. Preparation of 6-azaindoles as I κ B kinase inhibitors for treating diabetes and inflammatory diseases. WO 2005097129 A3, Oct 20, 2005.
- ¹⁵ Tan, L.; Tao, Y.; Wang, T.; Zou, F.; Zhang, S.; Kou, Q.; Niu, A.; Chen, Q.; Chu, W.; Chen, X.; Wang, H.; Yang, Y. Discovery of Novel Pyridone-Conjugated Monosulfactams as Potent and Broad-Spectrum Antibiotics for Multidrug-Resistant Gram-Negative Infections. *J. Med. Chem.* **2017**, *60*, 2669–2684.
- ¹⁶ Grünewald, J.; Jin, Y.; Vance, J.; Read, J.; Wang, X.; Wan, Y.; Zhou, H.; Ou, W.; Klock, H. E.; Peters, E. C.; Uno, T.; Brock, A.; Geierstanger, B. H. Optimization of an Enzymatic Antibody-Drug Conjugation Approach Based on Coenzyme A Analogs. *Bioconjugate Chem.* **2017**, *28*, 1906–1915.
- ¹⁷ Ge, Y.; Wu, X.; Zhang, D.; Hu, L. 3-Aminoxypropionate-based linker system for cyclization activation in prodrug design. *Bioorg. Med. Chem. Lett.* **2009**, *19*, 941–944.
- ¹⁸ Liao, X.; Pearson, N. D.; Pendrak, I.; Sano, M. Preparation of Cephalosporins as Antibacterial Compounds. WO 2013052568 A1. Apr 11, 2013.
- ¹⁹ Yamawaki, K.; Nomura, T.; Yasukata, T.; Uotani, K.; Miwa, H.; Takeda, K.; Nishitani, Y. A novel series of parenteral cephalosporins exhibiting potent activities against *Pseudomonas aeruginosa* and other Gram-negative pathogens: Synthesis and structure-activity relationships. *Bioorg. Med. Chem.* **2007**, *15*, 6716–6732.
- ²⁰ Nishitani, Y.; Yamawaki, K.; Takeoka, Y.; Sugimoto, H.; Hisakawa, S.; Aoki, T. Preparation of cephalosporins having catechol group as antibacterial agents. WO 2010050468 A1. May 6, 2010.
- ²¹ Koomanachai, P.; Kim, A.; Nicolau, D. P. Pharmacodynamic evaluation of tigecycline against *Acinetobacter baumannii* in a murine pneumonia model. *J Antimicrob Chemother.*

2009, 63, 982–987.

²² Drusano, G. L.; Lodise, T. P.; Melnick, D. et al. Meropenem penetration into epithelial lining fluid in mice and humans and delineation of exposure targets. *Antimicrob Agents Chemother.* **2011**, 55, 3406–3412.

Chapter IV Stereoselective Synthesis of Tricyclic β -lactam Core

IV-1. Introduction

β -Lactam antibiotics have released people from the threat of bacterial infections since the discovery of penicillin, but their use has also led to the emergence of serious resistant strains. The U.S. CDC and the WHO have sent out alerts about the urgent need for new treatment options for infections with carbapenem-resistant Enterobacterales (CREs), as cases of antimicrobial resistance (AMR) has become a significant worldwide public health.¹

In Chapter III, the author identified the novel identified tricyclic β -lactam **3** as a promising drug candidate for infectious diseases caused by CREs. The structure of **3** is a merger of the third-generation cephalosporin ceftazidime (**1**) and a cycloserine natural product named lactivicin (LTV, **2**) (Figure 4-1).² The unique tricyclic β -lactam exhibits potent antibacterial activities against several problematic β -lactamase-producing CREs without the use of β -lactamase inhibitors.

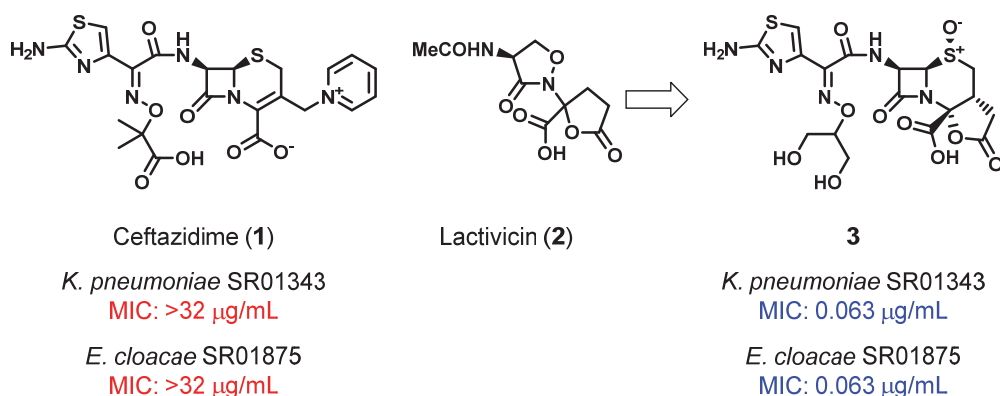
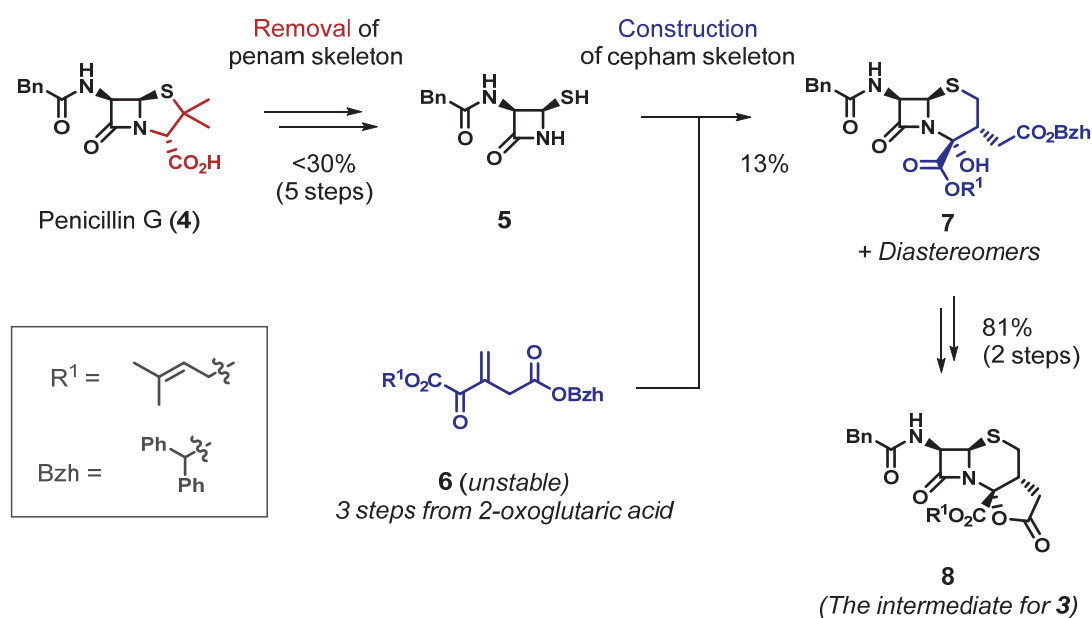


Figure 4-1. Structure and Minimum Inhibitory Concentration (MIC) of Ceftazidime **1**, Lactivicin **2** and **3**

While **3** showed attractive in vitro and in vivo antibiological activity, the complexity of the tricyclic β -lactam structure had posed a challenge to the scale-up of materials. **3** has a tricyclic fused high-Fsp³ core, including consecutive N–S and N–O acetals. Five chiral stereocenters determined by the X-ray crystal structure are essential for both the recognition mimicking *D*-alanyl-*D*-alanine of substrates by penicillin-binding proteins (PBPs), which play an essential role in bacterial cell wall synthesis, and the escape from the recognition by β -lactamase. It has been reported that regioisomers of such tricyclic β -lactams have significantly reduced antibacterial activities.

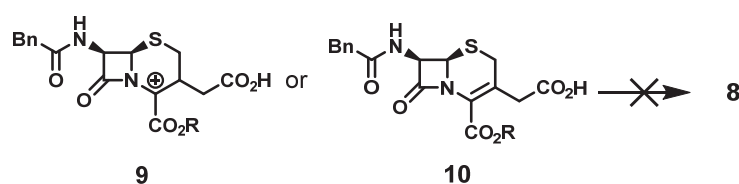
Scientists at Takeda synthesized **8**, an intermediate leading to **3**, by two transformations from penicillin in the 1980s:³ (a) ring opening and removal of the penam structure of **4** to form **5** and (b) reaction with **6** to construct the six-membered ring, which possesses functional groups enabling the third lactone cyclization (Scheme 4-1).



Scheme 4-1. Known Synthetic Route for Tricyclic β -lactam Core **8**

This route enabled to commence structure-activity relationship (SAR) effort, but challenges remained for scale-up of the synthesis and sufficient supply of the intermediate for further backup SAR. The issues related to the synthesis of the key intermediate **8** were (a) the long route (eight linear steps) from penicillin G, (b) the use of the labile enone **6**, which easily isomerizes and polymerizes, and (c) the formation of undesired diastereomers of **7**. He was also concerned from the viewpoint of atom economy that the four carbon atoms originally constituting the penicillin ring had not been used, requiring another unit of **6** in order to rebuild the second ring. Thus, a second-generation synthetic route of the unique tricyclic β -lactam core **8** was required..

Stereocontrol of the chiral center at the N–O acetal of **8** is the most important point. Epimerization of the hemiaminal of **7** was observed in the previous synthesis, which could be explained by the similar nature to **2** existing as epimers.⁴ In contrast, no epimerization was observed for cyclized lactone **8**. Therefore, he considered stereoselective lactone formation. Initial attempts at nucleophilic addition of a carboxylic group to a cationic intermediate or direct lactonization failed (Scheme 4-2).

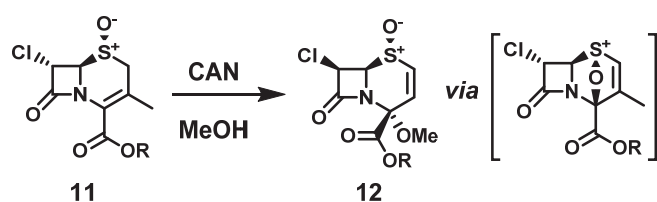


Scheme 4-2. Failed Attempts at Cyclization

He concluded that such a cationic intermediate might be disfavored and that direct lactonization might also be disfavored because the double bond is less reactive with

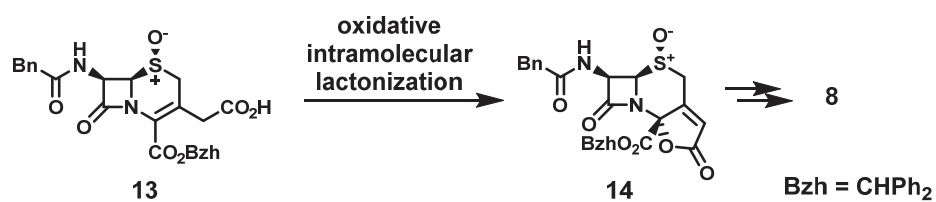
electrophiles as a result of the carboxyl group at C4. Indeed, Balsamo et al. reported that reduction of the carboxyl group to the alcohol influences the reactivity of the olefin.⁵

In 1994, Alpegiani et al. reported that oxidation of **11** using cerium ammonium nitrate (CAN) in methanol gave alkoxyated compound **12** (Scheme 4-3).⁶



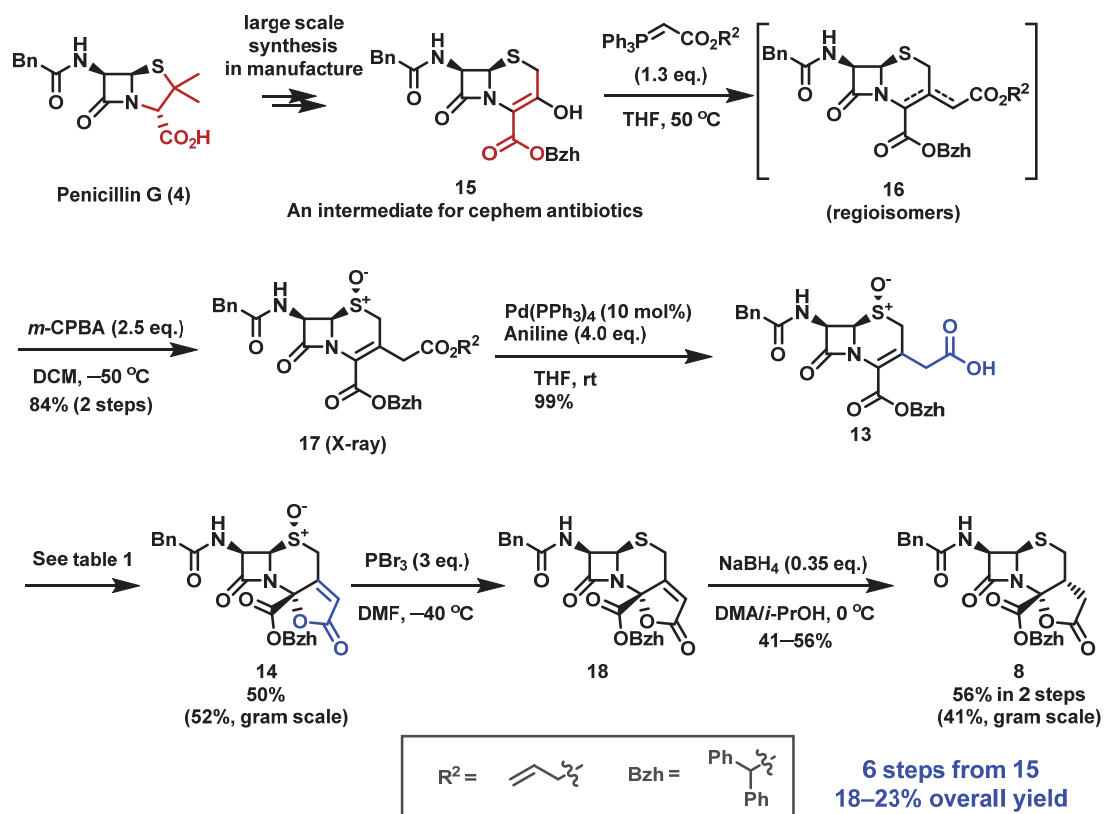
Scheme 4-3. Stereo-Controlled Oxidative Alkoxylation of Sulfoxide Reported by Alpegiani *et al.*

Interestingly, the alkoxylation proceeded in a stereoselective manner, and they assumed that the reaction would proceed via a sulfonium intermediate followed by stereoselective addition of alcohol. Inspired by their work, he envisioned that the tricyclic β -lactam core would be constructed by sulfoxide-directed⁷ oxidative intramolecular lactonization from cephem sulfoxide **13** (Scheme 4-4). To access the cyclization precursor **13**, the author focused on readily available cephem compound **15**, which can be converted to cephem antibiotics such as ceftaroline,⁸ ceftibuten,⁹ cefixime,⁹ and cefaclor.¹⁰ Therefore, **15** serves as an inexpensive intermediate and is commercially available in large quantities. Unlike the previous synthetic route of **8** via a single β -lactam ring **5**, **15** can be synthesized from penicillin G with its carbon atoms being maintained.¹¹



Scheme 4-4. Sulfoxide-Directed Intramolecular Lactonization

Scheme 4-5 shows an overview of the second-generation synthetic route of key intermediate **8**.

Scheme 4-5. Synthesis of Tricyclic β -lactam Core **8** from **15**

The key precursor **13** for lactonization was synthesized from **15** in three steps in 84% yield without purification with silica gel column chromatography. Wittig reaction of **15** afforded **16** as a mixture of olefin regioisomers. He found that the subsequent sulfide oxidation with *m*-CPBA converged to a single isomer **17**, the structure of which was confirmed by single-crystal X-ray analysis (Figure 4-2). Deprotection of the allyl group gave the cyclization precursor **13**.

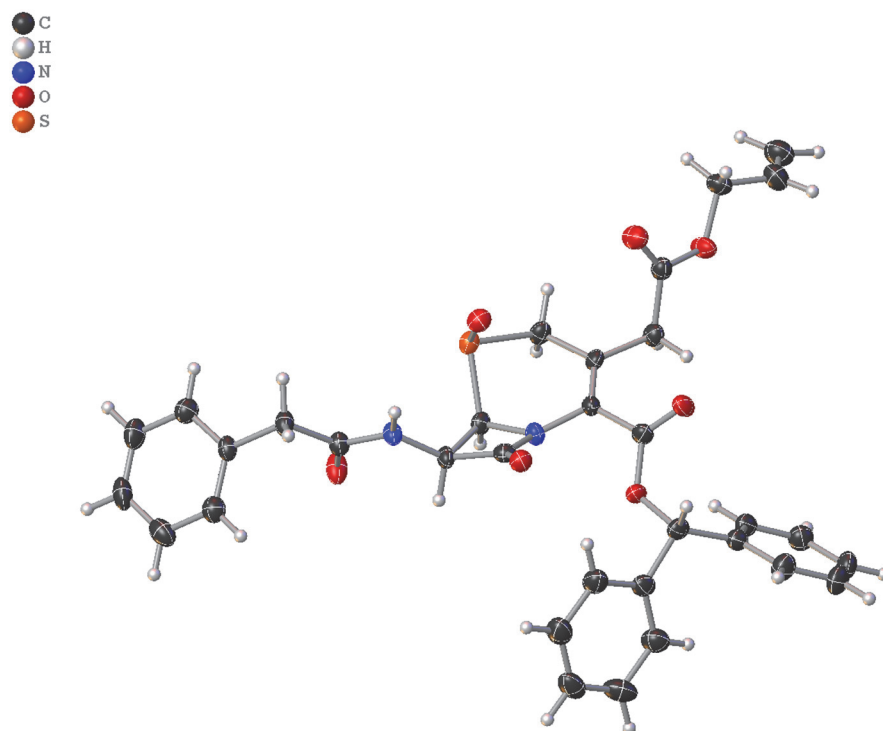


Figure 4-2. Molecular Structure of **17**; Thermal ellipsoids are set at 30% probability

IV-2. Sulfoxide-Directed Oxidative Intramolecular Cyclization

Investigation of the key sulfoxide-directed oxidative intramolecular cyclization is described in Table 4-1. According to precedent, he conducted the reaction with CAN in

methanol as the initial trial, but neither the desired product **14** nor the corresponding alkoxylation product (e.g., **12**) was observed under the conditions, and **13** remained (Table 4-1, entry 1).

Table 4-1. Results of Sulfoxide-Directed Oxidative Intramolecular Lactonization

Entry	Scale of 13	CAN (x eq.)	Pyridine (y eq.)	Note	Yield of 14 ^a
1	10 mg	5	-	in MeOH, 3 hr	ND
2	10 mg	5	10		(53%)
3	10 mg	5	-		ND
4	10 mg	-	10		ND
5	10 mg	5	10	in DMF	(22%)
6	10 mg	5	10	in <i>i</i> -PrOH	ND
7	10 mg	5	10	in MeOH/DMF	(26%)
8	100 mg	5	8		49% (48%)
9	1 g	5	8		50%
10	10 g	5	8		52% ^b

^a Yields after purification by silica gel column chromatography. Yields in parentheses were determined by ¹H NMR analysis with phenanthrene as an internal standard without isolation.

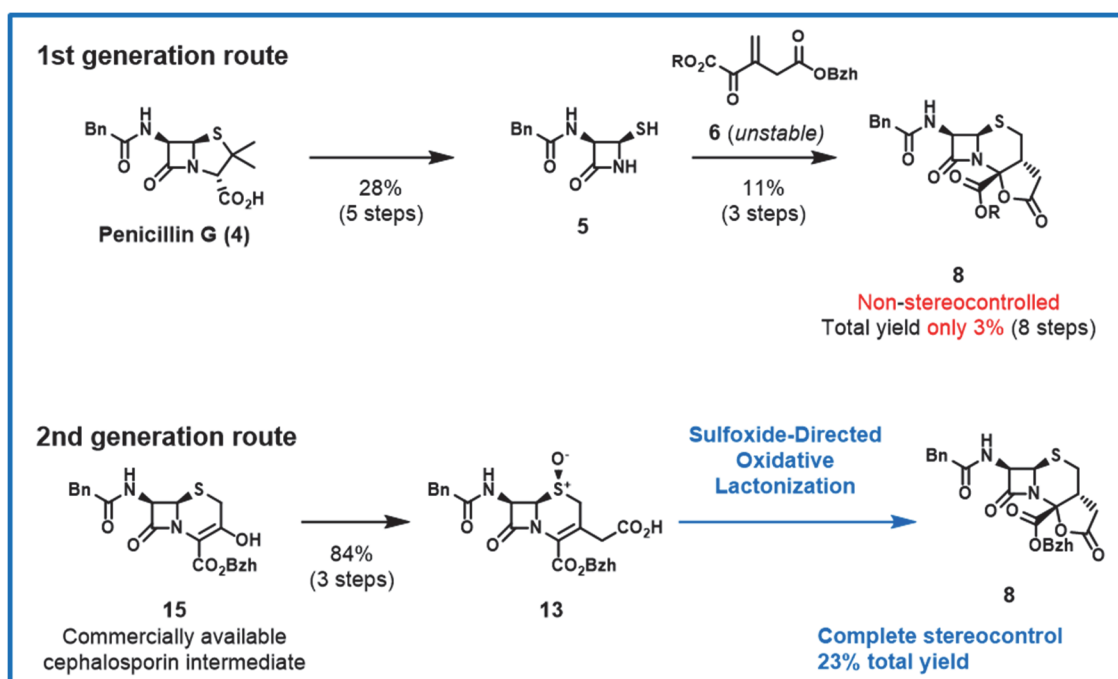
^b Isolated yield without silica gel column chromatography.

He hypothesized that the nucleophilicity of the carboxylic acid might not be sufficient under acidic conditions because of the strong acidity of CAN.¹² Therefore, he added pyridine to the reaction mixture in isopropyl alcohol (*i*-PrOH), and DMF, which increased the solubility of **13**, was used as a cosolvent. As a result, **14** was obtained in a good yield

of 53% as a single desired stereoisomer (Table 1, entry 2). The position of the olefin of **14** was determined by 2D ^1H NMR analysis. Both pyridine and CAN are necessary for the reaction (Table 1, entries 3 and 4). In the absence of *i*-PrOH, the yield decreased to 22%, probably because the active species would be produced by exchange of the alcohol and the nitrate anion of CAN (Table 1, entry 5).¹³ DMF and *i*-PrOH would be important to dissolve the starting materials (Table 1, entries 6 and 7). The reaction scale could be increased to 1 and 10 g, affording consistent yields of 49–52% (Table 1, entries 8–10).

Reduction of sulfoxide **14** by phosphorus tribromide followed by convex-face-selective reduction by sodium borohydride afforded the key intermediate **8** in 41–56% yield in two steps on a gram scale.

IV-3. Conclusion



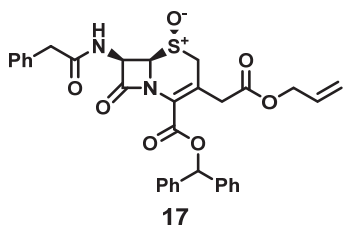
A highly stereoselective synthesis of the tricyclic β -lactam cepham core **8** has been developed as a key intermediate for preparation of **3**. The known synthetic route consists

of two transformations for removal of the five membered ring of the penam nucleus and construction of the cepham ring utilizing labile intermediate **6**, requiring eight steps (linear) in 3% yield and 11 steps (including synthesis of the labile compound **6**) with formation of the undesired stereoisomer of **7**. To resolve these issues, he developed a sulfoxide-directed oxidative intramolecular lactonization that enabled the synthesis of **8** in six steps from inexpensive and readily available cephem intermediate **13** in 18–23% overall yield on a gram scale. This methodology provided enough intermediate for further studies on the SAR of tricyclic β -lactams to combat clinically challenging CREs and allow scaleup synthesis.

Experimental

Unless otherwise noted, reactions were performed under a nitrogen atmosphere. All commercial reagents and solvents were used as purchased without further purification. Compound **15** was purchased from Shanghai iChemical Technology. ^1H and ^{13}C NMR spectra were recorded on Bruker Avance 400 and 100 MHz spectrometers, respectively. Spectral data are reported as follows: chemical shift (integration, multiplicity, coupling constant). Chemical shifts (δ) are in parts per million from tetramethylsilane (in CDCl_3 and $\text{DMSO-}d_6$) or sodium 2,2-dimethyl-2-silapentane-5-sulfonate (in D_2O). Multiplicities are reported as s = singlet, d = doublet, dd = doublet of doublets, dt = doublet of triplets, t = triplet, q = quartet, m = multiplet, br = broad. Analytical thin-layer chromatography was run on silica gel F254 precoated plates. Visualization of the developed chromatograms was done using fluorescence quenching or Vaughn's reagent. Flash column chromatography was carried out on an automated purification system using Yamazen or Fuji Silysia preppacked silica gel columns. High-resolution mass spectral data

were acquired with an Orbitrap Q Exactive Plus (ESI).



Synthesis of Benzhydryl (5*S*,6*R*,7*R*)-3-(2-(Allyloxy)-2-oxoethyl)-8-oxo-7-(2-phenylacetamido)-5-thia-1-azabicyclo[4.2.0]oct-2-ene-2-carboxylate 5-Oxide (17)

To a solution of allyl (triphenylphosphoranylidene)acetate (6.92 g, 15.7 mmol) in THF (37 mL) was added compound **15** (6.12 g, 12.1 mmol). The mixture was stirred at 50 °C with a heating block for 8 h. Water was added to the reaction mixture, followed by extraction with ethyl acetate. The organic layer was washed with a saturated aqueous solution of sodium bicarbonate, water, and brine in that order and dried over anhydrous magnesium sulfate. After filtration, the filtrate was concentrated under reduced pressure to afford crude **16** (13.4 g). ¹H NMR analysis of crude **16** showed that the main impurity was consistent with triphenylphosphine oxide (theoretically 4.37 g). **16** was used in the next step without further purification.

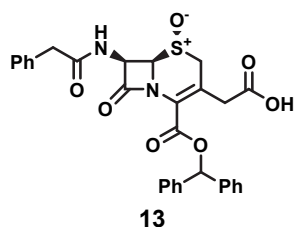
To a solution of crude **16** (13.4 g) in dichloromethane (DCM) (35 mL) was added *m*-CPBA (3.15 g, 12.7 mmol) in DCM (36 mL) at -50 °C, and the resulting mixture was stirred at the same temperature for 30 min. Further *m*-CPBA (1.04 g, 4.2 mmol) in DCM (12 mL) was added twice (8.4 mmol in total) at -50 °C followed by stirring at the same temperature for 30 min. Next, a 15% aqueous solution of sodium thiosulfate was added to the reaction mixture, followed by extraction with DCM. The organic layer was washed with a 5% aqueous solution of sodium bicarbonate and water in that order and then dried over anhydrous magnesium sulfate. After filtration, the filtrate was concentrated under

reduced pressure. The residue was precipitated with ethyl acetate–diisopropyl ether (50:50) to obtain compound **17** (6.07 g, 84%) as a white solid.

^1H NMR (400 MHz, CDCl_3): δ 7.46–7.43 (2H, m), 7.38–7.26 (13H, m), 6.90 (1H, s), 6.73 (1H, d, $J = 9.9$ Hz), 6.07 (1H, dd, $J = 9.9, 4.8$ Hz), 5.82 (1H, ddt, $J = 17.2, 10.4, 5.8$ Hz), 5.30–5.21 (2H, m), 4.52–4.49 (3H, m), 4.25 (1H, d, $J = 17.4$ Hz), 3.68–3.59 (3H, m), 3.42 (1H, d, $J = 18.6$ Hz), 3.16 (1H, d, $J = 17.4$ Hz).

$^{13}\text{C}\{^1\text{H}\}$ NMR (100 MHz, CDCl_3): δ 171.2, 169.1, 164.0, 160.0, 139.15, 139.07, 133.6, 131.5, 129.4, 129.1, 128.6, 128.5, 128.18, 128.15, 127.6, 127.5, 127.1, 125.4, 120.6, 118.9, 80.2, 67.0, 66.0, 58.9, 48.9, 43.5, 38.2.

HRMS (ESI) m/z : $[\text{M} + \text{H}]^+$ calcd for $\text{C}_{33}\text{H}_{31}\text{O}_7\text{N}_2\text{S}$, 599.1846; found, 599.1845.



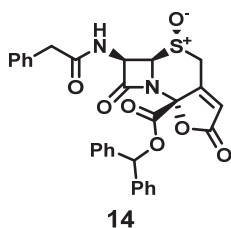
Synthesis of 2-((5*S*,6*R*,7*R*)-2-((Benzhydryloxy)carbonyl)-5-oxido-8-oxo-7-(2-phenylacetamido)-5-thia-1-azabicyclo[4.2.0]oct-2-en-3-yl)acetic Acid (**13**)

To a solution of **17** (2.00 g, 3.34 mmol) in tetrahydrofuran (20 mL) were added aniline (1.22 mL, 13.36 mmol) and tetrakis(triphenylphosphine)palladium (0.386 g, 0.334 mmol). The mixture was stirred at room temperature for 2 h. Next, the solvent was evaporated under reduced pressure, and isopropyl acetate, water, and 2 mol/L hydrochloric acid (7 mL, 14 mmol) were added, followed by filtration and washing with water and isopropyl acetate to afford compound **13** (1.85 g, 99%) as a cream-colored solid.

^1H NMR (400 MHz, DMSO- d_6): δ 12.54 (1H, br s), 8.34 (1H, d, $J = 8.5$ Hz), 7.64–7.22 (15H, m), 6.89 (1H, s), 5.90 (1H, dd, $J = 8.4, 4.6$ Hz), 4.95 (1H, d, $J = 4.6$ Hz), 3.89 (1H, d, $J = 18.8$ Hz), 3.76–3.55 (4H, m), 3.28 (1H, d, $J = 17.1$ Hz).

$^{13}\text{C}\{^1\text{H}\}$ NMR (100 MHz, DMSO- d_6): δ 171.0, 170.5, 164.3, 160.0, 140.0, 139.8, 135.7, 134.4, 130.7, 129.0, 128.4, 128.3, 128.2, 127.7, 127.6, 126.6, 126.5, 126.4, 123.4, 123.3, 78.7, 66.4, 57.6, 48.2, 41.4, 37.8.

HRMS (ESI) m/z : $[\text{M} + \text{H}]^+$ calcd for $\text{C}_{30}\text{H}_{27}\text{O}_7\text{N}_2\text{S}$, 559.1533; found, 559.1532.



Synthesis of Benzhydryl (5*S*,5*aR*,6*R*,8*aR*)-2,7-Dioxo-6-(2-phenylacetamido)-2,4,5*a*,6-tetrahydro-7*H*,8*aH*-azeto[2,1-*b*]furo[2,3-*d*][1,3]thiazine-8*a*-carboxylate 5-Oxide (14)

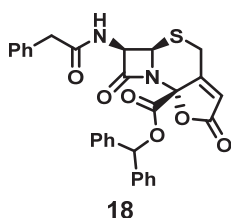
To a suspension of **13** (1.00 g, 1.79 mmol) and pyridine (1.44 mL, 17.9 mmol) in *i*-PrOH (10 mL) and DMF (10 mL) was added CAN (4.91 g, 8.95 mmol) at 0 °C. The mixture was stirred at room temperature for 30 min. Next, a 10% aqueous solution of sodium hydrogen sulfite and ethyl acetate were added to the reaction mixture, followed by acidification with 2 mol/L hydrochloric acid and extraction with ethyl acetate. The organic layer was washed with water, a saturated aqueous solution of sodium bicarbonate, and brine in that order and dried over anhydrous magnesium sulfate. After filtration, the filtrate was concentrated under reduced pressure. The obtained residue was purified by

silica gel column chromatography (50–100% ethyl acetate–*n*-hexane) to afford compound **14** (0.495 g, 50%) as an orange foam.

^1H NMR (400 MHz, CDCl_3): δ 7.69–7.65 (1H, m), 7.57–7.44 (2H, m), 7.37–7.24 (12H, m), 6.95 (1H, s), 6.83 (1H, d, $J = 10.0$ Hz), 6.13 (1H, d, $J = 1.9$ Hz), 6.00 (1H, dd, $J = 10.0, 4.8$ Hz), 4.46 (1H, d, $J = 15.4$ Hz), 4.41 (1H, d, $J = 4.8$ Hz), 3.62 (1H, d, $J = 15.6$ Hz), 3.58–3.54 (2H, m).

$^{13}\text{C}\{^1\text{H}\}$ NMR (100 MHz, CDCl_3): δ 171.0, 167.2, 162.7, 160.6, 152.8, 138.4, 138.3, 133.5, 132.2, 132.1, 132.0, 129.4, 129.1, 128.64, 128.61, 128.58, 128.5, 127.6, 127.4, 127.2, 121.6, 87.0, 81.5, 68.7, 59.4, 50.4, 43.4.

HRMS (ESI) m/z : $[\text{M} - \text{H}]^-$ calcd for $\text{C}_{30}\text{H}_{23}\text{O}_7\text{N}_2\text{S}$, 555.1220; found, 555.1233.



Synthesis of Benzhydryl (5a*R*,6*R*,8a*R*)-2,7-Dioxo-6-(2-phenylacetamido)-2,4,5a,6-tetrahydro-7*H*,8a*H*-azeto[2,1-*b*]furo[2,3-*d*][1,3]thiazine-8a-carboxylate (**18**)

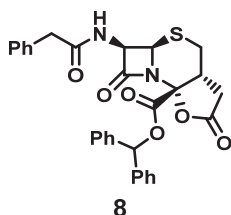
To a solution of **14** (0.495 g, 0.889 mmol) in DMF (5 mL) was added phosphorus tribromide (0.126 mL, 1.334 mmol) at -40 °C. The mixture was stirred at -40 °C for 1 h. Water was added to the reaction mixture, followed by extraction with ethyl acetate. The organic layer was washed with water, a saturated aqueous solution of sodium bicarbonate, and brine in that order and dried over anhydrous magnesium sulfate. After filtration, the filtrate was concentrated under reduced pressure to afford crude **18** (0.526 g) as a brown

foam. **18** was used in the next step without further purification.

^1H NMR (400 MHz, CDCl_3): δ 7.37–7.24 (15H, m), 6.92 (1H, s), 6.21–6.18 (2H, m), 5.66 (1H, dd, $J = 9.2, 4.5$ Hz), 5.02 (1H, d, $J = 4.5$ Hz), 3.92 (1H, d, $J = 13.3$ Hz), 3.64 (1H, d, $J = 15.8$ Hz), 3.58 (1H, d, $J = 15.8$ Hz), 3.51 (1H, dd, $J = 13.3, 2.3$ Hz).

$^{13}\text{C}\{^1\text{H}\}$ NMR (100 MHz, CDCl_3): δ 170.8, 167.7, 164.3, 161.3, 156.3, 138.5, 138.1, 133.6, 129.4, 129.1, 128.7, 128.63, 128.58, 127.7, 127.3, 127.1, 120.7, 87.0, 81.2, 60.4, 56.6, 43.3, 22.6.

HRMS (ESI) m/z : $[\text{M} - \text{H}]^-$ calcd for $\text{C}_{30}\text{H}_{23}\text{O}_6\text{N}_2\text{S}$, 539.1271; found, 539.1288.



Synthesis of Benzhydryl (3a*R*,5a*R*,6*R*,8a*R*)-2,7-Dioxo-6-(2-phenylacetamido)hexahydro-7*H*,8a*H*-azeto[2,1-*b*]furo[2,3-*d*][1,3]thiazine-8a-carboxylate (**8**)

To a solution of **18** (0.53 g) in *i*-PrOH (5 mL) and *N,N*-dimethylacetamide (DMA) (5 mL) was added 1 mol/L sodium borohydride in DMA (0.311 mL, 0.311 mmol) at -10 °C. The mixture was stirred at -10 to 0 °C for 1 h. Acetic acid (0.153 mL, 2.67 mmol) was added at -40 °C, and the mixture was stirred at -40 °C for 5 min. Next, 2 mol/L hydrochloric acid was added to the reaction mixture, followed by extraction with ethyl acetate. The organic layer was washed with water, a saturated aqueous solution of sodium bicarbonate, and brine in that order and then dried over anhydrous magnesium sulfate.

After filtration, the filtrate was concentrated under reduced pressure. The obtained residue was purified by silica gel column chromatography (20–60% ethyl acetate–*n*-hexane) to afford compound **8** (0.271 g, 56%) as a pale-yellow foam.

^1H NMR (400 MHz, CDCl_3): δ 7.38–7.24 (15H, m), 6.93 (1H, s), 6.21 (1H, d, $J = 8.7$ Hz), 5.52 (1H, dd, $J = 8.7, 4.8$ Hz), 4.98 (1H, d, $J = 4.8$ Hz), 3.65 (1H, d, $J = 16.1$ Hz), 3.60 (1H, d, $J = 16.1$ Hz), 3.13–3.08 (1H, m), 2.90 (1H, dd, $J = 14.5, 4.5$ Hz), 2.60 (1H, dd, $J = 14.5, 9.6$ Hz), 2.52 (1H, s), 2.51 (1H, d, $J = 0.9$ Hz).

$^{13}\text{C}\{^1\text{H}\}$ NMR (100 MHz, CDCl_3): δ 171.4, 171.0, 164.1, 163.7, 138.8, 138.2, 133.7, 129.5, 129.2, 128.7, 128.55, 128.51, 128.45, 127.7, 127.6, 127.0, 86.9, 80.9, 60.2, 56.3, 43.3, 35.6, 33.2, 27.0.

HRMS (ESI) m/z : $[\text{M} + \text{H}]^+$ calcd for $\text{C}_{30}\text{H}_{27}\text{N}_2\text{O}_6\text{S}$, 543.1584; found, 543.1581.

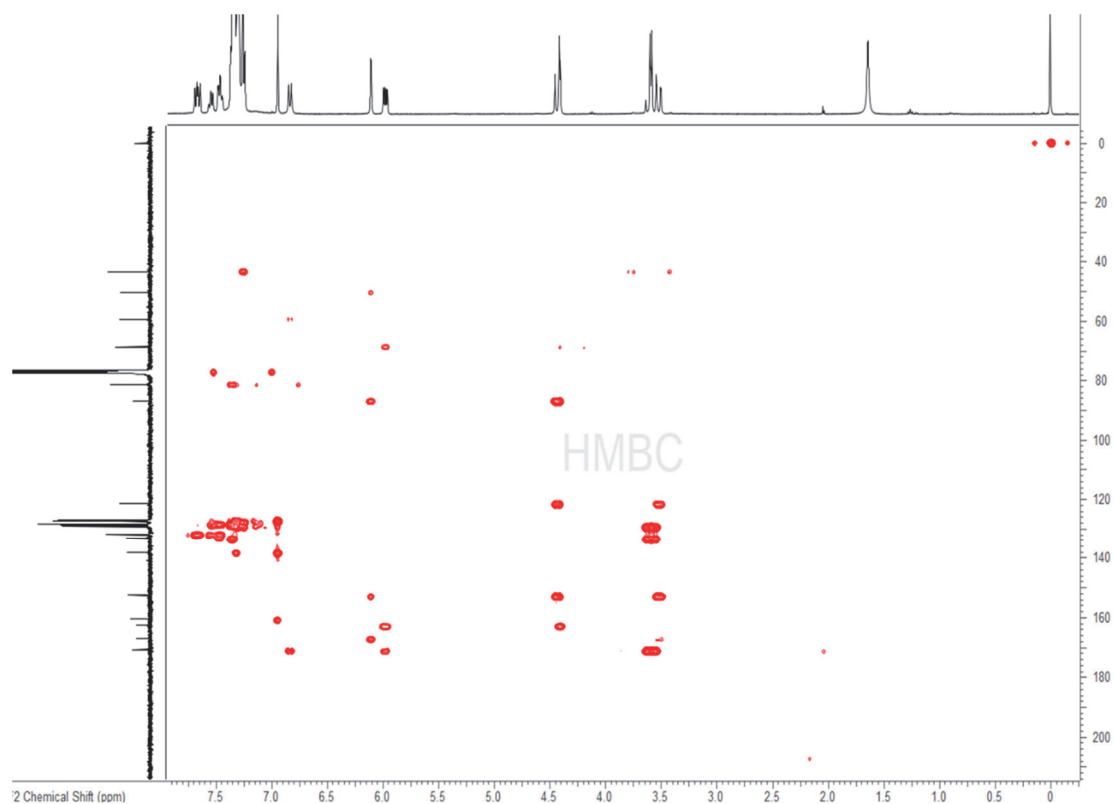
Gram-Scale Synthesis of **8**

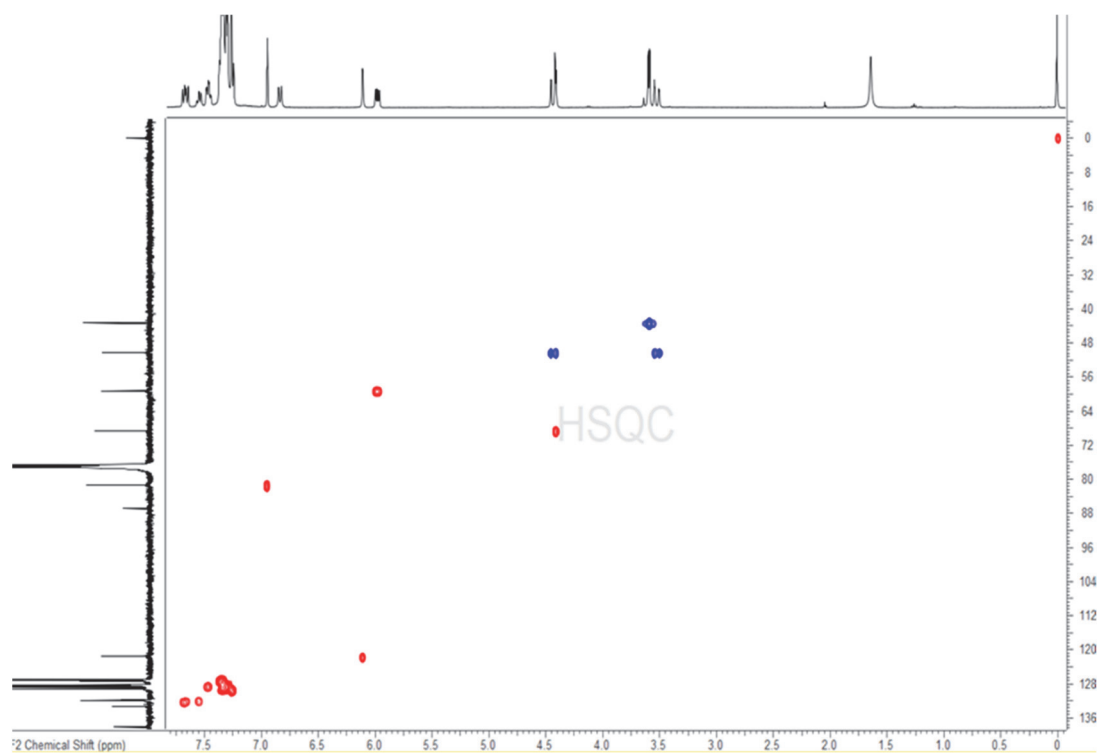
From **13** (10.0 g, 17.9 mmol), **14** (5.20 g, 9.34 mmol, 52%) was obtained as an orange foam according to the same procedure, except that activated carbon (20 g) was added during drying with anhydrous magnesium sulfate, and the crude product was used for the next step without silica gel column chromatography. From **14** (5.20 g), **18** (3.82 g, 7.07 mmol, 76%) was obtained as an orange foam according to the same procedure, except that the extraction was performed with *n*-hexane–ethyl acetate (1:1) and the filtration was performed through a 10 g silica gel pad with *n*-hexane–ethyl acetate (1:1). From **18** (3.82 g), **8** (2.06 g, 3.80 mmol, 54%) was obtained as a pale-yellow foam according to the same procedure, except that activated carbon (8 g) was added during drying with anhydrous

magnesium sulfate. The NMR spectra were consistent with the data given above.

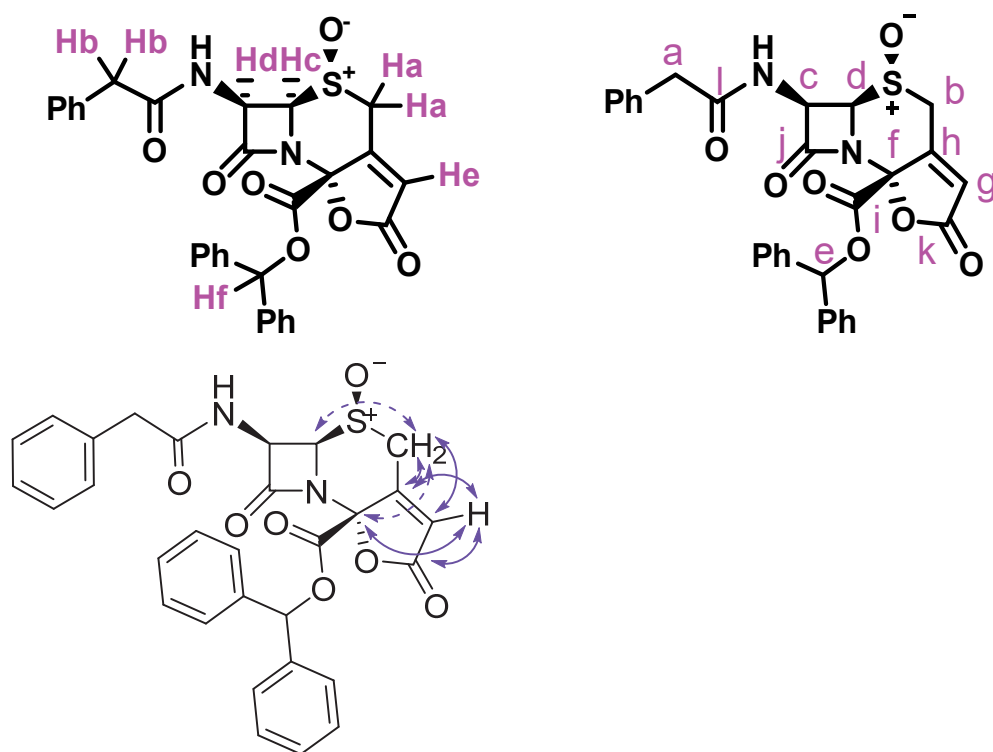
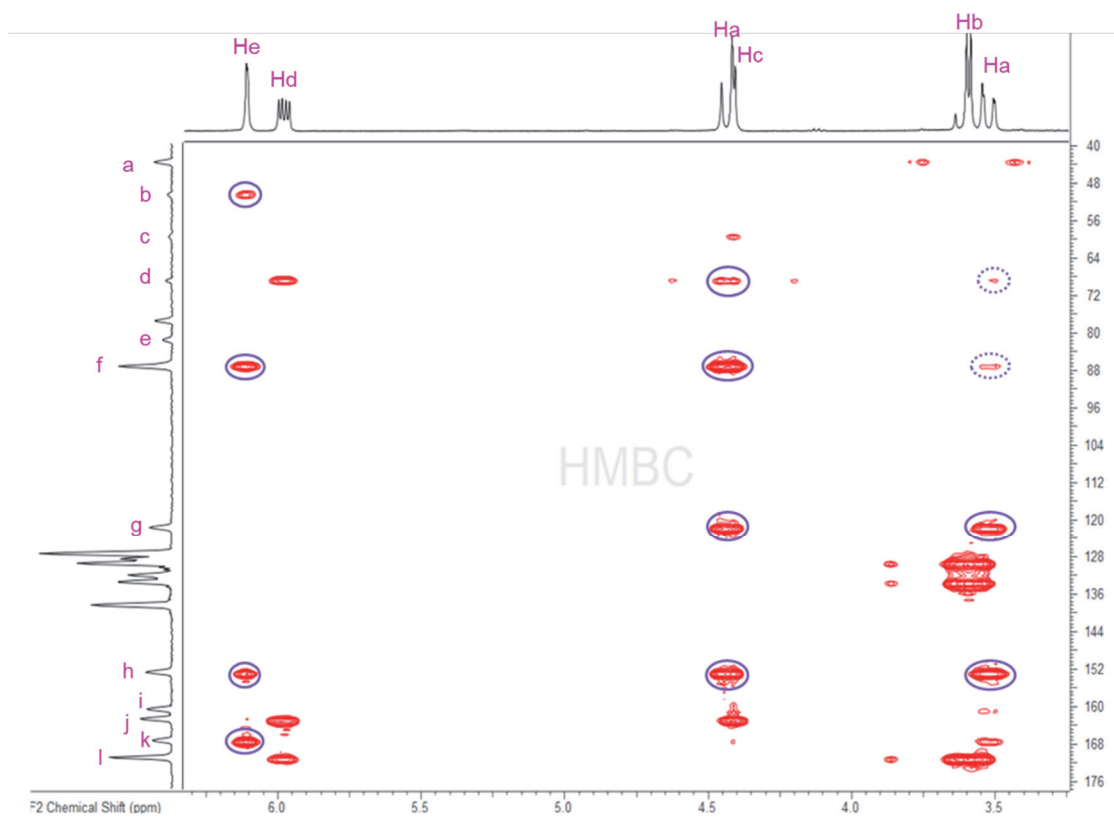
HMBC and HSQC spectra of compound 14

HMBC spectra of Compound 14 in CDCl₃



HSQC spectra of compound **14** in CDCl₃

Structural analysis of compound 14



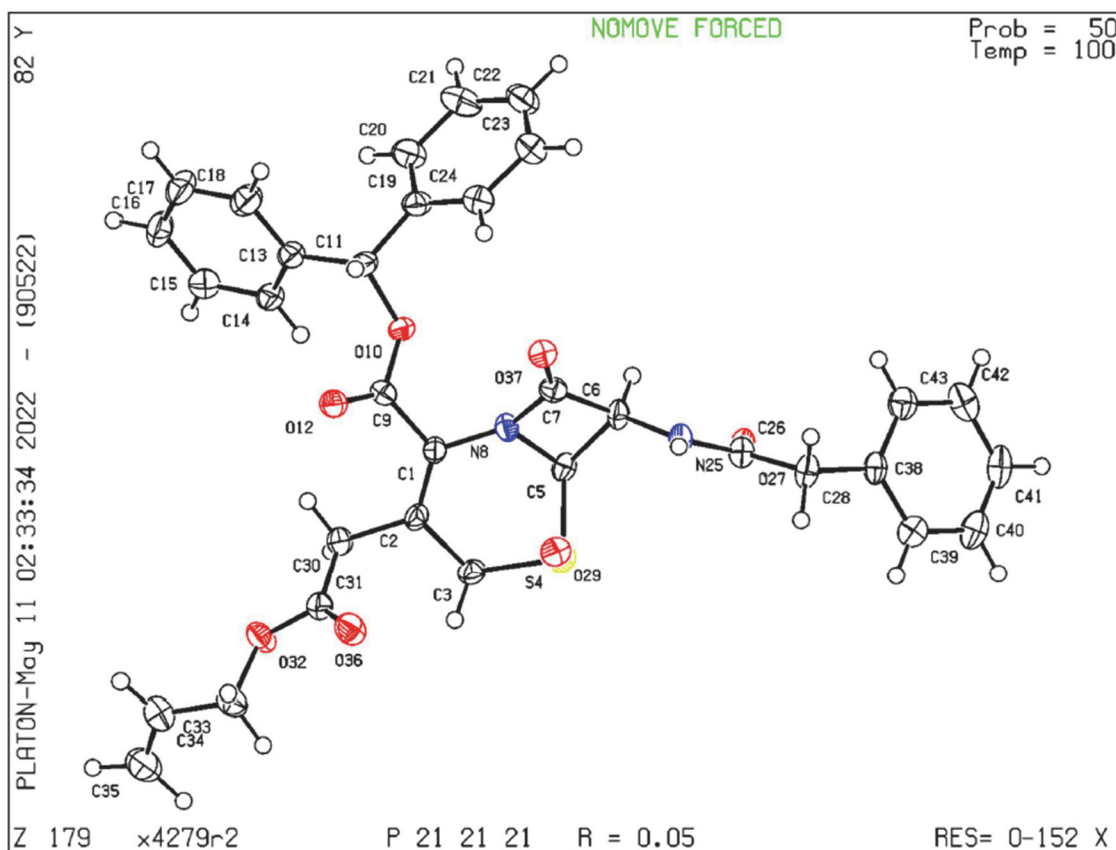
X-ray crystallographic data of compound 17

X-ray Crystallography: The diffraction data of **17** were collected on an XtaLAB AFC10 (RCD3): quarter-chi single diffractometer. The crystal was kept at 100.0 K during data collection. Using Olex2,1 the structure was solved with the ShelXT2 structure solution program using Intrinsic Phasing and refined with the ShelXL3 refinement package using Least Squares minimization.

Sample Preparation: X-ray quality crystal was prepared by vapor diffusion method using dichloromethane–*n*-hexane at room temperature

Compound 17

CCDC Deposition Number; 2171963



Identification code; X4279r2

Empirical formula; C₃₃H₃₀N₂O₇S

Formula weight; 598.65

Temperature; 100 K

Crystal system; orthorhombic

Space group; P2₁2₁2₁

Unit cell dimension;

$$\alpha = 4.7678(3) \text{ \AA} \quad \alpha = 90^\circ$$

$$\beta = 23.2697(17) \text{ \AA} \quad \beta = 90^\circ$$

$$\gamma = 26.2723(16) \text{ \AA} \quad \gamma = 90^\circ$$

Volume; 2914.8(3) Å³

Z; 4

Density (calculated) 1.364 g/cm³

Absorption coefficient; 1.431 μ/mm⁻¹

F(000); 1256.0

Crystal size; 0.2 × 0.02 × 0.01 mm

Radiation; CuKα (λ = 1.54184 Å)

2θ range for data collection; 6.728 to 147.598 °

Index ranges; -5 ≤ h ≤ 5, -27 ≤ k ≤ 24, -32 ≤ l ≤ 25

Reflections collected; 16020

Independent reflections; 5697 [R_{int} = 0.0930, R_{sigma} = 0.1056]

Data / restraints / parameters; 5697 / 0 / 396

Goodness-of-fit on F²; 0.976

Final R indexes [I >= 2σ (I)]; R₁ = 0.0493, wR₂ = 0.1025

Final R indexes [all data]; $R_1 = 0.0773$, $wR_2 = 0.1134$

Largest diff. peak / hole; $0.41 / -0.37 \text{ e\AA}^{-3}$

Flack parameter; $0.00(3)$

Reference

- ¹ (a) Centers for Disease Control and Prevention (CDC). *Antibiotic Resistance Threats in the United States 2019*, Atlanta, GA; U.S. Department of Health and Human Services, CDC, 2019. Retrieved from <https://www.cdc.gov/drugresistance/pdf/threats-report/2019-ar-threats-report-508.pdf> (accessed November 22, 2022). (b) World Health Organization. *Global priority list of antibiotic-resistant bacteria to guide research, discovery, and development of new antibiotics*; WHO, February 27, 2017. Retrieved from <https://www.aidsdatahub.org/resource/who-global-priority-list-antibiotic-resistant-bacteria> (accessed November 22, 2022).
- ² Nozaki, Y.; Katayama, N.; Ono, H.; Tsubotani, S.; Harada, S.; Okazaki, H.; Nakao, Y. Binding of a non- β -lactam antibiotic to penicillin-binding proteins. *Nature* **1987**, *325*, 179–180.
- ³ Morimoto, A.; Noguchi, N.; Chou, N. Tricyclic cepham compounds, their production and use. EP253337 A2. Jan 20, 1988.
- ⁴ Harada, S.; Tsubotani, S.; Hida, T.; Ono, H.; Okazaki, H. Structure of lactivicin, an antibiotic having a new nucleus and similar biological activities to β -lactam antibiotics. *Tetrahedron Lett.* **1986**, *27*, 6229–6232.
- ⁵ Balsamo, A.; Macchia, B.; Macchia, F.; Rossello, A.; Scatena, P.; Domiano, P. Conversion reactions of cepham into penam systems. A route to determine the relative

configurations of two diastereoisomeric 3-bromo-4-methoxycepham derivatives. *J. Org. Chem.* **1986**, *51*, 540–543.

⁶ Alpegiani, M.; Bissolino, P.; Borghi, D.; Perrone, E. Cerium ammonium nitrate promoted alkoxylation of cephem sulfoxides and sulfones. *Synlett* **1994**, *1994*, 233–234.

⁷ (a) Waters, M.; Onofiok, E.; Tellers, D.; Chilenski, J.; Song, Z. Enantioselective Synthesis of 1,4-Dihydrobenzoxathiins via Sulfoxide-Directed Borane Reduction. *Synthesis* **2006**, 3389–3396. (b) Carreno, M. C.; Hernandez-Torres, G.; Urbano, A.; Colobert, F. Sulfoxide-directed stereocontrolled access to 2H-chromans: total synthesis of the (*S,R,R,R*)-enantiomer of the antihypertensive drug nebivolol. *Eur. J. Org. Chem.* **2008**, *12*, 2035–2038. (c) Fernandez de la Pradilla, R.; Tortosa, M.; Castellanos, E.; Viso, A.; Baile, R. Sulfoxide-directed intramolecular [4 + 2] cycloadditions between 2-sulfinyl butadienes and unactivated alkynes. *J. Org. Chem.* **2010**, *75*, 1517–1533. (d) Fernandez de la Pradilla, R.; Simal, C.; Bates, R. H.; Viso, A.; Infantes, L. Sulfoxide-Directed Enantioselective Synthesis of Functionalized Tetrahydropyridines. *Org. Lett.* **2013**, *15*, 4936–4939.

⁸ (a) Ishikawa, T.; Matsunaga, N.; Tawada, H.; Kuroda, N.; Nakayama, Y.; Ishibashi, Y.; Tomimoto, M.; Ikeda, Y.; Tagawa, Y.; Iizawa, Y.; Okonogi, K.; Hashiguchi, S.; Miyake, A. TAK-599, a novel N-Phosphono type prodrug of anti-MRSA cephalosporin T-91825: synthesis, physicochemical and pharmacological properties. *Bioorg. Med. Chem.* **2003**, *11*, 2427–2437. (b) Yoshida, Y.; Matsuda, K.; Sasaki, H.; Matsumoto, Y.; Matsumoto, S.; Tawara, S.; Takasugi, H. Studies on anti-*Helicobacter pylori* agents. Part 2: New cephem derivatives. *Bioorg. Med. Chem.* **2000**, *8*, 2317–2335.

⁹ Kameyama, Y. Process for the preparation of 3-sulfonyloxy-3-cephem compounds. WO 2001021622 A1, March 29, 2001.

-
- ¹⁰ (a) Zhao, J. Preparation method of high purity cefaclor. CN 111187284 A, May 22, 2020. (b) Kameyama, Y.; Yamada, T.; Suh, D. S. Process for preparation of 7-amino-3-cephem-4-carboxylic acid compounds from 7-(acylamino)-3-cephem-4-carboxylic acids. WO 2000001703 A1, January 13, 2000.
- ¹¹ Tanaka, H.; Taniguchi, M.; Kameyama, Y.; Monnin, M.; Torii, S.; Sasaoka, M.; Shiroy, T.; Nagao, S.; Yamada, T.; Tokumaru, Y. Synthesis of 3-hydroxycephems from penicillin G through cyclization of chlorinated 4-(phenylsulfonylthio)-2-azetidinones promoted by a BiCl₃/Sn or TiCl₄/Sn bimetal redox system. *Bull. Chem. Soc. Jpn.* **1995**, *68*, 1385–1391.
- ¹² Sridharan, V.; Menendez, J. C. Cerium(IV) ammonium nitrate as a catalyst in organic synthesis. *Chem. Rev.* **2010**, *110*, 3805–3849.
- ¹³ Torii, S.; Tanaka, H.; Inokuchi, T.; Nakane, S.; Akada, M.; Saito, N.; Sirakawa, T. Indirect electrooxidation (an ex-cell method) of alkylbenzenes by recycle use of diammonium hexanitratocerate in various solvent systems. *J. Org. Chem.* **1982**, *47*, 1647–1652.

Chapter V Conclusion

This thesis summarizes the results of research on the pharmacological activity and new synthetic route of novel tricyclic β -lactam sulfoxides with the aim of discovery new treatment options for infections caused by carbapenem-resistant Enterobacterales (CREs), which become a worldwide clinical and public health problem in recent years.

Chapter I “Introduction” describes the problem of multidrug-resistant bacteria, especially CREs and the urgent need for new treatment options.

Furthermore, the author describes the resistance mechanisms of CRE, and the combination of β -lactam and β -lactamase inhibitor (BL/BLI) currently developed against the production of β -lactamase, which is the major resistance mechanism of CRE. He notes that the BL/BLI strategy should be one of the therapeutic options for infections caused by CRE, however, they do not offer sufficient antibacterial activities against MBL-producing strains and these activities would be lost against clinical isolates with resistance mechanisms other than β -lactamase production.

Based on this background, he mentions the need to resolve the problem of CRE by using a single molecule of β -lactam without the β -lactamase inhibitor. To achieve this goal, the author believes that it is necessary to discover a new β -lactam agent which is not easily recognized and hydrolyzed by various classes of β -lactamases and can provide sufficient antibacterial activities against CREs without a BLI. The author was interested in lactivicin (LTV) **1** and its derivative, tricyclic β -lactam **2**, and started exploratory research to discover a new β -lactam agent, because the antibacterial activities of LTVs against various β -lactamase producing strains have been reported from the late 2000's (Figure 5-1).

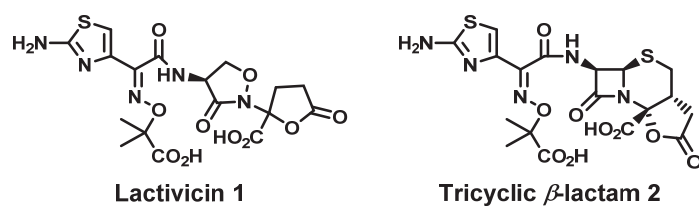
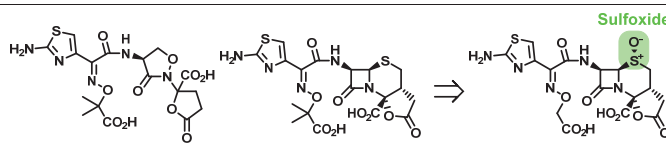


Figure 5-1. Lactivicin 1 and Tricyclic β -lactam 2

In Chapter II “Discovery of a tricyclic β -lactam sulfoxide core”, the antibacterial activities of lactivicin 1 and tricyclic β -lactam 2 against various kinds of β -lactamase producers were evaluated and the results show that tricyclic β -lactam 2 has potent activities against class A, B and D β -lactamase producers but not the class C β -lactamase producer. With these findings in mind, because there are multiple β -lactamase producers, including the class C β -lactamase among the clinical isolates, the author conducted exploratory research of compounds with potent activities against several problematic β -lactamase producers by improving the activity against class C β -lactamase producers.

By optimizing the aminothiazole side chain of tricyclic β -lactam 2 and introduction a sulfoxide to the tricyclic β -lactam core, the author succeeded to identify a novel scaffold which exerts potent antibacterial activities against class C β -lactamase producers while maintaining antibacterial activities against class A, B and D β -lactamase producers (Table 5-1).

Table 5-1. Antibacterial Activities of **1–3** against Clinical Isolates


Strain	Phenotype (Ambler classification)	1	2	3
<i>E. coli</i> NIHJJC-2	Susceptible	0.25	0.5	0.063
<i>E. coli</i> SR34100	CTX-M-15 (class A)	4	1	0.125
<i>E. cloacae</i> SR01875	NDM-1 (class B)	1	0.5	0.063
<i>E. cloacae</i> SR36276	AmpC (class C)	>32	16	0.063
<i>K. pneumoniae</i> SR08787	OXA-48 (class D)	1	2	0.25

In addition, evaluation of antibacterial activities against clinical isolates shows that **3** exhibited lower MIC₉₀ values than those of the already approved BL/BLI and also shows a potent therapeutic efficacy in the neutropenic mouse lung infection model. These results demonstrate that this tricyclic β -lactam scaffold deserves further study in the search for new antimicrobial agents against CREs.

Chapter III “Optimization of the aminothiazole side chain” describes the discovery of a promising drug candidate **4** which has improved the antibacterial activities against CREs with reduced outer membrane permeability and the four-amino acid insertion into penicillin-binding protein 3 (PBP3) by optimizing the aminothiazole side chain of compound **3** which was identified in the previous chapter.

It is first mentioned that the reduction of outer membrane permeability caused by porin deficiency with β -lactamase production or the insertion of four amino acids into PBP3 are noticed as resistance mechanisms other than β -lactamase production, and these are also problems in BL/BLIs. The MICs of **3** also increased against the strains harboring them. Based on studies about porin permeability, he proposed that converting the carboxylic acid group on the alkoxyimino moiety of the aminothiazole side chain into a

non-anionic group and/or introducing a non-bulky hydrophilic functional group should improve the permeability of porin and consequently its antibacterial activities against the porin-deficient strains. This strategy should simultaneously improve the antibacterial activities against the four-amino acid inserted strains, because it has been reported that the binding of β -lactams, which have a large substituent at the position of the aminothiazole side chain, to PBP3 is hindered by the four-amino acid insertion.

Based on this hypothesis, he identified potent compound **4** by converting the carboxylic acid group at the alkoxyimino moiety of the aminothiazole side chain to a non-anionic hydroxyl group and introduction another hydroxyl group as a non-bulky hydrophilic functional group. **4**, as expected, overcomes the reduction of outer membrane permeability caused by porin deficiency with β -lactamase production (Table 5-2) and the insertion of four amino acids into PBP3, which significantly increases the MICs of new BL/BLI combinations currently under clinical development, such as monobactam aztreonam (ATM) and avibactam (AVI) (Table 5-3).

Table 5-2. Antibacterial Activities against *K. pneumoniae* NVT2001S and Its OmpK35/36-Deletion Strains

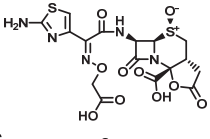
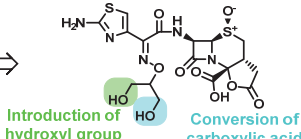
strain	Knock-out porin	Carrying β -lactamase	 3	 4
NVT2001S	Parent	-	0.031	0.031
SR-L3006	Δ OmpK35	-	0.125	0.063
SR-L3007	Δ OmpK36	-	0.063	0.031
SR-L3008	Δ OmpK35 & Δ OmpK36	-	1	0.25
SR-L3014	-	pACYC177:: <i>bla</i> _{KPC-2}	0.063	0.031
SR 9872	Δ OmpK35 & Δ OmpK36	pACYC177:: <i>bla</i> _{KPC-2}	1	0.25

Table 5-3. Antibacterial Activities of **3** and **4** against Porin-Deficient Enterobacterales

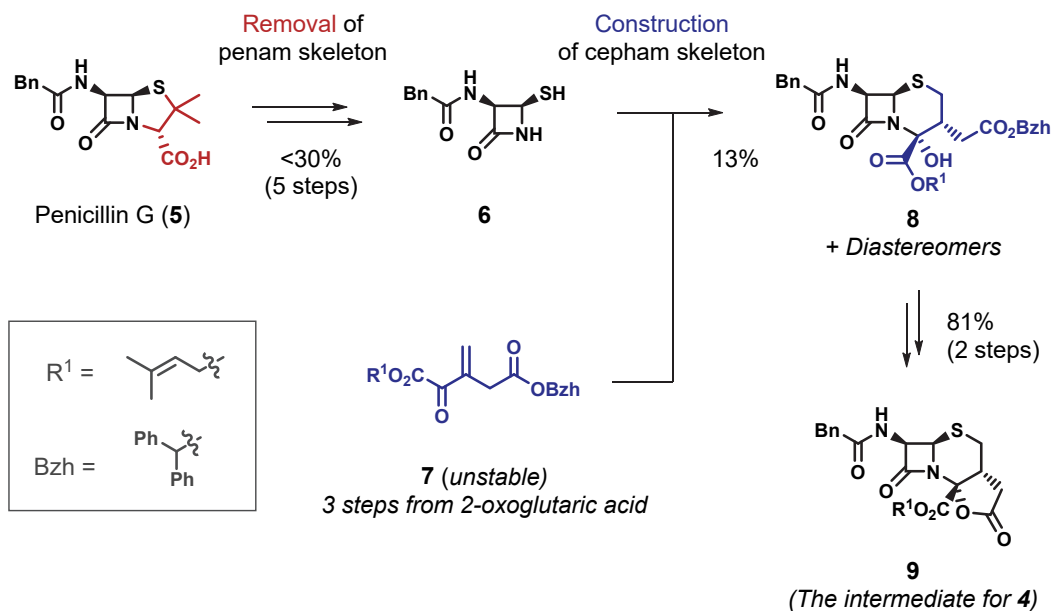
Strain	Characteristics	MIC ($\mu\text{g/mL}$)	
		4	ATM /AVI
<i>E. coli</i> SR08587	NDM-1, YRIN-inserted in PBP3	2	4
<i>E. coli</i> SR01463	NDM-1, YRIN-inserted in PBP3	2	8
<i>E. coli</i> SR08586	NDM-1, YRIK-inserted in PBP3	4	16
<i>E. coli</i> SR01442	NDM-1, ΔOmpF , YRIK-inserted in PBP3	4	16
<i>E. coli</i> SR200040	NDM-1, YRIK-inserted in PBP3	4	32

4 also exerts strong therapeutic efficacy that is significantly superior to BL/BLIs in the neutropenic mouse lung infection model and a low frequency of the production of spontaneous resistant mutants, which is similar to the already approved BL/BLI. These results demonstrate that **4** is a promising drug candidate for infections caused by CREs including those with reduced outer membrane permeability and the four-amino acid insertion into PBP3, in addition to β -lactamase production.

In Chapter IV “Stereoselective synthesis of a tricyclic β -lactam core”, the author notes that challenges remained for scale-up of the synthesis and sufficient supply of the intermediate for further backup SAR.

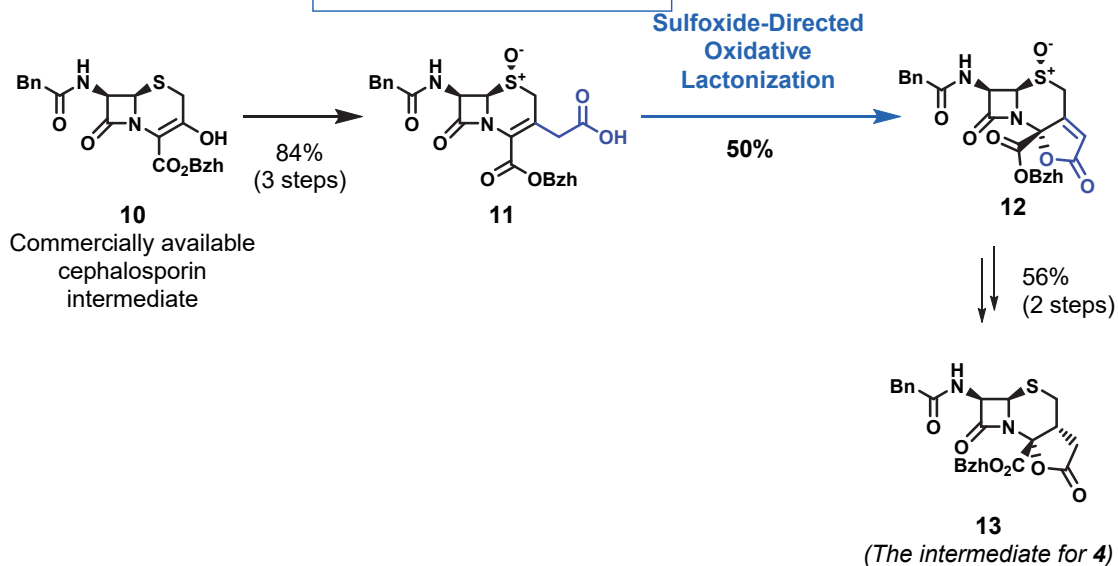
1st generation route

Non-stereocontrolled
Total yield **only 3%** (8 steps)



2nd generation route

Complete stereocontrol
23% total yield (6 steps)

Scheme 5-1. Synthetic Routes for Tricyclic β -lactam Core

In known synthetic routes, compound **9**, an intermediate leading to **3**, is synthesized by two transformations from penicillin: (a) ring opening and removal of the penam structure of **5** to form **6** and (b) reaction with **7** to construct the six-membered ring, which possesses functional groups enabling the third lactone cyclization. This route required 11 steps (including synthesis of the labile compound **7**) in 3% yield with formation of the undesired stereoisomer of **8**.

To resolve these issues, he developed a sulfoxide-directed oxidative intramolecular lactonization that takes advantage of sulfoxide stereochemistry. This enables the synthesis of **13** in six steps from inexpensive and readily available cephem intermediate **10** in 23% overall yield on a gram scale. This methodology provided enough intermediate for further studies on the SAR of tricyclic β -lactams to combat clinically challenging CREs and allow scaleup synthesis (Scheme 5-1).

In summary, this thesis describes exploratory research on novel tricyclic β -lactam sulfoxides. The author succeeded to identify a novel tricyclic β -lactam sulfoxide **4**, which is not easily recognized and hydrolyzed by various classes of β -lactamases and can provide sufficient antibacterial activities against carbapenem-resistant Enterobacterales (CREs) without a β -lactamase inhibitor (BLI).

Starting from a known tricyclic β -lactam **2**, the author succeeded to obtain a tricyclic β -lactam sulfoxide **3** which exerts potent antibacterial activities against several problematic β -lactamase producers without BLI by the introduction of a sulfoxide into the tricyclic β -lactam core. By further optimizing the aminothiazole side chain, he has identified a promising drug candidate **4** for infectious diseases caused by CREs that exerts potent activities against clinical isolates with resistance mechanisms other than β -lactamase

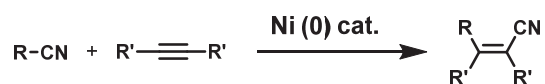
production. Furthermore, he has developed a sulfoxide-directed oxidative intramolecular lactonization for second-generation synthetic route of the unique tricyclic β -lactam to provide enough intermediate for further studies on the SAR of tricyclic β -lactams to combat clinically challenging CREs and allow scaleup synthesis.

The results of this thesis are expected to become a new treatment option for infections caused by CRE and contribute to future exploratory research on new tricyclic β -lactams to combat clinically challenging antimicrobial resistant bacteria such as CRE.

Appendix Ni-catalyzed Arylcyanation Reaction of Norbornene and Norbornadiene

A-1. Introduction

The author is interested in the introduction of functional groups to a carbon-carbon double bond as shown in Chapter IV. Although this reaction proceeds stereoselectively, it only introduces one functional group across a carbon-carbon double bond. Reactions that allow simultaneous formation of two carbon-carbon bonds in regio-, stereo-, and chemoselective manners should have innovative utility in organic synthesis. In this context, direct addition reactions of aryl and allyl cyanides across alkynes were reported to give variously functionalized nitriles in a single operation with perfect atom economy (Scheme A-1).¹



Scheme A-1. Nickel-Catalyzed Arylcyanation and Allylcyanation of Alkynes

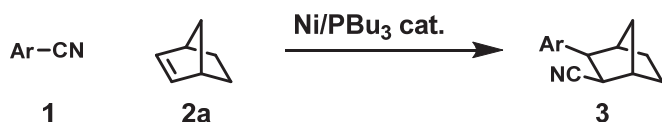
The author was intrigued by this reaction, which allows the introduction of two functional groups in one operation, therefore he started to investigate the application of the arylcyanation reaction to carbon-carbon double bonds.²

A-2. Arylcyanation of Norbornene

Initially, the reaction of 4-trifluoromethylbenzotrile (**1a**: 1.0 mmol) with norbornene (**2a**: 1.2 mmol) in toluene at 100 °C for 20 h in the presence of Ni(cod)₂ (5 mol %) and

PBu₃ (10 mol %) was investigated and found to obtain (2*R**,3*S**)-2-cyano-3-[4-(trifluoromethyl)phenyl]bicyclo[2.2.1]heptane (**3aa**) in 95% yield (Table A-1, Entry 1).

Table A-1. Arylcyanation of Norbornene (**2a**) Catalyzed by Ni/PBu₃^a



Entry	Ar	Time / h	Yield / % ^b
1	4-F ₃ C-C ₆ H ₄ (1a)	20	95 (3aa)
2	4-F-C ₆ H ₄ (1b)	20	91 (3ba)
3	4-Me(O)C-C ₆ H ₄ (1c)	20	86 (3ca)
4	4-MeO ₂ C-C ₆ H ₄ (1d)	20	89 (3da)
5 ^c	4-H(O)C-C ₆ H ₄ (1e)	38	56 (3ea)
6	4-Ph-C ₆ H ₄ (1f)	54	67 (3fa)
7 ^d	4-Me-C ₆ H ₄ (1g)	77	84 (3ga)
8 ^d	4-MeO-C ₆ H ₄ (1h)	77	76 (3ha)
9 ^d	3,4,5-(MeO) ₃ -C ₆ H ₂ (1i)	54	66 (3ia)
10 ^d	2-F ₃ C-C ₆ H ₄ (1j)	77	55 (3ja)
11 ^d	5-F-2-Me-C ₆ H ₃ (1k)	77	73 (3ka)
12 ^d	2-Pyridyl (1l)	-	<5 (3la)
13	3-Pyridyl (1m)	48	88 (3ma)
14	4-Pyridyl (1n)	48	92 (3na)
15	2-Furyl (1o)	48	94 (3oa)
16 ^e	2-Thienyl (1p)	48	90 (3pa)
17 ^e	1-Boc-3-indolyl (1q)	48	71 (3qa)

^a Reactions were carried out in toluene (0.60 mL) using an aryl cyanide (1.00 mmol) and **2a** (1.20 mmol) in the presence of Ni(cod)₂ (50 μmol) and PBu₃ (0.100 mmol). ^b Isolated yields based on an aryl cyanide.

^c PMe₃ (0.100 mmol) was used as a ligand. ^d **2a** (1.50 mmol), Ni(cod)₂ (0.100 mmol), and PBu₃ (0.20 mmol) were used. ^e PMe₂Ph (0.100 mmol) was used as a ligand.

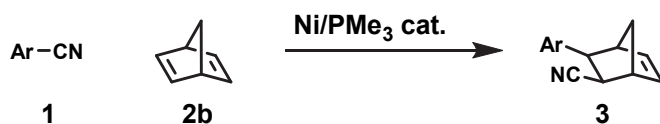
These conditions were found effective for the addition of various aryl cyanides across **2a**. A variety of electron-withdrawing functional groups including fluoro, keto, and ester were tolerated to give the corresponding adducts in good yields (Entries 2–4). In the case of the formyl group (**1e**), the use of PMe_3 as a ligand was important due presumably to competitive C–H activation of the formyl group under the standard catalyst system (Entry 5).³ The electronically neutral 4-phenylbenzonitrile (**1f**) required longer reaction times for the reaction completion (Entry 6). For electron-rich functional groups and ortho-substitutions, 10 mol% of catalyst was required to afford the corresponding arylcyanation products in modest to good yields (Entries 7–11). This reaction is also adaptable to heteroaryl cyanides, giving various $(2R^*,3S^*)$ -2-cyano-3-heteroaryl[bicyclo[2.2.1]heptanes in good yields from heteroaryl cyanides such as 3- and 4-pyridyl- and 2-furyl cyanides (Entries 13–15). Unfortunately, 2-cyanopyridine (**11**) did not react with **2a** and was recovered (Entry 12). 2-Cyanothiophene (**1p**) and 1-Boc-3-cyanoindole (**1q**) gave the adducts in good yields by using PMe_2Ph as a ligand (Entries 16 and 17).

A-3. Arylcyanation of Norbornadiene

The resulting $(2R^*,3S^*)$ -2-cyano-3-organobicyclo[2.2.1]hept-5-enes would find further applications as precursors for functionalized cyclopentanes or monomers for ring-opening metathesis polymerization⁴, therefore arylcyanation of norbornadiene (**2b**) would be also synthetically valuable. Although the standard conditions were not applicable to arylcyanation of **2b**, the reaction of **1a** with **2b** in the presence of $\text{Ni}(\text{cod})_2$ (5 mol %) and PMe_3 (15 mol %) was yielded the expected arylcyanation product **3ab** in 77% yield (Table A-2, Entry 1). This catalyst system could be applied to the reactions of

electron-poor aryl cyanides and heteroaryl cyanides to give the corresponding adducts in modest to good yields (Entries 2–7). On the other hand, the sluggish reaction (<20%) of electron-neutral or rich aryl cyanides is presumably due to reluctant oxidative addition of unactivated aryl cyanides to Ni(0)/PMe₃. None of double addition products were observed in all cases.

Table A-2. Arylcyanation of Norbornadiene (**2b**) Catalyzed by Ni/PMe₃^a



Entry	Ar	Time / h	Yield / % ^b
1	4-F ₃ C-C ₆ H ₄ (1a)	21	77 (3ab)
2	4-Me(O)C-C ₆ H ₄ (1c)	19	51 (3cb)
3	4-MeO ₂ C-C ₆ H ₄ (1d)	24	52 (3db)
4	4-Pyridyl (1n)	20	60 (3nb)
5 ^c	2-Furyl (1o)	21	81 (3ob)
6	2-Thienyl (1p)	35	79 (3pb)
7	1-Boc-3-indolyl (1q)	35	34 (3qb)

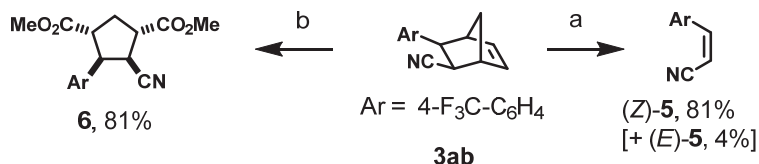
^a Reactions were carried out in toluene (0.67 mL) using an aryl cyanide (1.00 mmol) and **2b** (1.50 mmol) in the presence of Ni(cod)₂ (50 μmol) and PMe₃ (0.150 mmol). ^b Isolated yields based on an aryl cyanide.

^c Ni(cod)₂ (0.100 mmol) and PMe₃ (0.300 mmol) was used as a ligand.

A-4. Transformation of Arylcyanation Product

The retro-Diels-Alder reaction of the arylcyanation product **3ab** proceeded at 190 °C in xylene to give (*Z*)-2-[4-(trifluoromethyl)-phenyl]acrylonitrile [(*Z*)-**5**] along with a small amount of (*E*)-**5** that might be derived from thermal isomerization of (*Z*)-**5**.⁵ In

addition, the ruthenium-catalyzed oxidative cleavage of the remaining double bond in **3ab** followed by methyl esterification with $\text{Me}_3\text{SiCHN}_2$ afforded functionalized cyclopentane **6** in a stereospecific manner (Scheme A-2).

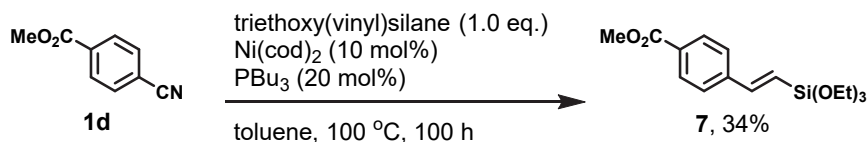


Reagents and conditions: (a) xylene, 190 °C, 24 h
 (b) $\text{RuCl}_3 \cdot 3\text{H}_2\text{O}$ cat., NaIO_4 , $\text{CCl}_4 / \text{CH}_3\text{CN} / \text{H}_2\text{O}$, 0 °C to rt, 1 h,
 then $\text{Me}_3\text{SiCHN}_2$, $\text{MeOH} / \text{C}_6\text{H}_6$, 35 °C, 1 h.

Scheme A-2. Transformations of **3ab**

A-5. Heck-type Reaction

Although other bicyclic alkenes such as *N*-Boc-7-azabicyclo[2.2.1]heptene and bicyclo[2.2.2]octene as well as simple alkenes such as styrene, 1-hexene, and cyclopentene were not amenable to this reaction and did not give the desired arylcyanation product, methyl 4-cyanobenzoate (**1d**) reacted with triethoxy(vinyl)silane under the standard conditions and gave (*E*)-alkenylsilane **7** in 34% yield (Scheme A-3).

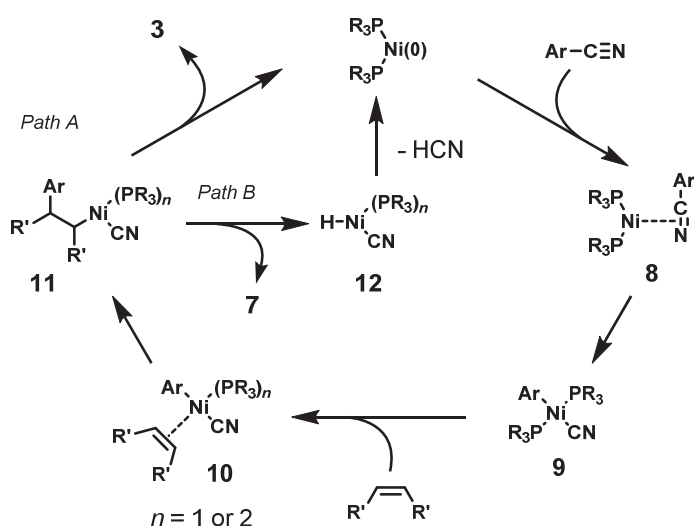


Scheme A-2. Heck-type Reaction of Vinylsilane

This result indicates that the aryl cyanide acts as an arylating agent, presumably via the Heck-type reaction.

A-6. Plausible Mechanism of Arylcyanation

The formation of **7** clearly provides a mechanistic clue that arylnickelation should be involved in the catalytic cycle shown in Scheme A-3. Hence, it is reasonable to assume that the reaction should be initiated by the oxidative addition of an Ar–CN bond to Ni(0) to give *trans*-Ni(II) complex **9** via π -coordinating intermediate **8**.⁶ The nickel center of **9** would be coordinated by an alkene substrate to give four- or five-coordinated Ni(II) intermediate **10**. Subsequent insertion of norbornene or norbornadiene into the Ni–Ar bond (arylnickelation) giving alkylnickel **11**, which reductively eliminates an arylcyanation product and regenerates the Ni(0) (path A), whereas that of triethoxy(vinyl)silane followed by β -hydrogen elimination appears likely to give alkenylsilane **7** (path B).



Scheme A-3. Plausible Mechanism

As already reported,⁷ the fact that an electron density of the *exo*-face of norbornene is higher than that of the *endo*-face should be responsible for the exclusive *exo*-selectivity observed in the present reaction.

A-7. Conclusion

The author demonstrated that arylcyanation, which can introduce two functional groups in one operation, can be applied to carbon–carbon double bonds. The arylcyanation reactions of norbornene and norbornadiene take place with a broad scope of substrates to allow a direct synthesis of (2*R**,3*S**)-3-aryl-2-cyanobicyclo[2.2.1]heptanes and (2*R**,3*S**)-3-aryl-2-cyanobicyclo[2.2.1]hept-5-enes. Also demonstrated was the Heck-type arylation of triethoxy(vinyl)silane using an aryl cyanide, suggesting that an arylnickelation pathway would be operative in the catalytic cycle.

Experimental

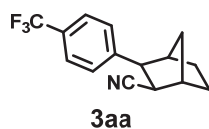
General. All manipulations of oxygen- and moisture-sensitive materials were conducted with a standard Schlenk technique under an argon atmosphere or in a dry box under a nitrogen atmosphere. Flash column chromatography was performed using Merck silica gel 60 (40–63 μm) or Kanto Chemical silica gel 60 (spherical, 40–50 μm). Analytical thin layer chromatography (TLC) was performed on Merck Kieselgel 60 F₂₅₄ (0.25 mm) plates. Visualization was accomplished with UV light (254 nm) and/or an aqueous alkaline KMnO₄ solution followed by heating.

Apparatus. Proton and carbon nuclear magnetic resonance spectra (¹H NMR and ¹³C NMR) were recorded on a Varian UNITY-INOVA 500 (¹H NMR, 500 MHz; ¹³C NMR, 126 MHz) spectrometer or Varian Mercury 400 (¹H, 400 MHz; ¹³C, 101 MHz)

spectrometer with solvent resonance (^1H NMR, CHCl_3 at 7.26 ppm; ^{13}C NMR, CDCl_3 at 77.0 ppm) or CFCl_3 (^{19}F NMR, 0 ppm) as the internal standard. ^1H NMR data are reported as follows: chemical shift, multiplicity (s = singlet, d = doublet, t = triplet, q = quartet, m = multiplet, br m = broad multiplet), coupling constants (Hz), and integration. IR spectra recorded on a Shimadzu FT-IR 8400 spectrometer are reported in cm^{-1} . Melting points (mp) were measured on a Yanaco Mp-500D and are uncorrected. Elemental analyses were performed by Elemental Analysis Center of Kyoto University. High-resolution mass spectra were obtained with a JEOL JMS-700 (EI) spectrometer.

Chemicals. Unless otherwise noted, reagents were commercially available and were used without purification. Toluene was distilled from sodium/benzophenone ketyl. 1-(*tert*-Butoxycarbonyl)-3-cyanoindole (from 3-cyanoindole)⁸ was prepared following the literature procedures.

Arylcyanation of norbornene. *A general procedure.* To a mixture of an aryl cyanide (1.00 mmol) and norbornene (113 mg, 1.20 mmol) was added a solution of $\text{Ni}(\text{cod})_2$ (14.0 mg, 50 μmol) and PBU_3 (20 mg, 0.10 mmol) in toluene (0.60 mL) in a dry box. The vessel was taken outside the dry box and heated at 100 $^\circ\text{C}$. After the time specified in Table A-1, the mixture was filtered through a silica gel pad, concentrated in vacuo, and purified by flash chromatography on silica gel to give arylcyanation products.



(2*R,3*S**)-2-Cyano-3-[4-(trifluoromethyl)phenyl]bicyclo[2.2.1]heptane (3aa).**

A colorless solid (mp = 79.7–80.0 $^\circ\text{C}$), R_f 0.47 (hexane–ethyl acetate = 4:1).

^1H NMR (400 MHz, CDCl_3): δ 7.60 (d, $J = 8.2$ Hz, 2H), 7.35 (d, $J = 8.2$ Hz, 2H), 3.11 (d, $J = 9.2$ Hz, 1H), 3.03 (dd, $J = 9.2, 1.3$ Hz, 1H), 2.76 (br s, 1H), 2.69 (br s, 1H), 2.07 (d, $J = 10.8$ Hz, 1H), 1.80–1.37 (m, 5H).

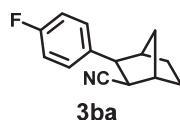
^{13}C NMR $\{^1\text{H}\}$ (101 MHz, CDCl_3): δ 145.0, 129.2 (q, $J = 32.8$ Hz), 128.1, 125.6 (q, $J = 3.6$ Hz), 124.1 (q, $J = 270.7$ Hz), 119.9, 49.7, 42.6, 41.3, 40.9, 36.9, 30.4, 27.6.

IR (KBr): 2966, 2876, 2235, 1618, 1423, 1329, 1298, 1165, 1124, 1111, 1069, 1016, 843, 772, 601 cm^{-1} .

Anal.: $\text{C}_{15}\text{H}_{14}\text{F}_3\text{N}$.

Calcd: C, 67.91; H, 5.32 (%).

Found: C, 67.88; H, 5.47 (%).



(2*R,3*S**)-2-Cyano-3-(4-fluorophenyl)bicyclo[2.2.1]heptane (3ba).**

A colorless solid (mp = 67.5–67.8 °C), R_f 0.49 (hexane–ethyl acetate = 2:1).

^1H NMR (400 MHz, CDCl_3): (br d, $J = 1.7$ Hz, 1H), 2.63 (br d, $J = 1.5$ Hz, 1H), 2.05 (dt, $J = 10.8, 1.8$ Hz, 1H), 1.78–1.51 (m, 3H), 1.43–1.32 (m, 2H).

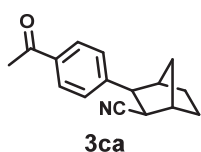
^{13}C NMR $\{^1\text{H}\}$ (101 MHz, CDCl_3): δ 161.7 (d, $J = 244.0$ Hz), 136.8 (d, $J = 3.6$ Hz), 129.2 (d, $J = 8.4$ Hz), 120.1, 115.4 (d, $J = 21.3$ Hz), 49.2, 42.6, 41.6, 41.1, 36.8, 30.4, 27.6.

IR (KBr): 2959, 2878, 2233, 1601, 1508, 1223, 1159, 1097, 839, 820, 758, 538 cm^{-1} .

Anal.: $\text{C}_{14}\text{H}_{14}\text{FN}$.

Calcd: C, 78.11; H, 6.56 (%).

Found: C, 77.84; H, 6.51 (%).



(2*R,3*S**)-3-(4-Acetylphenyl)-2-cyanobicyclo[2.2.1]heptane (3ca).**

A colorless solid (mp = 89.6–89.9 °C), R_f 0.26 (hexane–ethyl acetate = 2:1).

^1H NMR (400 MHz, CDCl_3): δ 7.94 (d, J = 8.3 Hz, 2H), 7.33 (d, J = 8.3 Hz, 2H), 3.11 (d, J = 9.3 Hz, 1H), 3.02 (dd, J = 9.3, 1.8 Hz, 1H), 2.75 (br d, J = 2.6 Hz, 1H), 2.70 (br d, J = 1.3 Hz, 1H), 2.58 (s, 3H), 2.07 (dt, J = 10.6, 1.8 Hz, 1H), 1.79–1.68 (m, 2H), 1.59 (dt, J = 10.8, 1.6 Hz, 1H), 1.44–1.35 (m, 2H).

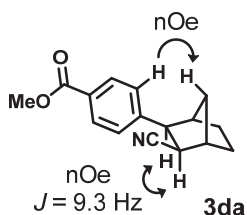
^{13}C NMR { ^1H } (101 MHz, CDCl_3): δ 197.6, 146.4, 135.8, 128.7, 128.0, 119.9, 49.8, 42.6, 41.3, 40.7, 36.9, 30.3, 27.6, 26.5.

IR (KBr): 2957, 2876, 2232, 1682, 1607, 1570, 1420, 1362, 1263, 1184, 962, 860, 835, 766, 598 cm^{-1} .

Anal.: C₁₆H₁₇NO.

Calcd: C, 80.30; H, 7.16 (%).

Found: C, 80.27; H, 7.25 (%).



(2*R,3*S**)-2-Cyano-3-[4-(methoxycarbonyl)phenyl]bicyclo[2.2.1]heptane (3da).**

A colorless solid (mp = 130.4–130.9 °C), *R_f* 0.25 (hexane–ethyl acetate = 2:1).

¹H NMR (500 MHz, CDCl₃): δ 8.01 (d, *J* = 8.4 Hz, 2H), 7.30 (d, *J* = 8.4 Hz, 2H), 3.90 (s, 3H), 3.09 (d, *J* = 9.3 Hz, 1H), 3.00 (dd, *J* = 9.3, 1.3 Hz, 1H), 2.73 (br d, *J* = 2.2 Hz, 1H), 2.68 (br s, 1H), 2.05 (d, *J* = 10.7 Hz, 1H), 1.77–1.63 (m, 2H), 1.56 (d, *J* = 10.7 Hz, 1H), 1.42–1.33 (m, 2H).

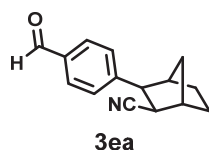
¹³C NMR {¹H} (126 MHz, CDCl₃): δ 166.7, 146.2, 129.8, 128.6, 127.7, 119.8, 51.9, 49.7, 42.5, 41.2, 40.6, 36.8, 30.2, 27.4.

IR (KBr): 2966, 2953, 2872, 2233, 1717, 1609, 1450, 1427, 1283, 1258, 1184, 1109, 1018, 862, 745, 712 cm⁻¹.

Anal.: C₁₆H₁₇NO₂.

Calcd: C, 75.27; H, 6.71 (%).

Found: C, 75.28; H, 6.71 (%).



(2R*,3S*)-2-Cyano-3-(4-formylphenyl)bicyclo[2.2.1]heptane (3ea).

A colorless solid (mp 103.8–104.8 °C), R_f 0.33 (hexane–ethyl acetate = 3:1).

^1H NMR (400 MHz, CDCl_3): δ 9.99 (s, 1H), 7.87 (d, $J = 8.1$ Hz, 2H), 7.41 (d, $J = 8.1$ Hz, 2H), 3.14 (d, $J = 9.3$ Hz, 1H), 3.03 (dd, $J = 9.3, 1.6$ Hz, 1H), 2.77 (br d, $J = 2.4$ Hz, 1H), 2.72 (br d, $J = 1.5$ Hz, 1H), 2.05 (dt, $J = 10.8, 1.8$ Hz, 1H), 1.84–1.66 (m, 2H), 1.60 (dt, $J = 10.8, 1.5$ Hz, 1H), 1.50–1.33 (m, 2H).

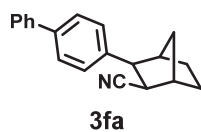
^{13}C NMR $\{^1\text{H}\}$ (101 MHz, CDCl_3): δ 191.8, 148.0, 135.2, 130.1, 128.5, 119.8, 50.0, 42.6, 41.3, 40.7, 37.0, 30.4, 27.6.

IR (KBr): 3447, 2968, 2878, 2235, 1693, 1607, 1574, 1454, 1312, 1215, 1167, 853, 833, 760, 527 cm^{-1} .

Anal.: $\text{C}_{15}\text{H}_{15}\text{NO}$.

Calcd: C, 79.97; H, 6.71 (%).

Found: C, 79.92; H, 6.76 (%).



(2R*,3S*)-3-(4-Biphenyl)-2-cyanobicyclo[2.2.1]heptane (3fa).

A colorless solid (mp = 125.6–125.9 °C), R_f 0.47 (hexane–ethyl acetate = 2:1).

^1H NMR (400 MHz, CDCl_3): δ 7.61–7.57 (m, 4H), 7.43 (t, $J = 7.5$ Hz, 2H), 7.35–7.31 (m, 3H), 3.10 (d, $J = 9.3$ Hz, 1H), 3.03 (dd, $J = 9.3, 1.6$ Hz, 1H), 2.76 (br d, $J = 2.7$ Hz, 1H), 2.71 (br s, 1H), 2.13 (dt, $J = 10.6, 1.6$ Hz, 1H), 1.79–1.36 (m, 5H).

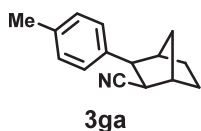
^{13}C NMR $\{^1\text{H}\}$ (101 MHz, CDCl_3): δ 140.7, 140.1, 139.7, 128.7, 128.2, 127.3, 127.2, 127.0, 120.3, 49.7, 42.6, 41.6, 41.1, 37.0, 30.5, 27.7.

IR (KBr): 2953, 2872, 2233, 1487, 1452, 1406, 837, 752, 737, 691, 669 cm^{-1} .

Anal.: $\text{C}_{20}\text{H}_{19}\text{N}$.

Calcd: C, 87.87; H, 7.01 (%).

Found: C, 87.60; H, 7.13 (%).



(2*R,3*S**)-2-Cyano-3-(4-methylphenyl)bicyclo[2.2.1]heptane (3ga).**

A colorless solid (mp 58.1–58.4 °C), R_f 0.53 (hexane–ethyl acetate = 2:1).

^1H NMR (400 MHz, CDCl_3): δ 7.18–7.12 (m, 4H), 3.03 (d, $J = 9.3$ Hz, 1H), 2.97 (dd, $J = 9.3, 1.6$ Hz, 1H), 2.73 (br d, $J = 2.9$ Hz, 1H), 2.66 (br s, 1H), 2.34 (s, 3H), 2.09 (dt, $J = 10.6, 1.7$ Hz, 1H), 1.83–1.32 (m, 5H).

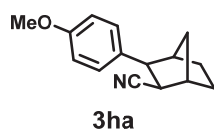
^{13}C NMR $\{^1\text{H}\}$ (101 MHz, CDCl_3): δ 138.0, 136.4, 129.2, 127.5, 120.4, 49.5, 42.5, 41.6, 40.9, 36.9, 30.4, 27.6, 21.0.

IR (KBr): 2961, 2876, 2232, 1514, 822, 754, 534, 484 cm^{-1} .

Anal.: $\text{C}_{15}\text{H}_{17}\text{N}$.

Calcd: C, 85.26; H, 8.11 (%).

Found: C, 85.35; H, 8.19 (%).



(2*R,3*S**)-2-Cyano-3-(4-methoxyphenyl)bicyclo[2.2.1]heptane (3ha).**

A colorless solid (mp 64.9–65.3 °C), R_f 0.40 (hexane–ethyl acetate = 2:1).

^1H NMR (400 MHz, CDCl_3): δ 7.17 (d, J = 8.8 Hz, 2H), 6.88 (d, J = 8.8 Hz, 2H), 3.79 (s, 3H), 3.01 (d, J = 9.1 Hz, 1H), 2.95 (dd, J = 9.3, 1.3 Hz, 1H), 2.71 (br s, 1H), 2.63 (br s, 1H), 2.07 (d, J = 10.6 Hz, 1H), 1.77–1.61 (m, 2H), 1.53 (d, J = 10.6 Hz, 1H), 1.45–1.28 (m, 2H).

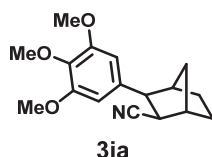
^{13}C NMR $\{^1\text{H}\}$ (101 MHz, CDCl_3): δ 158.2, 133.1, 128.6, 120.4, 113.8, 55.1, 49.1, 42.5, 41.6, 41.1, 36.8, 30.4, 27.6.

IR (KBr): 2959, 2866, 2232, 1612, 1514, 1456, 1308, 1294, 1246, 1182, 1040, 841, 536 cm^{-1} .

Anal.: C₁₅H₁₇NO.

Calcd: C, 79.26; H, 7.54 (%).

Found: C, 79.15; H, 7.53 (%).



(2*R,3*S**)-2-Cyano-3-(3,4,5-trimethoxyphenyl)bicyclo[2.2.1]heptane (3ia).**

A colorless solid (mp 108.4–108.6 °C), R_f 0.24 (hexane–ethyl acetate = 2:1).

¹H NMR (400 MHz, CDCl₃): δ 6.45 (s, 2H), 3.86 (s, 6H), 3.83 (s, 3H), 2.99 (s, 1H), 2.98 (s, 1H), 2.73 (br d, *J* = 3.1 Hz, 1H), 2.63 (br d, *J* = 1.6 Hz, 1H), 2.06 (dt, *J* = 10.6, 1.8 Hz, 1H), 1.78–1.63 (m, 2H), 1.55 (dt, *J* = 10.6, 1.6 Hz, 1H), 1.44–1.31 (m, 2H).

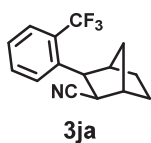
¹³C NMR {¹H} (101 MHz, CDCl₃): δ 153.1, 137.0, 136.7, 120.2, 105.0, 60.9, 56.1, 50.2, 42.5, 41.6, 41.2, 36.9, 30.5, 27.6.

IR (KBr): 2968, 2239, 1589, 1510, 1460, 1423, 1238, 1124, 1011 cm⁻¹.

Anal.: C₁₇H₂₁NO₃.

Calcd: C, 71.06; H, 7.37 (%).

Found: C, 70.77; H, 7.27 (%).



(2*R,3*S**)-2-Cyano-3-(2-trifluoromethylphenyl)bicyclo[2.2.1]heptane (3ja).**

A colorless solid (mp 79.8–80.1 °C), R_f 0.54 (hexane–ethyl acetate = 2:1).

^1H NMR (400 MHz, CDCl_3): δ 7.68 (d, $J = 7.9$ Hz, 1H), 7.61–7.56 (m, 2H), 7.42–7.35 (m, 1H), 3.36 (d, $J = 9.1$ Hz, 1H), 3.05 (d, $J = 9.1$ Hz, 1H), 2.72 (br d, $J = 3.7$ Hz, 1H), 2.67 (br d, $J = 1.8$ Hz, 1H), 2.19 (d, $J = 10.8$ Hz, 1H), 1.84–1.38 (m, 5H).

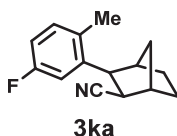
^{13}C NMR $\{^1\text{H}\}$ (101 MHz, CDCl_3): δ 139.7 (q, $J = 9.1$ Hz), 132.2, 128.4 (q, $J = 29.7$ Hz), 128.1, 127.0, 126.2 (q, $J = 6.2$ Hz), 124.4 (q, $J = 272.2$ Hz), 119.8, 45.4, 42.6, 42.1, 41.8, 37.7, 30.8, 27.3.

IR (KBr): 2972, 2239, 1450, 1312, 1161, 1140, 1124, 1107, 1063, 1038, 775, 729, 650 cm^{-1} .

Anal.: $\text{C}_{15}\text{H}_{14}\text{F}_3\text{N}$.

Calcd: C, 67.91; H, 5.32 (%).

Found: C, 67.68; H, 5.34 (%).



(2*R,3*S**)-2-Cyano-3-(5-fluoro-2-methylphenyl)bicyclo[2.2.1]heptane (3ka).**

A colorless solid (mp 125.9–126.1 °C), R_f 0.53 (hexane–ethyl acetate = 2:1).

^1H NMR (400 MHz, CDCl_3): δ 7.14 (dd, $J = 8.3, 6.1$ Hz, 1H), 7.02 (dd, $J = 10.5, 2.7$ Hz, 1H), 6.86 (td, $J = 8.2, 2.7$ Hz, 1H), 3.08–3.02 (m, 2H), 2.74 (br d, $J = 1.6$ Hz, 1H), 2.71 (br d, $J = 1.5$ Hz, 1H), 2.26 (s, 3H), 2.04 (dt, $J = 10.8, 1.7$ Hz, 1H), 1.83–1.68 (m, 2H), 1.58 (dt, $J = 10.6, 1.6$ Hz, 1H), 1.45–1.37 (m, 2H).

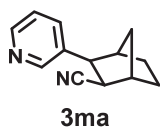
^{13}C NMR $\{^1\text{H}\}$ (101 MHz, CDCl_3): δ 161.4 (d, $J = 241.7$ Hz), 141.1 (d, $J = 6.8$ Hz), 131.7, 131.6 (d, $J = 7.6$ Hz), 119.5, 113.4 (d, $J = 20.6$ Hz), 112.9 (d, $J = 18.1$ Hz), 46.9, 42.6, 40.2, 40.0, 36.7, 30.2, 27.8, 19.2.

IR (KBr): 2959, 2878, 2232, 1611, 1587, 1495, 1454, 1265, 1242, 1153, 868, 820, 735 cm^{-1} .

Anal.: $\text{C}_{15}\text{H}_{16}\text{FN}$.

Calcd: C, 78.57; H, 7.03 (%).

Found: C, 78.37; H, 7.00 (%).



(2*R,3*S**)-2-Cyano-3-(3-pyridyl)bicyclo[2.2.1]heptane (3ma).**

A colorless solid (mp 80.1–80.4 °C), R_f 0.20 (hexane–ethyl acetate = 1:2).

^1H NMR (400 MHz, CDCl_3): δ 8.57–8.44 (m, 2H), 7.61 (dt, $J = 8.0, 1.8$ Hz, 1H), 7.30 (dd, $J = 7.9, 4.9$ Hz, 1H), 3.06 (d, $J = 9.3$ Hz, 1H), 3.01 (dd, $J = 9.3, 1.8$ Hz, 1H), 2.77 (br d, $J = 2.6$ Hz, 1H), 2.65 (br d, $J = 1.5$ Hz, 1H), 2.06 (dt, $J = 11.0, 1.8$ Hz, 1H), 1.83–1.65

(m, 2H), 1.59 (dt, $J = 10.8, 1.6$ Hz, 1H), 1.48–1.35 (m, 2H).

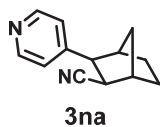
^{13}C NMR $\{^1\text{H}\}$ (101 MHz, CDCl_3): δ 149.4, 148.3, 136.6, 135.2, 123.5, 119.8, 47.5, 42.6, 41.3, 41.1, 36.9, 30.5, 27.5.

IR (KBr): 2968, 2878, 2359, 2341, 2233, 1574, 1481, 1425, 1028, 822, 754, 716, 629 cm^{-1} .

Anal.: $\text{C}_{13}\text{H}_{14}\text{N}_2$.

Calcd: C, 78.75; H, 7.12 (%).

Found: C, 78.59; H, 7.15 (%).



(2*R,3*S**)-2-Cyano-3-(4-pyridyl)bicyclo[2.2.1]heptane (3na).**

A colorless oil, R_f 0.11 (hexane–ethyl acetate = 2:1).

^1H NMR (400 MHz, CDCl_3): δ 8.53 (d, $J = 6.0$ Hz, 2H), 7.12 (d, $J = 6.0$ Hz, 2H), 2.98 (s, 2H), 2.72 (br d, $J = 1.8$ Hz, 1H), 2.64 (br s, 1H), 1.97 (dt, $J = 10.8, 1.8$ Hz, 1H), 1.78–1.30 (m, 5H).

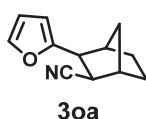
^{13}C NMR $\{^1\text{H}\}$ (101 MHz, CDCl_3): δ 149.9, 149.7, 122.9, 119.5, 49.0, 42.5, 40.7, 40.3, 36.8, 30.0, 27.4.

IR (KBr): 2964, 2878, 2235, 1601, 1418, 833, 760 cm^{-1} .

Anal.: $\text{C}_{13}\text{H}_{14}\text{N}_2$.

Calcd: C, 78.75; H, 7.12 (%).

Found: C, 78.74; H, 7.14 (%).



(2*R,3*S**)-2-Cyano-3-(2-furyl)bicyclo[2.2.1]heptane (3oa).**

A colorless oil, R_f 0.50 (hexane–ethyl acetate = 2:1).

^1H NMR (400 MHz, CDCl_3): δ 7.37 (dd, $J = 1.7, 0.7$ Hz, 1H), 6.32 (dd, $J = 3.2, 1.8$ Hz, 1H), 6.18 (d, $J = 3.2$ Hz, 1H), 3.11 (d, $J = 9.0$ Hz, 1H), 2.86 (dd, $J = 9.0, 1.7$ Hz, 1H), 2.70 (br d, $J = 1.8$ Hz, 1H), 2.60 (br d, $J = 1.6$ Hz, 1H), 2.11 (dt, $J = 10.6, 1.6$ Hz, 1H), 1.75–1.58 (m, 2H), 1.47 (dt, $J = 10.6, 1.7$ Hz, 1H), 1.42–1.25 (m, 2H).

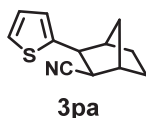
^{13}C NMR { ^1H } (101 MHz, CDCl_3): δ 154.4, 141.7, 120.0, 110.0, 106.0, 44.3, 42.5, 40.7, 39.1, 36.5, 29.2, 27.6.

IR (neat): 2964, 2878, 2235, 1593, 1506, 1456, 1300, 1157, 1013, 739 cm^{-1} .

Anal.: $\text{C}_{12}\text{H}_{13}\text{NO}$.

Calcd: C, 76.98; H, 7.00 (%).

Found: C, 77.26; H, 7.28 (%).



(2*R,3*S**)-2-Cyano-3-(2-thienyl)bicyclo[2.2.1]heptane (3pa).**

A yellow oil, R_f 0.47 (hexane–ethyl acetate = 2:1).

^1H NMR (400 MHz, CDCl_3): δ 7.20 (dd, $J = 5.1, 1.0$ Hz, 1H), 6.98 (dd, $J = 5.1, 3.7$ Hz, 1H), 6.94 (dt, $J = 3.7, 1.0$ Hz, 1H), 3.31 (d, $J = 9.0$ Hz, 1H), 2.95 (dd, $J = 9.0, 1.8$ Hz, 1H), 2.75 (br dd, $J = 1.8, 1.1$ Hz, 1H), 2.66 (br d, $J = 1.2$ Hz, 1H), 2.15 (dt, $J = 10.8, 1.6$ Hz, 1H), 1.78–1.26 (m, 5H).

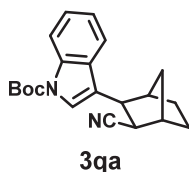
^{13}C NMR $\{^1\text{H}\}$ (101 MHz, CDCl_3): δ 144.2, 126.8, 124.8, 123.9, 119.9, 45.6, 43.4, 42.8, 41.7, 36.6, 29.9, 27.6.

IR (neat): 2962, 2876, 2235, 1452, 1437, 1298, 1238, 839, 698 cm^{-1} .

Anal.: $\text{C}_{12}\text{H}_{13}\text{NS}$.

Calcd: C, 70.89; H, 6.45 (%).

Found: C, 71.03; H, 6.44 (%).



(2*R,3*S**)-3-(1-*tert*-Butoxycarbonyl-3-indolyl)-2-cyanobicyclo[2.2.1]heptane (3qa).**

A colorless solid, mp 133.0–133.2 °C, R_f 0.10 (hexane–ethyl acetate = 10:1).

^1H NMR (400 MHz, CDCl_3): δ 8.07 (br s, 1H), 7.54 (br s, 1H), 7.43 (dd, $J = 7.7, 0.7$ Hz, 1H), 7.32 (td, $J = 7.7, 1.2$ Hz, 1H), 7.24 (td, $J = 7.3, 0.9$ Hz, 1H), 3.20 (d, $J = 9.0$ Hz, 1H), 3.05 (dd, $J = 9.0, 1.5$ Hz, 1H), 2.78 (br d, $J = 2.4$ Hz, 1H), 2.72 (br s, 1H), 2.09 (dt, $J = 10.6, 1.7$ Hz, 1H), 1.83–1.62 (m, 2H), 1.69 (s, 9H), 1.55 (dt, $J = 10.6, 1.6$ Hz, 1H), 1.49–1.39 (m, 2H).

^{13}C NMR $\{^1\text{H}\}$ (101 MHz, CDCl_3): δ 149.8, 130.2, 124.6, 122.5, 121.9, 121.1, 120.2, 118.4, 115.4, 109.7, 83.7, 43.4, 41.3, 41.1, 39.8, 36.4, 30.0, 28.2, 27.7.

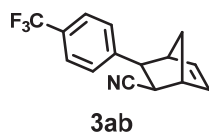
IR (KBr): 2968, 2931, 2880, 2233, 1730, 1456, 1375, 1261, 1223, 1155, 1088, 1020, 768, 750 cm^{-1} .

Anal.: $\text{C}_{21}\text{H}_{24}\text{N}_2\text{O}_2$.

Calcd: C, 74.97; H, 7.19 (%).

Found: C, 75.04; H, 7.31 (%).

Arylcyanation of norbornadiene. *A general procedure.* To a mixture of an aryl cyanide (1.00 mmol) and norbornadiene (138 mg, 1.50 mmol) was added a solution of $\text{Ni}(\text{cod})_2$ (14.0 mg, 50 μmol) and PMe_3 (11.4 mg, 0.150 mmol) in toluene (0.67 mL) in a dry box. The vessel was taken outside the dry box and heated at 100 $^\circ\text{C}$. After the time specified in Table A-2, the mixture was filtered through a silica gel pad, concentrated in vacuo, and purified by flash chromatography on silica gel to give arylcyanation products.



(2*R,3*S**)-2-Cyano-3-[4-(trifluoromethyl)phenyl]bicyclo[2.2.1]hept-5-ene (3ab).**

A colorless solid (mp = 69.1–70.4 °C), R_f 0.24 (hexane–ethyl acetate = 5:1).

^1H NMR (400 MHz, CDCl_3): δ 7.63 (d, $J = 8.3$ Hz, 2H), 7.38 (d, $J = 8.3$ Hz, 2H), 6.45 (dd, $J = 5.7, 3.3$ Hz, 1H), 6.23 (dd, $J = 5.7, 2.9$ Hz, 1H), 3.38 (s, 1H), 3.23 (d, $J = 1.5$ Hz, 1H), 3.11 (d, $J = 9.1$ Hz, 1H), 2.87 (dd, $J = 9.1, 1.8$ Hz, 1H), 2.09 (d, $J = 9.5$ Hz, 1H), 1.84 (dt, $J = 9.5, 1.8$ Hz, 1H).

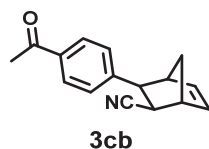
^{13}C NMR $\{^1\text{H}\}$ (101 MHz, CDCl_3): δ 144.2, 140.4, 135.6, 129.3 (q, $J = 32.2$ Hz), 128.5, 125.6 (q, $J = 3.8$ Hz), 124.1 (q, $J = 272.2$ Hz), 120.7, 48.3, 47.0, 46.2, 46.1, 36.3.

IR (KBr): 2991, 2972, 2949, 2235, 1618, 1454, 1418, 1333, 1159, 1146, 1119, 1070, 1016, 847, 787, 768, 739, 708, 652, 602 cm^{-1} .

Anal.: $\text{C}_{15}\text{H}_{12}\text{F}_3\text{N}$.

Calcd: C, 68.44; H, 4.59 (%).

Found: C, 68.28; H, 4.60 (%).



(2*R,3*S**)-3-(4-Acetylphenyl)-2-cyanobicyclo[2.2.1]hept-5-ene (3cb).**

A colorless solid (mp = 120.5–121.0 °C), R_f 0.31 (hexane–ethyl acetate = 2:1).

^1H NMR (400 MHz, CDCl_3): δ 7.96 (d, $J = 8.4$ Hz, 2H), 7.35 (d, $J = 8.4$ Hz, 2H), 6.45 (dd, $J = 5.7, 3.3$ Hz, 1H), 6.22 (dd, $J = 5.7, 3.1$ Hz, 1H), 3.37 (s, 1H), 3.25 (d, $J = 1.5$ Hz, 1H), 3.11 (dd, $J = 9.1, 1.3$ Hz, 1H), 2.87 (dd, $J = 9.1, 1.8$ Hz, 1H), 2.60 (s, 3H), 2.10 (d, $J = 9.5$ Hz, 1H), 1.84 (dt, $J = 9.5, 1.8$ Hz, 1H).

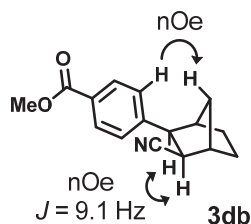
^{13}C NMR $\{^1\text{H}\}$ (101 MHz, CDCl_3): δ 197.6, 145.6, 140.4, 135.8, 135.5, 128.7, 128.3, 120.7, 48.2, 47.2, 46.2, 46.0, 36.4, 26.6.

IR (KBr): 2997, 2980, 2943, 2232, 1680, 1605, 1412, 1362, 1273, 841, 729, 608, 592 cm^{-1} .

Anal.: $\text{C}_{16}\text{H}_{15}\text{NO}$.

Calcd: C, 80.98; H, 6.37 (%).

Found: C, 80.79; H, 6.47 (%).



(2*R,3*S**)-2-Cyano-3-[4-(methoxycarbonyl)phenyl]bicyclo[2.2.1]hept-5-ene (3db).**

A colorless solid (mp = 108.1–111.3 °C), R_f 0.16 (hexane–ethyl acetate = 5:1).

^1H NMR (400 MHz, CDCl_3): δ 8.04 (d, $J = 8.4$ Hz, 2H), 7.33 (d, $J = 8.4$ Hz, 2H), 6.44

(dd, $J = 5.6, 3.2$ Hz, 1H), 6.21 (dd, $J = 5.7, 3.1$ Hz, 1H), 3.91 (s, 3H), 3.36 (s, 1H), 3.24 (d, $J = 1.3$ Hz, 1H), 3.11 (d, $J = 9.1$ Hz, 1H), 2.86 (dd, $J = 9.1, 1.6$ Hz, 1H), 2.09 (d, $J = 9.5$ Hz, 1H), 1.83 (dt, $J = 9.5, 1.6$ Hz, 1H).

^{13}C NMR $\{^1\text{H}\}$ (101 MHz, CDCl_3): δ 166.8, 145.4, 140.5, 135.5, 129.9, 128.9, 128.1, 120.7, 52.0, 48.2, 47.2, 46.2, 46.0, 36.4.

IR (KBr): 2988, 2949, 2230, 1717, 1611, 1433, 1283, 1192, 1115, 1018, 860, 756, 729, 716 cm^{-1} .

Anal.: $\text{C}_{16}\text{H}_{15}\text{NO}_2$.

Calcd: C, 75.87; H, 5.97 (%).

Found: C, 75.60; H, 6.08 (%).



(2*R,3*S**)-2-Cyano-3-(4-pyridyl)bicyclo[2.2.1]heptane (3nb).**

A brown oil, R_f 0.24 (hexane–ethyl acetate = 1:5).

^1H NMR (400 MHz, CDCl_3): δ 8.60 (d, $J = 5.7$ Hz, 2H), 7.18 (d, $J = 6.0$ Hz, 2H), 6.44 (dd, $J = 5.6, 3.2$ Hz, 1H), 6.23 (dd, $J = 5.7, 2.9$ Hz, 1H), 3.29 (s, 1H), 3.23 (s, 1H), 3.01 (d, $J = 9.1$ Hz, 1H), 2.87 (dd, $J = 9.3, 1.8$ Hz, 1H), 2.04 (d, $J = 9.5$ Hz, 1H), 1.84 (dt, $J = 9.5, 1.7$ Hz, 1H).

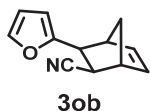
^{13}C NMR $\{^1\text{H}\}$ (101 MHz, CDCl_3): δ 150.0, 149.2, 140.2, 135.7, 123.3, 120.4, 48.3, 46.6, 46.2, 45.7, 36.1.

IR (neat): 3385, 3071, 3028, 2982, 2949, 2876, 2235, 1599, 1553, 1497, 1454, 1416, 1333, 1313, 1265, 1256, 1221, 1072, 997, 988, 918, 833, 770, 708, 644, 631, 554, 538, 513, 469 cm^{-1} .

Anal.: $\text{C}_{13}\text{H}_{12}\text{N}_2$.

Calcd: C, 79.56; H, 6.16 (%).

Found: C, 79.56; H, 6.42 (%).



(2*R,3*S**)-2-Cyano-3-(2-furyl)bicyclo[2.2.1]hept-5-ene (3ob).**

A brown oil, R_f 0.38 (hexane–ethyl acetate = 5:1).

^1H NMR (400 MHz, CDCl_3): δ 7.42–7.40 (m, 1H), 6.38–6.33 (m, 2H), 6.23 (dd, $J = 3.2$, 0.6 Hz, 1H), 6.19 (dd, $J = 5.7$, 2.9 Hz, 1H), 3.33 (s, 1H), 3.16 (d, $J = 0.7$ Hz, 1H), 3.08 (d, $J = 8.8$, 1.3 Hz, 1H), 2.72 (dd, $J = 8.9$, 1.9 Hz, 1H), 2.19 (dd, $J = 9.4$, 0.5 Hz, 1H), 1.74 (dt, $J = 9.5$, 1.7 Hz, 1H).

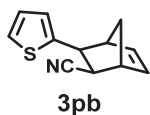
^{13}C NMR $\{^1\text{H}\}$ (101 MHz, CDCl_3): δ 153.7, 142.2, 139.4, 135.7, 120.6, 110.3, 106.8, 48.2, 46.7, 46.3, 41.6, 34.7.

IR (neat): 2984, 2237, 1715, 1591, 1504, 1454, 1325, 1165, 1140, 1016, 905, 766, 721, 687, 598 cm^{-1} .

Anal.: $\text{C}_{12}\text{H}_{11}\text{NO}$.

Calcd: C, 77.81; H, 5.99 (%).

Found: C, 77.94; H, 6.12 (%).



(2*R,3*S**)-2-Cyano-3-(2-thienyl)bicyclo[2.2.1]hept-5-ene (3pb).**

A colorless solid (mp = 83.4–83.9 °C), R_f 0.20 (hexane–ethyl acetate = 10:1).

^1H NMR (400 MHz, CDCl_3): δ 7.24 (dd, $J = 5.1, 1.3$ Hz, 1H), 7.01 (dd, $J = 5.0, 3.6$ Hz, 1H), 6.97 (dd, $J = 3.5, 1.0$ Hz, 1H), 6.41 (dd, $J = 5.7, 3.3$ Hz, 1H), 6.19 (dd, $J = 5.7, 2.9$ Hz, 1H), 3.37 (d, $J = 0.5$ Hz, 1H), 3.30 (dd, $J = 8.8, 1.5$ Hz, 1H), 3.19 (d, $J = 1.3$ Hz, 1H), 2.80 (dd, $J = 8.9, 1.9$ Hz, 1H), 2.21 (d, $J = 9.7$ Hz, 1H), 1.81 (dq, $J = 9.5, 1.8$ Hz, 1H).

^{13}C NMR $\{^1\text{H}\}$ (101 MHz, CDCl_3): δ 143.2, 140.0, 135.4, 127.0, 125.4, 124.4, 120.7, 48.9, 48.4, 46.2, 42.9, 36.8.

IR (KBr): 3103, 3061, 3011, 2980, 2953, 2918, 2876, 2233, 1435, 1321, 1271, 1258, 1244, 1042, 922, 903, 841, 760, 741, 716, 698, 538 cm^{-1} .

Anal.: C₁₂H₁₁NS.

Calcd: C, 71.60; H, 5.51 (%).

Found: C, 71.71; H, 5.43 (%).



(2*R,3*S**)-3-(1-*tert*-Butoxycarbonyl-3-indolyl)-2-cyanobicyclo[2.2.1]hept-5-ene**

(3qb).

A colorless solid (mp = 150.6–151.4 °C), R_f 0.13 (hexane–ethyl acetate = 10:1).

¹H NMR (400 MHz, CDCl₃): δ 8.09 (br s, 1H), 7.53 (br s, 1H), 7.40 (d, *J* = 7.7 Hz, 1H), 7.33 (td, *J* = 7.7, 1.1 Hz, 1H), 7.24 (td, *J* = 7.3, 0.9 Hz, 1H), 6.45 (dd, *J* = 5.7, 3.1 Hz, 1H), 6.24 (dd, *J* = 5.6, 3.0 Hz, 1H), 3.40 (s, 1H), 3.27 (s, 1H), 3.15 (d, *J* = 8.8 Hz, 1H), 2.88 (dd, *J* = 8.8, 1.6 Hz, 1H), 2.14 (d, *J* = 9.3 Hz, 1H), 1.81 (dt, *J* = 9.3, 1.6 Hz, 1H), 1.69 (s, 9H).

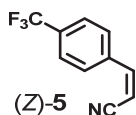
¹³C NMR {¹H} (101 MHz, CDCl₃): δ 149.8, 140.1, 135.3, 130.8, 124.7, 122.6, 122.0, 120.9, 120.7, 118.5, 115.5, 83.8, 49.1, 46.8, 46.1, 38.5, 35.0, 28.2.

IR (KBr): 3067, 2993, 2976, 2937, 2232, 1724, 1477, 1452, 1381, 1340, 1329, 1310, 1256, 1225, 1157, 1111, 1090, 1022, 872, 853, 768, 746, 721, 698 cm⁻¹.

Anal.: C₂₁H₂₂N₂O₂.

Calcd: C, 75.42; H, 6.63 (%).

Found: C, 75.18; H, 6.70 (%).



Retro-Diels-Alder reaction of **3ab**.

A solution of **3ab** (0.26 g, 1.00 mmol) in xylene (0.20 mL) was heated at 190 °C for 26 h and then concentrated in vacuo. The residue was purified by flash chromatography on silica to give (*Z*)-2-(4-trifluoromethylphenyl)acrylonitrile [(*Z*)-**5**, 161 mg, 81%, (*E*)-**5** was also obtained in 4% yield] as a colorless oil.

R_f 0.25 (hexane-ethyl acetate = 5:1).

¹H NMR (400 MHz, CDCl₃): δ 7.90 (d, *J* = 8.2 Hz, 2H), 7.71 (d, *J* = 8.2 Hz, 2H), 7.19 (d, *J* = 12.1 Hz, 1H), 5.61 (d, *J* = 12.1 Hz, 2H).

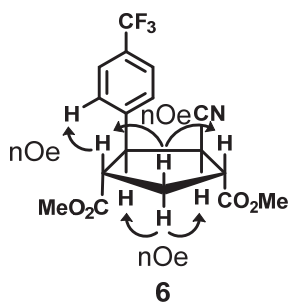
¹³C NMR {¹H} (101 MHz, CDCl₃): δ 147.0, 136.6, 132.3 (q, *J* = 32.2 Hz), 129.2, 125.9 (q, *J* = 3.8 Hz), 123.6 (q, *J* = 273.0 Hz), 116.6, 98.0.

IR (neat): 3071, 2218, 1618, 1420, 1325, 1171, 1126, 1069, 1016, 851, 606 cm⁻¹.

Anal.: C₁₀H₆F₃N.

Calcd: C, 60.92; H, 3.07 (%).

Found: C, 61.21; H, 3.36 (%).



Oxidative ring-opening reaction of **3ab**.

To a solution of **3ab** (0.26 g, 1.00 mmol) in $\text{CCl}_4\text{-CH}_3\text{CN-H}_2\text{O}$ (1.0:1.0:1.5, 3.1 mL) were added $\text{RuCl}_3\cdot 3\text{H}_2\text{O}$ (5.8 mg, 22 μmol) and NaIO_4 (0.96 g, 4.5 mmol) at 0 °C, and the resulting mixture was stirred at rt for 1 h. The mixture was diluted with acetone (10 mL), filtered through a Celite pad, and concentrated in vacuo. The dilution-filtration-concentration procedure was continued twice [acetonitrile (10 mL) was used for the third dilution]. The residue was again diluted with a crude dicarboxylic acid thus obtained was dissolved in MeOH-benzene (1.0:3.5, 9.0 mL) and a 2.0 M solution of $\text{Me}_3\text{SiCHN}_2$ in hexane (1.25 mL, 2.5 mmol) was added at rt. The resulting mixture was stirred at 35 °C for 1 h and then concentrated in vacuo. The residue was purified by flash chromatography on silica gel to give **6** (0.29 g, 81%) as a colorless oil.

R_f 0.30 (hexane–ethyl acetate = 2:1).

$^1\text{H NMR}$ (400 MHz, CDCl_3): δ 7.64 (d, $J = 8.1$ Hz, 2H), 7.45 (d, $J = 8.1$ Hz, 2H), 3.84 (dd, $J = 10.2, 8.3$ Hz, 1H), 3.79 (s, 3H), 3.76 (dd, $J = 8.2, 4.8$ Hz, 1H), 3.63 (s, 3H), 3.43–3.35 (m, 2H), 2.74 (dt, $J = 13.7, 8.7$ Hz, 1H), 2.30 (ddd, $J = 13.7, 9.5, 7.9$ Hz, 1H).

$^{13}\text{C NMR}$ $\{^1\text{H}\}$ (101 MHz, CDCl_3): δ 172.6, 172.0, 140.6, 130.0 (q, $J = 33.0$ Hz), 128.4, 125.6 (q, $J = 3.1$ Hz), 123.8 (q, $J = 272.2$ Hz), 118.6, 52.6, 52.2, 49.8, 47.5, 47.0, 38.6,

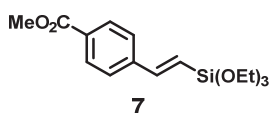
32.6.

IR (neat): 2957, 2243, 1732, 1620, 1439, 1329, 1271, 1200, 1171, 1123, 1070, 1018, 845, 760, 669, 409 cm^{-1} .

Anal.: $\text{C}_{17}\text{H}_{16}\text{F}_3\text{NO}_4$.

Calcd: C, 57.47; H, 4.54 (%).

Found: C, 57.19; H, 4.64 (%).



Heck-type reaction of triethoxy(vinyl)silane with methyl 4-cyanobenzote

To a mixture of methyl 4-cyanobenzote (161 mg, 1.00 mmol) and triethoxy(vinyl)silane (190 mg, 1.00 mmol) was added a solution of $\text{Ni}(\text{cod})_2$ (14.0 mg, 50 μmol) and PBU_3 (20 mg, 0.100 mmol) in toluene (0.60 mL) in a dry box. The vessel was taken outside the dry box and heated at 100 $^\circ\text{C}$ for 100 h. The mixture was filtered through a silica gel pad, concentrated in vacuo, and purified by flash chromatography on silica gel to give (*E*)-triethoxy[2-(4-methoxycarbonylphenyl)ethenyl]silane (**7**, 109 mg, 34%) as a colorless oil. R_f 0.44 (hexane–ethyl acetate = 5:1).

^1H NMR (400 MHz, CDCl_3): δ 8.00 (d, $J = 8.2$ Hz, 2H), 7.51 (d, $J = 8.2$ Hz, 2H), 7.22 (d, $J = 19.2$ Hz, 1H), 6.29 (d, $J = 19.2$ Hz, 1H), 3.90 (s, 3H), 3.88 (q, $J = 7.0$ Hz, 6H), 1.26 (t, $J = 7.0$ Hz, 9H).

^{13}C NMR $\{\text{}^1\text{H}\}$ (101 MHz, CDCl_3): δ 166.7, 147.7, 141.7, 129.9, 129.8, 126.6, 121.2, 58.6, 52.1, 18.2.

HRMS (EI) m/z : $[\text{M}]^+$ calcd for $\text{C}_{16}\text{H}_{24}\text{O}_5\text{Si}$, 324.1393; found, 324.1389.

Reference

- ¹ Nakao, Y. Metal-mediated C–CN Bond Activation in Organic Synthesis. *Chem. Rev.* **2021**, *121*, 327–344.
- ² For cyanoesterification, see: Nishihara, Y.; Inoue, Y.; Itazaki, M.; Takagi, K. Palladium-Catalyzed Cyanoesterification of Norbornenes with Cyanoformates via the NC-Pd-COOR (R = Me and Et) Intermediate. *Org. Lett.* **2005**, *7*, 2639–2641.
- ³ Tsuda, T.; Kiyoi, T.; Saegusa, T. Nickel(0)-catalyzed hydroacylation of alkynes with aldehydes to α,β -enones *J. Org. Chem.* **1990**, *55*, 2554–2558.
- ⁴ Yoshida, Y.; Goto, K.; Komiya, Z. Preparation and Properties of Ester or Cyano Group Substituted Ring-Opening Polymers and Their Hydrogenated Derivatives. *J. Appl. Polym. Sci.* **1997**, *66*, 367–375.
- ⁵ Arylcyanation of acetylene was unsuccessful. See Refs. 1a and 1b. For (Z)-selective synthesis of β -arylacrylonitriles, see: Kojima, S.; Fukuzaki, T.; Yamakawa, A.; Murai, Y. Highly (Z)-Selective Synthesis of β -Monosubstituted α,β -Unsaturated Cyanides Using the Peterson Reaction. *Org. Lett.* **2004**, *6*, 3917–3920.
- ⁶ a) Parshall, G. W. σ -Aryl Compounds of Nickel, Palladium, and Platinum. Synthesis and Bonding Studies. *J. Am. Chem. Soc.* **1974**, *96*, 2360–2366. b) Abila, M.; Yamamoto, T. Oxidative Addition of C–CN Bond to Nickel(0) Complex: Synthesis and Crystal

-
- Structures of Ni(CN)(o-C₆H₄CN)(bpy) and Ni(CN)(p-C₆H₄CN)(bpy). *J. Organomet. Chem.* **1997**, *532*, 267–270. c) Garcia, J. J.; Jones, W. D. Reversible Cleavage of Carbon–Carbon Bonds in Benzonitrile Using Nickel(0). *Organometallics* **2000**, *19*, 5544–5545.
- ⁷ a) Kondo, T.; Uenoyama, S.; Fujita, K.; Mitsudo, T. First Transition-Metal Complex Catalyzed Addition of Organic Disulfides to Alkenes Enables the Rapid Synthesis of vicinal-Dithioethers. *J. Am. Chem. Soc.* **1999**, *121*, 482–483. b) S Inagaki, S.; Fujimoto, H.; Fukui, K. Orbital mixing rule. *J. Am. Chem. Soc.* **1976**, *98*, 4054–4061.
- ⁸ Deng, W.-P.; Nam, G.; Fan, J.; Kirk, K. L. Syntheses of β,β -Difluorotryptamines. *J. Org. Chem.* **2003**, *68*, 2798–2802.

List of publications

- (1) A novel tricyclic β -lactam exhibiting potent antibacterial activities against carbapenem-resistant Enterobacterales: Synthesis and structure-activity-relationships.
Jun Sato, Hiroki Kusano, Toshiaki Aoki, Satoru Shibuya, Katsuki Yokoo, Kazuo Komano, Takuya Oguma, Shuhei Matsumoto, Takafumi Sato, Kazuya Yasuo, Kenji Yamawaki
Bioorg. Med. Chem. **2021**, *46*, 116343. Copyright 2021 Elsevier Ltd. Reproduced with permission. To access the final edited and published work, see [<https://doi.org/10.1016/j.bmc.2021.116343>].
- (2) Discovery of a Tricyclic β -Lactam as a Potent Antimicrobial Agent against Carbapenem-Resistant Enterobacterales, Including Strains with Reduced Membrane Permeability and Four-Amino Acid Insertion into Penicillin-Binding Protein 3: Structure–Activity-Relationships and *In Vitro* and *In Vivo* Activities.
Jun Sato, Hiroki Kusano, Toshiaki Aoki, Satoru Shibuya, Katsuki Yokoo, Kazuo Komano, Takuya Oguma, Shuhei Matsumoto, Rio Nakamura, Takafumi Sato, Kenji Yamawaki
ACS Infect. Dis. **2022**, *8*, 400–410. Copyright 2022 American Chemical Society. Reproduced with permission. To access the final edited and published work, see [<https://doi.org/10.1021/acsinfecdis.1c00549>].
- (3) Stereoselective Synthesis of Tricyclic β -Lactam by Sulfoxide-Directed Oxidative Lactonization from an Accessible Cephalosporin Intermediate.
Jun Sato, Takuya Oguma, Kenji Yamawaki
J. Org. Chem. **2022**, *87*, 11231–11236. Copyright 2022 American Chemical Society. Reproduced with permission. To access the final edited and published work, see

[<https://doi.org/10.1021/acs.joc.2c01113>].

(4) Arylcyanation of Norbornene and Norbornadiene Catalyzed by Nickel.

Yoshiaki Nakao, Akira Yada, **Jun Satoh**, Shiro Ebata, Shinichi Oda, Tamejiro Hiyama

Chem. Lett. **2006**, *35*, 790–791. Copyright 2006 The Chemical Society of Japan.

Reproduced with permission. To access the final edited and published work, see

[<https://doi.org/10.1246/cl.2006.790>].

Other Publications

- (1) Regio- and stereoselective decarbonylative carbostannylation of alkynes catalyzed by Pd/C.

Yoshiaki Nakao, **Jun Satoh**, Eiji Shirakawa, Tamejiro Hiyama

Angew. Chem. Int. Ed. **2006**, *45*, 2271–2274

- (2) Allylcyanation of Alkynes: Regio- and Stereoselective Access to Functionalized Di- or Trisubstituted Acrylonitriles.

Yoshiaki Nakao, Tomoya Yukawa, Yasuhiro Hirata, Shinichi Oda, **Jun Satoh**, Tamejiro Hiyama

J. Am. Chem. Soc. **2006**, *128*, 7116–7117

- (3) Cefiderocol (S-649266), A new siderophore cephalosporin exhibiting potent activities against *Pseudomonas aeruginosa* and other gram-negative pathogens including multi-drug resistant bacteria: Structure activity relationship.

Toshiaki Aoki, Hidenori Yoshizawa, Kenji Yamawaki, Katsuki Yokoo, **Jun Sato**, Shinya Hisakawa, Yasushi Hasegawa, Hiroki Kusano, Masayuki Sano, Hideki Sugimoto, Yasuhiro Nishitani, Takafumi Sato, Masakatsu Tsuji, Rio Nakamura, Toru Nishikawa, Yoshinori Yamano

Eur. J. Med. Chem. **2018**, *155*, 847–868

- (4) Synthesis of 2-Thio-Substituted 1,6-Diazabicyclo[3.2.1]octane Derivatives, Potent β -Lactamase Inhibitors.

Motohiro Fujiu, Katsuki Yokoo, Toshiaki Aoki, Satoru Shibuya, **Jun Sato**, Kazuo Komano, Hiroki Kusano, Soichiro Sato, Masayoshi Ogawa, and Kenji Yamawaki

J. Org. Chem. **2020**, *85*, 9650–9660

- (5) Introduction of a Thio Functional Group to Diazabicyclooctane: An Effective

Modification to Potentiate the Activity of β -Lactams against Gram-Negative Bacteria Producing Class A, C, and D Serine β -Lactamases.

Motohiro Fujiu, Katsuki Yokoo, **Jun Sato**, Satoru Shibuya, Kazuo Komano, Hiroki Kusano, Soichiro Sato, Toshiaki Aoki, Naoki Kohira, Satoshi Miyagawa, Tomoyuki Kawachi, and Kenji Yamawaki

ACS Infect. Dis. **2020**, *6*, 3034–3047.

(6) Discovery of 2-Sulfinyl-Diazabicyclooctane Derivatives, Potential Oral β -Lactamase Inhibitors for Infections Caused by Serine β -Lactamase-Producing Enterobacterales.

Motohiro Fujiu, Katsuki Yokoo, **Jun Sato**, Satoru Shibuya, Kazuo Komano, Hiroki Kusano, Soichiro Sato, Toshiaki Aoki, Naoki Kohira, Sachi Kanazawa, Ryosuke Watari, Tomoyuki Kawachi, Yuya Hirakawa, Daiki Nagamatsu, Emi Kashiwagi, Hideki Maki, and Kenji Yamawaki

J. Med. Chem. **2021**, *64*, 9496–9512.

Acknowledgment

I would like to express my deep gratitude to Professor Seijiro Matsubara of Kyoto University for giving the opportunity and the kind guidance in organizing this thesis.

The studies from Chapter I to V had been carried out from July 2014 to October 2019 at Shionogi & Co., Ltd. research center. The research in the Appendix was conducted from 2004 to 2006 at the Hiyama group in Department of Material Chemistry, Graduate School of Engineering, Kyoto University.

My heartfelt appreciation goes to Professor Tamejiro Hiyama and Professor Yoshiaki Nakao, whose comments, suggestions and encouragement were of inestimable value for my study.

I would also like to thank the members of the Hiyama Group.

I am deeply grateful to Dr. Kenji Yamawaki, Director of the Medicinal Chemistry Research Laboratories, Shionogi & Co., Ltd., for giving me the opportunity to conduct this research.

I also wish to express my deep gratitude to Dr. Takafumi Sato, Dr. Shuhei Matsumoto and Dr. Naoki Kohira of Shionogi & Co., Ltd., and Ms. Rio Nakamura of Shionogi Techno Advance Research Co., Ltd., for their advice on obtaining pharmacological data and interpreting the results.

I also thank Mr. Masayoshi Ogawa of Shionogi & Co., Ltd., for the single-crystal X-ray structure analysis and 2D NMR analysis and Dr. Kazuya Yasuo for his advice on molecular modeling of tricyclic β -lactams.

I extend my sincere gratitude to colleagues Mr. Hiroki Kusano, Mr. Toshiaki Aoki, Mr. Satoru Shibuya, Mr. Katsuki Yokoo, Dr. Kazuo Komano and Dr. Takuya Oguma for their suggestions.

Finally, I also thank Dr. Hirotohi Morita and Ms. Yumiko Takagi of Shionogi Techno Advance Research Co., Ltd., for obtaining the analysis data.

The studies presented in Appendix has been supported financially by Grant-in-Aid for Creative Scientific Research, No. 16GS0209 and COE Research on “United Approach to New Material Science” from MEXT. YN also acknowledges the NIPPON SHOKUBAI Award in Synthetic Organic Chemistry, Japan, Mitsubishi Chemical Corporation Fund, and NOVARTIS Foundation (Japan) for the Promotion of Science.